LOW-LATITUDE WESTERN NORTH ATLANTIC CLIMATE VARIABILITY DURING THE PAST MILLENNIUM: INSIGHTS FROM PROXIES AND MODELS

By

Casey Pearce Saenger
B.S., Bates College, 2002

Submitted in partial fulfillment of the requirements for the degree of
Doctor of Philosophy

at the
MASSACHUSETTS INSTITUTE OF TECHNOLOGY
and the
WOODS HOLE OCEANOGRAPHIC INSTITUTION

September 2009

Author……
Joint Program in Oceanography/Applied Ocean Science and Engineering
Department of Geology and Geophysics
Massachusetts Institute of Technology and Woods Hole Oceanographic Institution
July 28, 2009

Certified by……
Delia W. Oppo
Senior Scientist, Department of Geology and Geophysics, WHOI
Thesis Co-Supervisor

Certified by……
Anne L. Cohen
Research Specialist, Department of Geology and Geophysics, WHOI
Thesis Co-Supervisor

Accepted by……...
Bradford H. Hager
Professor of Earth, Atmospheric, and Planetary Sciences, MIT
Chairman, Joint Committee for Geology and Geophysics

LOW-LATITUDE WESTERN NORTH ATLANTIC CLIMATE VARIABILITY DURING THE PAST MILLENNIUM: INSIGHTS FROM PROXIES AND MODELS

By

Casey Pearce Saenger

Submitted to the MIT/WHOI Joint Program in Oceanography/Applied Ocean Science and Engineering on August 14, 2009 in partial fulfillment of the requirements for the degree of Doctor of Philosophy in Paleoceanography

Abstract

Estimates of natural climate variability during the past millennium provide a frame of reference in which to assess the significance of recent changes. This thesis investigates new methods of reconstructing low-latitude sea surface temperature (SST) and hydrography, and combines these methods with traditional techniques to improve the present understanding of western North Atlantic climate variability. A new strontium/calcium (Sr/Ca) - SST calibration is derived for Atlantic *Montastrea* corals. This calibration shows that *Montastrea* Sr/Ca is a promising SST proxy if the effect of coral growth is considered. Further analyses of coral growth using Computed Axial Tomography (CAT) imaging indicate growth in *Siderastrea* corals varies inversely with SST on interannual timescales. A 440-year reconstruction of low-latitude western North Atlantic SST based on this relationship suggests the largest cooling of the last few centuries occurred from ~1650-1730 A.D., and was ~1ºC cooler than today. Sporadic multidecadal variability in this record is inconsistent with evidence for a persistent 65-80 year North Atlantic SST oscillation. Volcanic and anthropogenic radiative forcing are identified as important sources of externally-forced SST variability, with the latter accounting for most of the 20th century warming trend. An 1800-year reconstruction of SST and hydrography near the Gulf Stream also suggests SSTs remained within about 1ºC of modern values. This cooling is small relative to other regional proxy records and may reflect the influence of internal oceanic and atmospheric circulation. Simulations with an atmospheric general circulation model (AGCM) indicate that the magnitude of cooling estimated by proxy records is consistent with tropical hydrologic proxy records.

Acknowledgements

I thank my advisors Anne Cohen and Delia Oppo for their time and support. Listening to their ideas has been inspirational, and their willingness to listen to mine has been appreciated. They will be role models to me throughout my scientific career. The generous and selfless contributions of my thesis committee, including Bill Curry, Ping Chang, Ed Boyle and Jeff Donnelly are also greatly appreciated. My only regret is not taking greater advantage of their collective knowledge.

I also express my appreciation to the members of WHOI's Paleoceanography group, within which the analytical efforts of Rindy Ostermann, Scot Birdwhistell, Simon Thorrold, Darlene Ketten, Julie Arruda, Kathyrn Rose and Luping Zou deserve special recognition. The support of the Academic Programs Office is unparalleled and is greatly appreciated. I also thank the Geology and Geophysics administrative staff, the MIT Education Office and WHOI's Facilities staff for their efforts to make daily operations run smoothly.

I am grateful to know my fellow Joint Program students and I thank them for their encouragement, shop talk and countless dinner parties. Thanks also to the larger Woods Hole community. I will miss sharing a smile and a wave as I ride past. Finally, to Em. My love. Her jokes, pies and unwavering faith in me have been the brightest points of graduate school.

Funding for this research was provided by a National Science Foundation Graduate Student Fellowship, National Science Foundation grants OCE-0402728, OCE-0623364, ATM-033746, the WHOI Ocean and Climate Change Institute, the WHOI Ocean Ventures Fund, the WHOI Ocean Life Institute, the MIT Student Assistance Fund, award number USA-0002, made by King Abdullah University of Science and Technology (KAUST), and the Inter-American Institute for Global Change Research.

Table of Contents

Chapter 1:

Introduction

Variations in Earth's climate primarily reflect interactions between intrinsic modes of ocean-atmosphere circulation and external radiative forcing. Externally-forced climate variability includes natural variations in solar and volcanic activity, and in recent centuries, anthropogenic impacts on atmospheric greenhouse gases, tropospheric aerosols and land-use [*Jansen et al*., 2007]. The significance of these anthropogenic effects must be interpreted in a longer-term context that captures the climatic response to natural internal and external forcing. During the past millennium, major climatic boundary conditions (ice volume, orbital geometry) were relatively constant, making this time interval appropriate for estimating the bounds of natural climate variability.

Proxy reconstructions of Northern Hemisphere climate during the last millennium suggest that the late 20th century was likely the warmest interval of the past 500 years [*Jansen et al*., 2007; *Mann et al*., 2008], and that this warming was mostly anthropogenic [*Hegerl et al*., 2007]. However, these reconstructions are based primarily on high-latitude terrestrial proxies, with relatively little data from the tropics or the ocean. Given that temperatures in the tropics, which are predominantly covered by oceans, closely follow the global mean [*National Research Council*, 2006], reconstructions of low-latitude sea-surface temperature (SST) variability may allow the significance of anthropogenic climate impacts to be assessed more accurately.

In this thesis I explore new methods of reconstructing tropical climate variability, and use these methods in parallel with traditional techniques to generate low-latitude climate reconstructions spanning the last millennium. Although my focus is on the western Atlantic, including the Caribbean Sea, a number of the questions I address are relevant to other regions. These questions are:

1. Does the growth rate of Atlantic *Montastrea* corals influence SST estimates based on their strontium/calcium ratios?
2. Can coral growth rates be used on their own to constrain SST trends and variability on interannual to centennial timescales?
3. How has the circulation of the ocean and the atmosphere affected regional climate on centennial and longer timescales?
4. Is evidence for small SST variability over the past millennium consistent with circum-Atlantic hydrologic proxies?

These questions are explored more thoroughly in Chapters 2 through 5 of this thesis.

Chapter 2 examines the climatic archive preserved within the aragonitic skeletons of massive, long-lived *Montastrea* corals. These skeletons consist of biogenic aragonite that can contain various minor and trace elements including strontium (Sr). Early investigations of coral Sr/Ca suggested a weak temperature dependence that was overwhelmed by growth rate effects [*Weber*, 1973]. Subsequent work concluded growth rate effects were negligible and proposed equations relating coral Sr/Ca to SST [*Smith et*

al., 1979; *Beck et al*., 1992] that paved the way for continuous, multi-centennial SST reconstructions [e.g. *Hendy et al*., 2002]. Rapid coral growth rates and annual density bands allow these long records to be generated at seasonal resolution in a number of species [*Quinn and Sampson*, 2002; *Swart et al*., 2002; *Bagnato et al*., 2004; *Cohen and Thorrold*, 2007; *Maupin et al*., 2008]. Simultaneous measurements of oxygen isotopic ratios ($\delta^{18}O$), which depend on SST and seawater $\delta^{18}O$, may allow hydrographic information to be extracted from the same samples [e.g. *Grottoli and Eakin,* 2007]. *Montastrea* are a dominant genus in both fossil and modern Atlantic reefs [*Weil and Knowlton*, 1994; *Hubbard et al*., 2005], and thus have the potential to be a valuable tool for reconstructing the region's climatic history over many centuries. However, differences in *Montastrea* Sr/Ca-SST calibrations [*Swart et al*., 2002; *Smith et al*., 2006] predict SST spanning more than 10ºC at a given Sr/Ca ratio, and make climatic interpretations using this species difficult. Evidence for growth-related effects on Sr/Ca in other coral genera [*deVilliers et al*., 1995; *Goodkin et al*., 2005] raises the possibility that disparate *Montastrea* calibrations may be related to growth.

In this chapter, I present analyses of the Sr/Ca and $\delta^{18}O$ in four *Montastrea* corals with growth rates ranging from 2.3 to 12.6 mm yr^{-1} [*Saenger et al*., 2008]. Systematic offsets in the Sr/Ca-SST calibrations of the four corals are inversely correlated with growth rate such that the slowest growing specimens have the highest average Sr/Ca. No growth rate dependence is evident in $\delta^{18}O$. The observed Sr/Ca growth-rate dependence is consistent with a Rayleigh fractionation model for coral biomineralization in which slower growing corals precipitate, on average, less aragonite from a batch of calcifying

fluid [*Gaetani and Cohen*, 2006; *Cohen et al.,* 2006]. To correct for this effect, I derive a growth-dependent Sr/Ca-SST calibration that describes *Montastrea* Sr/Ca as a function of both SST and growth rate. A conventional, nongrowth-dependent calibration calculates modern SSTs that are up to 9ºC cooler than observed, and estimates SST anomalies 5ºC cooler than today in a 450 year old subfossil *Montastrea*. In contrast, the growth-dependent calibration, which estimates SSTs within error of observed values, suggests little or no cooling in the same subfossil specimen. This suggests low-latitude western North Atlantic SST reconstructions based on *Montastrea* Sr/Ca that do not consider coral growth may estimate paleotemperatures that are several degrees too cool.

Chapter 3 further explores the link between coral growth and SST to investigate if variations in annual growth rate can be used to reconstruct the interannual to centennial-scale history of low-latitude western North Atlantic SST. The pattern of North Atlantic SST variability over the last 150 years shows evidence for a 65-80 year oscillation superimposed upon a background warming trend [*Schlesinger and Ramankutty,* 1994; *Andronova and Schlesinger*, 2000]. Model simulations [*Knight et al.,* 2005] suggest the multidecadal portion of this signal, often referred to as the Atlantic Multidecadal Oscillation (AMO), may be a persistent feature of Atlantic variability with large and potentially predictable climatic impacts [*Knight et al.,* 2006; *Keenlyside et al.,* 2008]. However, proxy evidence for the AMO predating the relatively brief instrumental record derives primarily from high-latitude terrestrial proxies [*Delworth and Mann,* 2000; *Gray et al.*, 2004]. To date, Atlantic reconstructions based strictly on oceanographic proxies do

not have the age control [*Haase-Schramm et al.,* 2003; *Lund and Curry,* 2006; *Black et al.,* 2007] or length [*Hetzinger et al.,* 2008; *Goodkin et al.,* 2008] necessary to separate the AMO from externally-forced SST variability.

This chapter presents a 440-year reconstruction of SST from the low-latitude western North Atlantic based on the annual growth rate of *Siderastrea siderea* corals [*Saenger et al.*, 2009a]. A calibration of annual average SST and *S. siderea* growth, derived from Computed Axial Tomography (CAT) imaging, suggests a significant correlation at periods longer than 6 years. Applying this relationship to *S. siderea* growth indicates coral-derived SST faithfully captures the timing and the magnitude of observed multidecadal trends. The entire 440-year SST reconstruction suggests that temperatures were as warm as today from about 1552-1570 A.D., then cooled by ~1ºC between 1650 and 1730 A.D. before warming toward the present. Approximately 35% of the variance in our SST reconstruction is attributed to external forcing, with the anthropogenic component accounting for most of the warming we observe after 1900 A.D. Our estimate of internal SST variability shows relatively persistent 15-25 year variability through most of the record, but only exhibits significant multidecadal variability after about 1730 A.D. This suggests that multidecadal SST variability may not be a persist feature of the low-latitude western North Atlantic, potentially complicating the ability to make accurate decadal climate forecasts.

Chapter 4 considers lower-frequency modes of regional variability that allow the multidecadal to centennial trends in Chapter 3 to be interpreted within a broader context.

The North Atlantic Oscillation (NAO) and the Meridional Overturning Circulation (MOC) are major influences on subtropical western North Atlantic atmospheric and oceanic variability [*Marshall et al.,* 2001; *Hurrell et al.,* 2003; *Visbeck et al.,* 2003]. Variations in the NAO and MOC can strongly impact regional climate on centennial and longer timescales, leading to trends that differ significantly from the Northern Hemisphere mean [*Goose et al.,* 2005; *deVernal and Hillaire-Marcel,* 2006]. Assessing the significance of observed climate change in the low-latitude western North Atlantic therefore requires proxy reconstructions that capture the complex dynamics of the region.

In this chapter, I present an 1800-year reconstruction of climate variability from the Carolina Slope in the subtropical western North Atlantic. Reconstructions of regional SST and hydrography based on planktonic foraminiferal Mg/Ca and $\delta^{18}O$ show small anomalies with patterns of variability that differ from those of the Northern Hemisphere mean. These differences are attributed to internal variations in oceanic and atmospheric circulation that may mask the response to external radiative forcing in the region.

Finally, Chapter 5 assesses if the small SST anomalies suggested in this thesis, and in other reconstructions of low-latitude western North Atlantic SST [*Lund and Curry,* 2006; *Black et al.,* 2007], are consistent with regional hydrologic proxies. A prolonged cool period from ~1400-1850 A.D., referred to as the Little Ice Age (LIA) [*Grove,* 1988], is a prominent feature of many North Atlantic SST reconstructions [*Keigwin* 1996; *Keigwin and Pickart,* 1999; *deMenocal et al.,* 2000; *Sicre et al.*, 2008]. Dry LIA conditions over Central and South America are thought to reflect a southerly migration of

precipitation associated with the Intertropical Convergence Zone (ITCZ) in response to North Atlantic cooling [*Haug et al.,* 2001; *Hodell et al.,* 2005]. Some proxy records estimate this cooling was as large as 3ºC in the low-latitude western North Atlantic [*Winter et al.,* 2000], while the reconstructions in this thesis find much smaller cool anomalies of a degree or less. Recent model simulations indicate extratropical North Atlantic climate can influence the meridional position of the ITCZ [*Chiang and Bitz*, 2005; *Broccoli et al*., 2006] without necessarily cooling the low latitudes [*Kang et al.,* 2008], which suggests the subtle LIA cooling suggested in previous chapters may be consistent with regional hydrologic reconstructions.

I further explore the relative influence of tropical and high-latitude SST on the latitude of the ITCZ in this chapter [*Saenger et al.,* 2009b]. Using an atmospheric general circulation model (AGCM) I assess the potential for extratropical SST anomalies to influence tropical precipitation in the absence of low-latitude cooling. Three sets of simulations are performed using the National Center for Atmospheric Research (NCAR) Community Atmosphere Model version 3 (CAM3) and the SST *pattern* from the "hosing" experiment of *Zhang and Delworth* [2005]. The first set of experiments cools the entire Atlantic north of the Equator, the second set of simulations applies cooling anomalies only north of 30ºN, and the third set applies anomalies from the Equator to 30ºN. Results clearly show that without coupling of the ocean and atmosphere, extratropical cooling cannot force southerly ITCZ migrations. However, the ITCZ does appear to be sensitive to very small SST anomalies of less than 0.5ºC, indicating that the

cooling anomalies estimated in previous chapters are consistent with circum-Atlantic hydrologic proxies.

References

Andronova, N. G. and M. E. Schlesinger, 2000: Causes of global temperature changes during the 19th and 20th centuries. *Geophysical Research Letters*, **27,** 2137-2140.

Bagnato, S., B. K. Linsley, S. S. Howe, G. M. Wellington, and J. Salinger, 2004: Evaluating the use of the massive coral Diploastrea heliopora for paleoclimate reconstruction. *Paleoceanography*, **19**.

Beck, J. W., R. L. Edwards, E. Ito, F. W. Taylor, J. Recy, F. Rougerie, P. Joannot, and C. Henin, 1992: Sea-Surface Temperature from Coral Skeletal Strontium Calcium Ratios. *Science*, **257,** 644-647.

Black, D. E., M. A. Abahazi, R. C. Thunell, A. Kaplan, E. J. Tappa, and L. C. Peterson, 2007: An 8-century tropical Atlantic SST record from the Cariaco Basin: Baseline variability, twentieth-century warming, and Atlantic hurricane frequency. *Paleoceanography*, **22**.

Broccoli, A. J., K. A. Dahl, and R. J. Stouffer, 2006: Response of the ITCZ to Northern Hemisphere cooling. *Geophysical Research Letters*, **33**.

Chiang, J. C. H. and C. M. Bitz, 2005: Influence of high latitude ice cover on the marine Intertropical Convergence Zone. *Climate Dynamics*, **25,** 477-496.

Cohen, A. L., G. A. Gaetani, T. Lundalv, B. H. Corliss, and R. Y. George, 2006: Compositional variability in a cold-water scleractinian, Lophelia pertusa: New insights into "vital effects". *Geochemistry Geophysics Geosystems*, **7**.

Cohen, A. L. and S. R. Thorrold, 2007: Recovery of temperature records from slow-growing corals by fine scale sampling of skeletons. *Geophysical Research Letters*, **34**.

de Vernal, A. and C. Hillaire-Marcel, 2006: Provincialism in trends and high frequency changes in the northwest North Atlantic during the Holocene. *Global and Planetary Change*, **54,** 263-290.

Delworth, T. L. and M. E. Mann, 2000: Observed and simulated multidecadal variability in the Northern Hemisphere. *Climate Dynamics*, **16,** 661-676.

deMenocal, P., J. Ortiz, T. Guilderson, and M. Sarnthein, 2000: Coherent high- and low-latitude climate variability during the holocene warm period. *Science*, **288,** 2198-2202.

deVilliers, S., B. K. Nelson and A. R. Chivas, 1995: Biological controls on coral Sr/Ca and delta ^{18}O reconstructions of sea surface temperatures. *Science*, **269**, 1247-1249.

Gaetani, G. A. and A. L. Cohen, 2006: Element partitioning during precipitation of

aragonite from seawater: A framework for understanding paleoproxies. *Geochimica Et Cosmochimica Acta*, **70,** 4617-4634.

Goodkin, N. F., K. A. Hughen, A. L. Cohen and S. R. Smith, 2005: Record of Little Ice Age sea surface temperatures at Bermuda using a growth-dependent calibration of coral Sr/Ca. *Paleoceanography*, **20**.

Goodkin, N. F., K. A. Hughen, W. B. Curry, S. C. Doney, and D. R. Ostermann, 2008: Sea surface temperature and salinity variability at Bermuda during the end of the Little Ice Age. *Paleoceanography*, **23**.

Goosse, H., H. Renssen, A. Timmermann, and R. S. Bradley, 2005: Internal and forced climate variability during the last millennium: a model-data comparison using ensemble simulations. *Quaternary Science Reviews*, **24,** 1345-1360.

Gray, S. T., L. J. Graumlich, J. L. Betancourt, and G. T. Pederson, 2004: A tree-ring based reconstruction of the Atlantic Multidecadal Oscillation since 1567 AD. *Geophysical Research Letters*, **31**.

Grottoli, A. G. and C. M. Eakin, 2007: A review of modern coral delta O-18 and Delta C-14 proxy records. *Earth-Science Reviews*, **81,** 67-91.

Grove, J. M., 1988: The Little Ice Age, Methuen, New York, 498 pp.

Haase-Schramm, A., F. Bohm, A. Eisenhauer, W. C. Dullo, M. M. Joachimski, B. Hansen, and J. Reitner, 2003: Sr/Ca ratios and oxygen isotopes from sclerosponges: Temperature history of the Caribbean mixed layer and thermocline during the Little Ice Age. *Paleoceanography*, **18**.

Haug, G. H., K. A. Hughen, D. M. Sigman, L. C. Peterson, and U. Rohl, 2001: Southward migration of the intertropical convergence zone through the Holocene. *Science*, **293,** 1304-1308.

Hegerl, G. C., T. J. Crowley, M. Allen, W. T. Hyde, H. N. Pollack, J. Smerdon, and E. Zorita, 2007: Detection of human influence on a new, validated 1500-year temperature reconstruction. *Journal of Climate*, **20,** 650-666.

Hendy, E. J., M. K. Gagan, C. A. Alibert, M. T. McCulloch, J. M. Lough, and P. J. Isdale, 2002: Abrupt decrease in tropical Pacific Sea surface salinity at end of Little Ice Age. *Science*, **295,** 1511-1514.

Hetzinger, S., M. Pfeiffer, W. C. Dullo, N. Keenlyside, M. Latif, and J. Zinke, 2008: Caribbean coral tracks Atlantic Multidecadal Oscillation and past hurricane activity. *Geology*, **36,** 11-14.

Hodell, D. A. M. Brenner, J. H. Curtis, R. Medina-Gonzales, E. Ildefonso-Chan Can, A. Albornaz-Pat, and T. P. Guilderson, 2005: Climate change on the Yucatan Peninsula during the Little Ice Age, *Quaternary Research*, **63**, 109-121.

Hurrell, J. W., Y. Kushnir, G. Ottersen and M. Visbeck, 2003: An Overview of the North Atlantic Oscillation, *in*, Hurrell, J. W., Y. Kushnir, G. Ottersen and M. Visbeck (eds.) The North Atlantic Oscillation: Climate Significance and Environmental Impact, American Geophysical Union, Washington D.C., p. 1-35.

Hubbard, D. K., H. Zankl, I. Van Heerden, and I. P. Gill, 2005: Holocene reef development along the Northeastern St. Croix Shelf, Buck Island, US Virgin Islands. *Journal of Sedimentary Research*, **75,** 97-113.

Jansen et al., 2007: Paleoclimate, *in*, Climate Change 2007: The Physical Science Basis. Contribution of Working Group I to the Fourth Assessment Report of the Intergovernmental Panel on Climate Change, Solomon, S., D. Qin, M. Manning, Z. Chen, M. Marquis, K. B. Averyt, M. Tignor and H. L. Miller (eds.), Cambridge University Press, Cambridge and New York. 996 pp.

Kang, S. M., I. M. Held, D. M. W. Frierson, and M. Zhao, 2008: The response of the ITCZ to extratropical thermal forcing: Idealized slab-ocean experiments with a GCM. *Journal of Climate*, **21,** 3521-3532.

Keenlyside, N. S., M. Latif, J. Jungclaus, L. Kornblueh, and E. Roeckner, 2008: Advancing decadal-scale climate prediction in the North Atlantic sector. *Nature*, **453,** 84-88.

Keigwin, L. D., 1996: The Little Ice Age and Medieval warm period in the Sargasso Sea. *Science*, **274,** 1504-1508.

Keigwin, L. D., and R. S. Pickart, 1999: Slope water current over the Laurentian Fan on interannual to millennial timescales. *Science*, **286**, 520-523.

Knight, J. R., R. J. Allan, C. K. Folland, M. Vellinga, and M. E. Mann, 2005: A signature of persistent natural thermohaline circulation cycles in observed climate. *Geophysical Research Letters*, **32**.

Knight, J. R., C. K. Folland, and A. A. Scaife, 2006: Climate impacts of the Atlantic Multidecadal Oscillation. *Geophysical Research Letters*, **33**.

Lund, D. C. and W. Curry, 2006: Florida Current surface temperature and salinity variability during the last millennium. *Paleoceanography*, **21**.

Mann, M. E., Z. H. Zhang, M. K. Hughes, R. S. Bradley, S. K. Miller, S. Rutherford, and F. B. Ni, 2008: Proxy-based reconstructions of hemispheric and global surface temperature variations over the past two millennia. *Proceedings of the National Academy of Sciences of the United States of America*, **105,** 13252-13257.

Marshall, J., Y. Kushner, D. Battisti, P. Chang, A. Czaja, R. Dickson, J. Hurrell, M. McCartney, R. Saravanan, and M. Visbeck, 2001: North Atlantic climate variability: Phenomena, impacts and mechanisms. *International Journal of Climatology*, **21,** 1863-1898.

Maupin, C. R., T. M. Quinn, and R. B. Halley, 2008: Extracting a climate signal from the skeletal geochemistry of the Caribbean coral Siderastrea siderea. *Geochemistry Geophysics Geosystems*, **9**.

National Research Council, 2006: Surface temperature reconstructions for the last 2,000 years. National Academies Press, Washington, D.C. 196 pp.

Quinn, T. M. and D. E. Sampson, 2002: A multiproxy approach to reconstructing sea surface conditions using coral skeleton geochemistry. *Paleoceanography*, **17**.

Saenger, C., A. L. Cohen, D. W. Oppo and D. Hubbard, 2008: Interpreting sea surface temperature from strontium/calcium in *Montastrea* corals: Link with growth rate and implications for proxy reconstructions. *Paleoceanography,* **23**

Saenger, C., A. L. Cohen, D. W. Oppo, R. B. Halley, and J. E. Carilli, 2009a: Surface temperature trends and variability in the low-latitude North Atlantic since 1552. *Nature Geoscience*, **2**, 492-495.

Saenger, C., P. Chang, L. Ji, D. W. Oppo, and A. L. Cohen, 2009b: Tropical Atlantic climate response to low-latitude and extratropical sea-surface temperature: A Little Ice Age perspective. *Geophysical Research Letters*, **36**.

Schlesinger, M. E. and N. Ramankutty, 1994: An Oscillation in the Global Climate System of Period 65-70 Years. *Nature*, **367,** 723-726.

Sicre, M. A., J. Jacob, U. Ezat, S. Rousse, C. Kissel, P. Yiou, J. Eiriksson, K. L. Knudsen, E. Jansen, and J. L. Turon, 2008: Decadal variability of sea surface temperatures off North Iceland over the last 2000 years. *Earth and Planetary Science Letters*, **268,** 137-142.

Smith, S. V., R. W. Buddemeier, R. C. Redalje, and J. E. Houck, 1979: Strontium-Calcium Thermometry in Coral Skeletons. *Science*, **204,** 404-407.

Smith, J. M., T. M. Quinn, K. P. Helmle, and R. B. Halley, 2006: Reproducibility of

geochemical and climatic signals in the Atlantic coral Montastraea faveolata. *Paleoceanography*, **21**.

Swart, P. K., H. Elderfield, and M. J. Greaves, 2002: A high-resolution calibration of Sr/Ca thermometry using the Caribbean coral Montastraea annularis. *Geochemistry Geophysics Geosystems*, **3**.

Visbeck, M., E. P. Chassignet, R. G. Curry, T. L. Delworth, R.R. Dickson, and G. Krahmann, 2003: The Ocean's Response to North Atlantic Oscillation Variability, *in*, Hurrell, J. W., Y. Kushnir, G. Ottersen and M. Visbeck (eds.) The North Atlantic Oscillation: Climate Significance and Environmental Impact, American Geophysical Union, Washington D.C., p. 113-145.

Weber, J. N., 1973: Incorporation of strontium into reef coral skeletal carbonate. *Geochimica et Cosmochimica Acta,* **37**, 2173-2190.

Weil, E. and N. Knowlton, 1994: A Multi-Character Analysis of the Caribbean Coral Montastraea-Annularis (Ellis and Solander, 1786) and Its 2 Sibling Species, M-Faveolata (Ellis and Solander, 1786) and M-Franksi (Gregory, 1895). *Bulletin of Marine Science*, **55,** 151-175.

Winter, A., H. Ishioroshi, T. Watanabe, T. Oba, and J. Christy, 2000: Caribbean sea surface temperatures: two-to-three degrees cooler than present during the Little Ice Age. *Geophysical Research Letters*, **27,** 3365-3368.

Zhang, R. and T. L. Delworth, 2005: Simulated tropical response to a substantial weakening of the Atlantic thermohaline circulation. *Journal of Climate*, **18,** 1853-1860.

Chapter 2:

Interpreting sea surface temperature from strontium/calcium ration in *Montastrea* corals: Link with growth rate and implications for proxy reconstructions

Reprinted with the permission of the American Geophysical Union.

Saenger, C., A. L. Cohen, D. W. Oppo and D. Hubbard, 2008: Interpreting sea surface temperature from strontium/calcium in *Montastrea* corals: Link with growth rate and implications for proxy reconstructions. *Paleoceanography,* **23,** PA3102, doi:10.1029/2007PA001572

Abstract

We analyzed strontium/calcium ratios (Sr/Ca) in four colonies of the Atlantic coral genus *Montastrea* with growth rates ranging from 2.3 to 12.6 mm yr^{-1}. Derived Sr/Ca–sea surface temperature (SST) calibrations exhibit significant differences among the four colonies that cannot be explained by variations in SST or seawater Sr/Ca. For a single coral Sr/Ca ratio of 8.8 mmol mol^{-1}, the four calibrations predict SSTs ranging from 24.0 to 30.9ºC. We find that differences in the Sr/Ca–SST relationships are correlated systematically with the average annual extension rate (ext) of each colony such that Sr/Ca (mmol mol^{-1}) = 11.82 (±0.13) – 0.058 (±0.004) * ext (mm yr^{-1}) – 0.092 (±0.005) * SST (ºC). This observation is consistent with previous reports of a link between coral Sr/Ca and growth rate. Verification of our growth-dependent Sr/Ca–SST calibration using a coral excluded from the calibration reconstructs the mean and seasonal amplitude of the actual recorded SST to within 0.3ºC. Applying a traditional, nongrowth-dependent Sr/Ca–SST calibration derived from a modern *Montastrea* to the Sr/Ca ratios of a conspecific coral that grew during the early Little Ice Age (LIA) (400 years B.P.) suggests that Caribbean SSTs were >5ºC cooler than today. Conversely, application of our growth-dependent Sr/Ca–SST calibration to Sr/Ca ratios derived from the LIA coral indicates that SSTs during the 5-year period analyzed were within error (±1.4ºC) of modern values.

PALEOCEANOGRAPHY, VOL. 23, PA3102, doi:10.1029/2007PA001572, 2008

Interpreting sea surface temperature from strontium/calcium ratios in *Montastrea* corals: Link with growth rate and implications for proxy reconstructions

Casey Saenger,[1] Anne L. Cohen,[2] Delia W. Oppo,[2] and Dennis Hubbard[3]

Received 17 November 2007; revised 30 April 2008; accepted 30 May 2008; published 31 July 2008.

[1] We analyzed strontium/calcium ratios (Sr/Ca) in four colonies of the Atlantic coral genus *Montastrea* with growth rates ranging from 2.3 to 12.6 mm a^{-1}. Derived Sr/Ca–sea surface temperature (SST) calibrations exhibit significant differences among the four colonies that cannot be explained by variations in SST or seawater Sr/Ca. For a single coral Sr/Ca ratio of 8.8 mmol mol^{-1}, the four calibrations predict SSTs ranging from 24.0° to 30.9°C. We find that differences in the Sr/Ca–SST relationships are correlated systematically with the average annual extension rate (ext) of each colony such that Sr/Ca (mmol mol^{-1}) = 11.82 (±0.13) – 0.058 (±0.004) × ext (mm a^{-1}) – 0.092 (±0.005) × SST (°C). This observation is consistent with previous reports of a link between coral Sr/Ca and growth rate. Verification of our growth-dependent Sr/Ca–SST calibration using a coral excluded from the calibration reconstructs the mean and seasonal amplitude of the actual recorded SST to within 0.3°C. Applying a traditional, nongrowth-dependent Sr/Ca–SST calibration derived from a modern *Montastrea* to the Sr/Ca ratios of a conspecific coral that grew during the early Little Ice Age (LIA) (400 years B.P.) suggests that Caribbean SSTs were >5°C cooler than today. Conversely, application of our growth-dependent Sr/Ca–SST calibration to Sr/Ca ratios derived from the LIA coral indicates that SSTs during the 5-year period analyzed were within error (±1.4°C) of modern values.

Citation: Saenger, C., A. L. Cohen, D. W. Oppo, and D. Hubbard (2008), Interpreting sea surface temperature from strontium/calcium ratios in *Montastrea* corals: Link with growth rate and implications for proxy reconstructions, *Paleoceanography*, *23*, PA3102, doi:10.1029/2007PA001572.

1. Introduction

[2] Several distinct, although not necessarily global, climatic events during the last 1000 years, such as the Little Ice Age (LIA, ~500–100 years B.P.), suggest that recent anthropogenically forced climate change is superimposed upon natural centennial-scale climate variability [*Jones and Mann*, 2004; *National Research Council*, 2006]. Separating the impact of anthropogenic activity on climate from the natural background variability requires accurate reconstructions of the nature and magnitude of past climate variability. While geochemical proxy records from biogenic carbonates have provided valuable information about the behavior of the climate system over this time period [e.g., *Hendy et al.*, 2002; *Cronin et al.*, 2003; *Black et al.*, 2004; *Lund and Curry*, 2006], inconsistent results in some regions have prevented a robust characterization of natural climatic changes. For example, proxy reconstructions suggest that sea surface temperatures (SSTs) in the Caribbean region during the LIA were <1° to >3°C cooler than today, and some data sets suggest that the surface ocean was fresher while others indicate more saline conditions than modern [*Winter et al.*, 2000; *Watanabe et al.*, 2001; *Nyberg et al.*, 2002; *Lund and Curry*, 2006]. There are several possible reasons for such discrepant results including seasonally biased SST estimates derived from foraminifera [*Thunell and Reynolds*, 1984; *Mohiuddin et al.*, 2004], smoothing due to bioturbation, chronological uncertainties associated with large errors on radiocarbon dates, and uncertainties associated with the calibration and interpretation of geochemical proxies.

[3] Massive, long-lived corals are unique archives of ocean climate that may circumvent some of the uncertainties of other reconstructions. Dense and rapidly extending coral skeletons can be sampled at subseasonal resolution with absolute age control because of annual density bands. Long-lived corals can provide continuous proxy records over multiple centuries [e.g., *Hendy et al.*, 2002] that are not prone to bioturbation, and young fossil coral can be U/Th dated to within ±5 years [*Cobb et al.*, 2003]. Nevertheless, interpreting coral geochemistry in terms of climatic parameters is not always straightforward [*Lough*, 2004]. For example, Sr/Ca–SST calibrations derived to date from single colonies of the Atlantic coral *Montastrea,* a predominant genus in both modern and fossil reefs [*Weil and Knowlton*, 1994; *Hubbard et al.*, 2005] show significant, yet unexplained differences [*Swart et al.*, 2002; *Smith et al.*, 2006]. This implies that paleo-SST estimates derived using these calibrations depend heavily on which calibration is applied. For example, applying

[1] MIT/WHOI Joint Program in Oceanography, Woods Hole, Massachusetts, USA.
[2] Department of Geology and Geophysics, Woods Hole Oceanographic Institution, Woods Hole, Massachusetts, USA.
[3] Department of Geology, Oberlin College, Oberlin, Ohio, USA.

0883-8305/08/2007PA001572$12.00

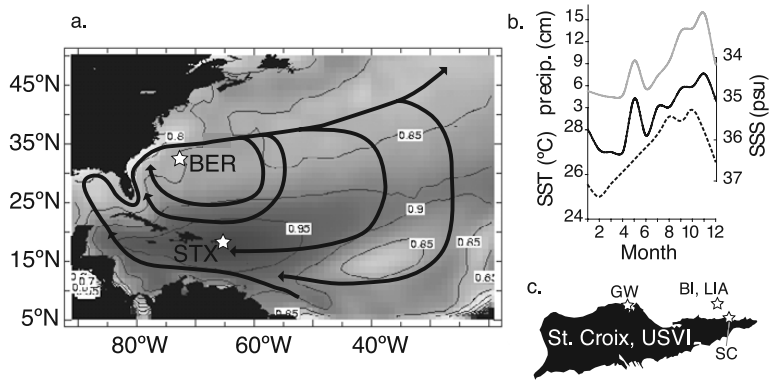

Figure 1. (a) Correlation of IGOSS sea surface temperature (SST) at St. Croix (STX) with the greater tropical and subtropical North Atlantic. Contours are correlation coefficient (r) values. Black arrows indicate general oceanic circulation. STX and Bermuda (BER) are coral collection sites. (b) Climatological St. Croix precipitation, SST, and sea surface salinity (SSS) [*Department of Conservation and Cultural Affairs*, 1986]. (c) Local STX map showing collection sites for modern (GW, SC, and BI) and Little Ice Age fossil (LIA) corals.

existing *Montastrea* Sr/Ca–SST calibrations [*Swart et al.*, 2002; *Smith et al.*, 2006] to a coral with a typical skeletal Sr/Ca ratio of 8.8 mmol mol^{-1} predicts paleo-SSTs ranging from 29.0° to 40.9°C.

[4] In this study we measured Sr/Ca in four *Montastrea* colonies that had mean annual extension rates ranging from 2.3 to 12.6 mm a^{-1}. Oxygen isotopic ratios ($\delta^{18}O_c$) also were measured in the three fastest growing corals. The derived Sr/Ca–SST calibrations exhibited systematic offsets that were correlated with differences in the annual average skeletal extension rate of each colony. No growth rate effect was evident in $\delta^{18}O_c$. We derived a growth rate–dependent Sr/Ca–SST calibration using three corals, and independently verified its accuracy using the fourth coral. We also applied our growth rate–dependent calibration to a fossil *Montastrea* that grew in the early LIA (400 years B.P.), and compared our result with that predicted using a traditional, nongrowth-dependent Sr/Ca–SST calibration.

2. Study Site

[5] St. Croix, U.S. Virgin Islands (17° 45′N, 64° 45′W) lies in the eastern Caribbean Sea and is bathed by water of predominantly North Atlantic subtropical gyre origin [*Hernandez-Guerra and Joyce*, 2000]. SST is highly correlated with SST throughout the broader tropical Atlantic (Figure 1a) suggesting that our study site is well situated to capture regional SST variability. The seasonal amplitude of SST at St Croix is ~4°C with an annual minimum in February and an annual maximum in September (Figure 1b). The influence of freshwater river discharge is small, and the regional hydrologic budget is controlled largely by precipitation [*Yoo and Carton*, 1990]. Precipitation varies seasonally in association with annual insolation-driven meridional migrations of the Intertropical Convergence Zone (ITCZ), a band of increased precipitation at the confluence of interhemispheric easterly trade winds.

3. Methods

3.1. Coral Collection and Sampling

[6] Live *Montastrea faveolata* corals were collected from three sites on St. Croix (GW, SC and BI) (Figure 1c). An additional specimen, a slow growing *Montastrea franksi* colony collected on Bermuda's (BER) south shore reef [*Cohen and Thorrold*, 2007], was also included in this study. GW and SC corals were collected from ~1 m of water, while BI and BER samples were recovered from water depths of 10 and 13 m, respectively. In addition to the live modern corals, we also analyzed a *Montastrea faveolata* specimen that grew during the early LIA. A ~10-cm-long piece was retrieved from a drill core taken in 6 m of water along the southeastern submerged Holocene reef of Buck Island, St. Croix [*Hubbard et al.*, 2005]. The drill core specimen was AMS radiocarbon dated to have a calibrated age of 400 years B.P. (conventional $^{14}C = 750 \pm 60$ years, 2σ range 490–270 years B.P.) [*Hubbard et al.*, 2005; *Hughen et al.*, 2004; M. Stuvier, P. J. Reimer, and R. W. Reimer, CALIB radiocarbon calibration, execute version 5.0.2, http://calib.qub.ac.uk/calib/, 2005].

[7] All corals were slabbed parallel to the axis of maximum growth using a water-cooled tile saw, and briefly ultrasonicated in deionized water. A 7-mm-wide slab was removed from the center of each colony and x-rayed to obtain information about coral growth rates and to establish a chronology from the annual density bands. X-radiographs were taken at the local hospital in Falmouth, MA, using settings of 55 kV and 1.6 mAs, a focal distance of 1 m and exposure time of 0.16 s. The LIA specimen was assessed for

diagenetic alteration using x-ray diffraction [*Hubbard et al.*, 2005] and examination of skeletal ultrastructure in petrographic thin sections.

[8] A Merchantek micromill was used to remove powdered subsamples from the St. Croix corals. Because *Montastrea* corals exhibit variability in $\delta^{18}O_c$ and Sr/Ca ratios among different skeletal elements [*Leder et al.*, 1996; *Smith et al.*, 2006], we removed subsamples from the exothecal wall only. Our sampling tracks were continuous, ~300 μm deep, ~100 μm wide, and advanced in ~400 μm increments along the coral growth axis. ~100 μg of powder was split into aliquots of ~30 μg for $\delta^{18}O_c$ and ~70 μg for Sr/Ca analyses. The $\delta^{18}O_c$ was determined using a Finnigan MAT 252 mass spectrometer with an analytical error of ±0.07‰ [*Ostermann and Curry*, 2000]. Sr/Ca ratios were analyzed using a ThermoFinnigan Element II inductively coupled plasma mass spectrometer (ICP-MS) following the method of *Rosenthal et al.* [1999]. Precision for Sr/Ca is ±0.02 mmol mol^{-1} based on replicate standard analyses (n = 73).

[9] To avoid significant dampening of the annual Sr/Ca cycle in the slow growing coral, Sr/Ca ratios from the BER *Montastrea franksi* were measured by a Cameca 3f ion microprobe as described by *Cohen et al.* [2004] and *Gaetani and Cohen* [2006]. BER data were generated at 50 μm intervals that are equivalent to a temporal resolution of ~10 days. Seasonally resolved $\delta^{18}O_c$ measurements were not generated for the slow growing BER, and no $\delta^{18}O_c$ data are reported for this coral.

3.2. Water Collection and Sampling

[10] Monthly surface water samples (~1 m depth) were collected at GW, SC and BI sites from January to May 2006 (n = 12). High-density polyethylene vials (60 mL volume) were triple rinsed with seawater, filled to overflowing, sealed with parafilm and shipped to the Woods Hole Oceanographic Institution for analysis. Sr/Ca ratios of seawater samples were measured using a ThermoFinnigan Element II high sector field ICP-MS following the protocol of *Gaetani and Cohen* [2006].

3.3. Instrumental SST Records

[11] Local St. Croix SST data were provided from three sources. First, we installed Onset HOBO data loggers at BI, GW and SC to measure bihourly water temperature at the depth of coral collection. Loggers recorded SST from 7 May 2006 to 7 February 2007, with a precision of ±0.2°C. Second, the National Park Service provided bihourly water temperature data for Buck Island, St. Croix from 1 January 1992 to 23 January 2007. A Ryan TempMentor 1.0 at a depth of 10 m collected these data. Third, the National Oceanographic and Atmospheric Administration's (NOAA) monitoring station at Salt River, St. Croix (http://www.coral.noaa.gov/crw/real_data.shtml), adjacent to the GW site, supplied hourly SST data from 1 January 2005 to 4 May 2006. In addition, we used the Integrated Global Ocean Services System (IGOSS) satellite-derived SST (1° × 1° grid box) to obtain weekly

Table 1. Summary of Coral Geochemical Data and Reconstructed SST[a]

Sample	Age (years B.P.)	Years (A.D.)	Growth Rate (mm a^{-1})	Sr/Ca (Mean/Amplitude) (mmol mol^{-1})	$\delta^{18}O$ (Mean/Amplitude) (‰)	Seawater Sr/Ca (mmol mol^{-1})	Growth-Dependent SST (Mean/Amplitude) (°C)	ΔIGOSS (°C)	Nongrowth-Dependent SST (Mean/Amplitude) (°C)	Δ IGOSS (°C)
BI	Modern	2002–2006	12.6	8.50/0.26	−4.7/0.9	8.46 ± 0.01	28.0/2.6	0.14/−0.72	27.9/3.3	0.02/0.06
GW	Modern	1995–2000	10.1	8.73/0.34	−4.7/1	8.48 ± 0.02	27.3/3.4	−0.14/0.57	25.5/5.0	−2.52/1.97
SC	Modern	1997–2000	8.0	8.84/0.28	−4.7/0.7	8.53 ± 0.02	27.4/3.0	−0.27/−0.29	23.5/3.7	−4.19/0.67
BER	Modern	1998–2001	2.3	9.46/0.78	–	–	24.3/8.6	0.15/0.24	15.3/10.6	−8.92/10.62
LIA	400 ± 60	5 years	5.2	8.88/0.35	−3.5/1.1	–	28.4/3.5	–	22.6/4.3	–

[a]Mean values amplitudes are calculated from annual maxima and minima following equations (1) and (2). ΔIGOSS is IGOSS SST subtracted from coral-based SST reconstructions.

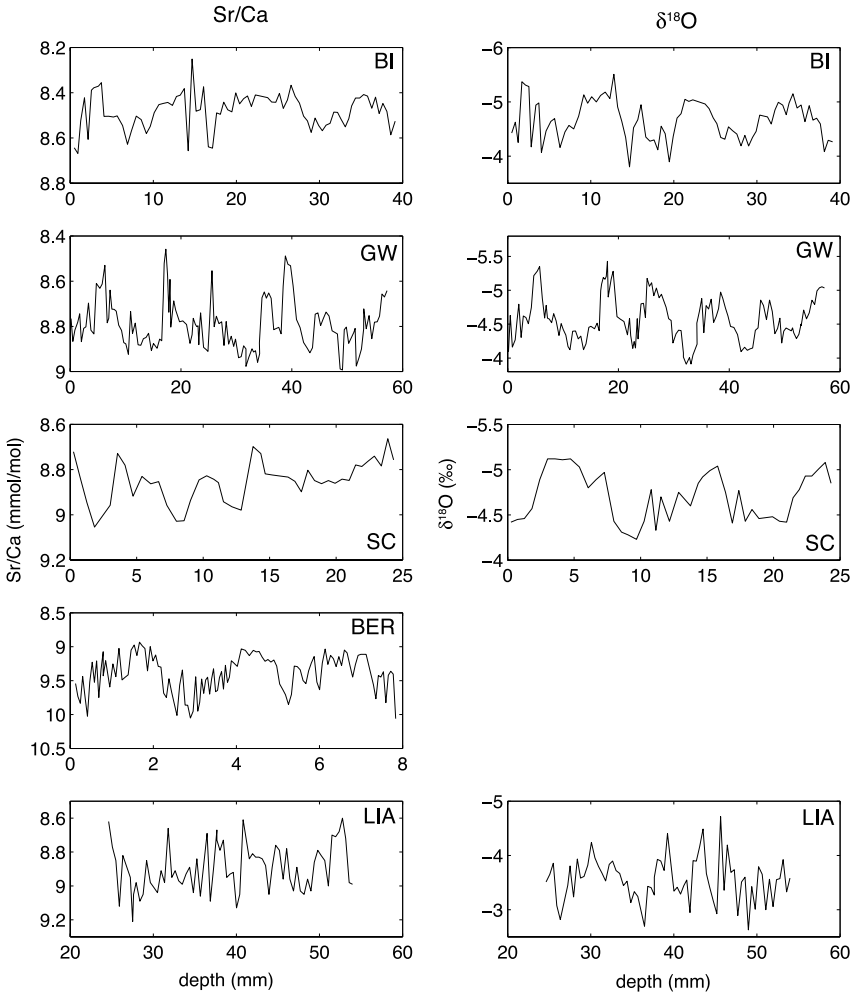

Figure 2. (left) Sr/Ca and (right) δ^{18}O data versus sampling depth in *Montastrea* from modern STX (BI, GW, SC), modern Bermuda (BER) and a Little Ice Age fossil (LIA). A slow extension rate prevented high-resolution δ^{18}O measurements of BER.

regional SST at both St. Croix and Bermuda [*Reynolds and Smith*, 1994] from 1 January 1983 to 7 February 2007.

4. Results

4.1. Instrumental SST Records

[12] In situ SST records from the three St. Croix sites were highly correlated (r^2 = 0.91–0.96) and consistent between 7 May 2006 and 7 February 2007. Maximum and minimum SSTs were within 0.25°C at all sites. Peak SC SST was ~0.25°C warmer than the average high, while minimum GW SST was ~0.25°C cooler than the average low. IGOSS SSTs were ~0.1°C cooler than our logged in situ SSTs in the summer, and ~0.1°C warmer in winter. Since intersite SST differences were negligible, and since logged SSTs were consistent with IGOSS satellite data, we constructed Sr/Ca–SST calibrations at each site using the weekly resolved IGOSS data.

4.2. Seawater Sr/Ca Ratios

[13] Seawater Sr/Ca at each site had typical ocean values [*deVilliers*, 1999], but exhibited small intersite differences. The Sr/Ca ratios of GW and BI seawater were within error: 8.46 ± 0.01 (1σ) and 8.48 ± 0.02 mmol mol^{-1}, respectively (Table 1). Site SC had a seawater Sr/Ca value of 8.53 ± 0.02 mmol mol^{-1}.

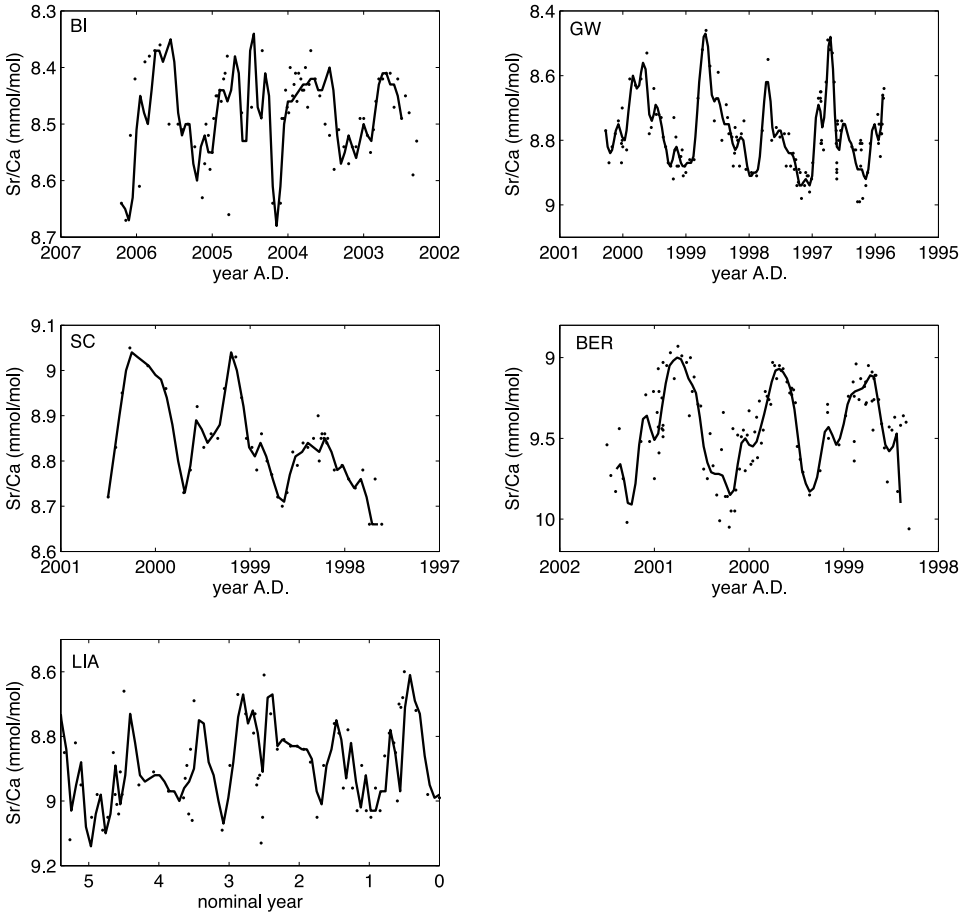

Figure 3. Unfiltered (points) and low-pass filtered (line) Sr/Ca versus age for *Montastrea* from three modern STX sites (BI, GW, and SC), Bermuda (BER), and a Little Ice Age fossil (LIA). Our age model fixes Sr/Ca maxima and minima to SST minima and maxima.

4.3. Modern Coral Extension Rate, Sr/Ca, and $\delta^{18}O_c$

[14] The mean annual extension rate of each colony was determined by measuring the distance between annual high-density bands in the x-radiographs. These measurements were independently cross-checked against the mean distance between $\delta^{18}O_c$ maxima and minima in BI, GW and SC. While variability within a colony was small (±4–7% RSD), mean annual extension rates ranged from 2.3 to 12.6 mm a^{-1} between the colonies studied (Table 1).

[15] Annual cycles were detected in coral Sr/Ca and $\delta^{18}O_c$ ratios at all sites (Figures 2 and 3). Geochemical data were assigned ages by tying Sr/Ca maxima and minima to SST minima and maxima, and linearly interpolating between tie points. The shape of the annual Sr/Ca cycles in modern corals differed from that of annual SST cycles because of intra-annual variability in skeletal extension rate. Our uniform sampling distance along the thecal wall means periods of faster extension were sampled more frequently. To avoid biasing data toward periods of higher extension rates, we compared data from each colony using the maximum and minimum values of each annual cycle rather than the entire annual data set.

[16] Annual Sr/Ca cycles were low-pass filtered to remove high-frequency variability with a periodicity of less than 60 days, such as that associated with tidal cycles [*Cohen and Sohn*, 2004]. To maintain consistency, the same Butterworth filter was applied to IGOSS SST and $\delta^{18}O_c$ data (Figure 3). The average of the three highest and three lowest values in each annual cycle was used to represent the annual maximum and minimum $\delta^{18}O_c$, and Sr/Ca ratio for each colony, as well as the relevant IGOSS SST. Mean Sr/Ca and $\delta^{18}O_c$ were then calculated as follows:

$$(\Sigma \max + \Sigma \min)/(n_{\max} + n_{\min}) \quad (1)$$

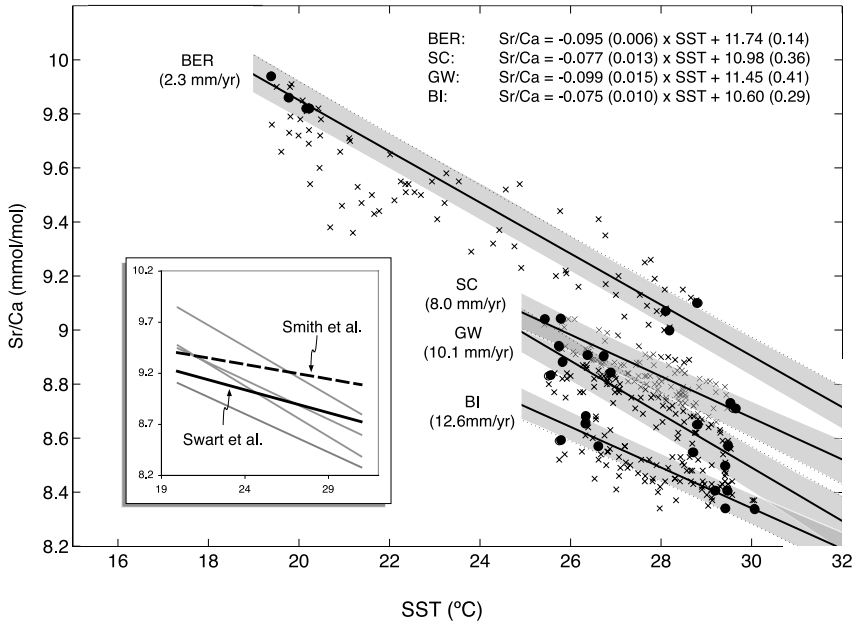

Figure 4. Sr/Ca–SST regressions from maxima and minima of filtered BI, GW, SC, and BER data (circles). All filtered data (crosses) are shown for comparison. Regressions exhibit systematic offsets toward higher Sr/Ca with slower mean annual extension rates. Shaded regions indicate standard error of reconstructed SST at the 95% confidence interval. (inset) Sr/Ca–SST regressions from this study (gray lines) differ from *Montastrea* Sr/Ca–SST calibrations of *Swart et al.* [2002] (black line) and *Smith et al.* [2006] (dashed line). See section 5.1.

The amplitude of Sr/Ca and $\delta^{18}O_c$ annual cycles was calculated as follows:

$$(\Sigma \max / n_{\max}) - (\Sigma \min / n_{\min}) \quad (2)$$

In both equations (1) and (2) max and min are the values of each coral's maxima and minima, and $n_{\max}$ and $n_{\min}$ are counts of the number of maxima and minima for a given coral.

[17] Mean Sr/Ca ratios exhibited an inverse correlation with mean annual extension rates. The mean Sr/Ca ratio of BI, growing at 12.6 mm a^{-1}, was 8.50 mmol mol^{-1}, while the mean Sr/Ca ratio of BER, growing at 2.3 mm a^{-1}, was 9.46 mmol mol^{-1} (Table 1). No relationship was found between extension rates and coral $\delta^{18}O_c$ in the St Croix corals over their growth rate range of 8.0–12.6 mm a^{-1}.

4.4. Sr/Ca–SST Calibration

[18] Sr/Ca–SST calibrations were generated for each of the four corals by linearly regressing Sr/Ca maxima and minima against IGOSS SST minima and maxima (Figure 4). We did not adjust coralline Sr/Ca ratios for the slight differences in seawater Sr/Ca between sites. Regression slopes were subparallel, but *y* intercepts were systematically offset from one another over the range of typical coral Sr/Ca ratios and Caribbean SSTs. These offsets were equivalent to a SST difference of over 6°C at a Sr/Ca value of 8.8 mmol mol^{-1}. Similar offsets were evident in unfiltered Sr/Ca–SST calibrations indicating the observed offsets were not an artifact of filtering.

[19] We used multiple linear regression to describe SST in terms of both Sr/Ca and mean annual extension rate. Data from three of the four corals analyzed (BI, GW and BER) were used to construct the regression. The best fit using this approach was:

$$\begin{aligned} \mathrm{Sr/Ca}\left(\mathrm{mmol\,mol^{-1}}\right) = {} & 11.82(\pm 0.13) - 0.058(\pm 0.004) \\ & \times \mathrm{ext} - 0.092(\pm 0.005) \\ & \times \mathrm{SST}(^{\circ}\mathrm{C}) \end{aligned} \quad (3)$$

where ext is the mean annual extension rate in mm a^{-1}. The error estimate on SST calculated from equation (3) is ±1.4°C at the 95% confidence interval using typical error propagation methods [*Bevington*, 1969].

[20] We used data from the fourth coral (SC) to assess the accuracy of our growth-dependent calibration. The mean and amplitude of SSTs derived from SC Sr/Ca ratios using equation (3) were both within 0.3°C of observed IGOSS values. SST maxima derived from SC were 0.4°C cooler than IGOSS, while minima were cooler by 0.1°C. These differences were all well within the ±1.4°C error for SSTs reconstructed from equation (3).

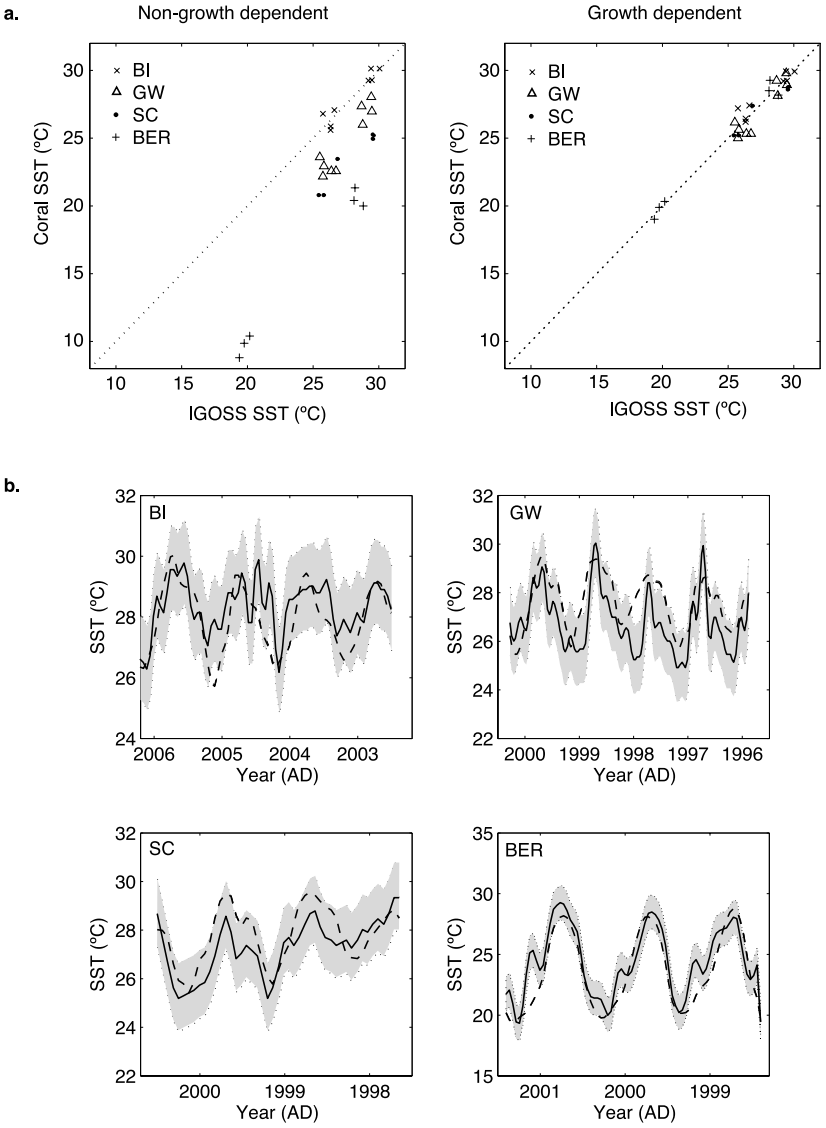

Figure 5. (a) Coral-derived SST versus IGOSS SST for growth-dependent and nongrowth-dependent calibrations. (left) Nongrowth-dependent SST estimates apply the BI calibration to annual Sr/Ca maxima and minima from BI (crosses), GW (triangles), SC (points), and BER (plus signs). (right) Growth-dependent SST estimates apply equation (3) to the same Sr/Ca maxima and minima data. Growth-dependent SSTs fall significantly closer to the 1:1 line than nongrowth-dependent SSTs, which can underestimate SST by over 9°C at slow growth rates. (b) Comparison of coral-derived SST from equation (3) (solid line) with IGOSS SST (dashed line) over the period of coral growth. Shaded areas indicate the standard error of reconstructed SST at the 95% confidence interval.

[21] Application of equation (3) to the Sr/Ca maxima and minima of all four corals accurately captured IGOSS SST maxima and minima using a single equation (Figure 5). The difference between coral-derived mean SST and IGOSS mean SST ranged from −0.14° to 0.15°C for the three corals used in the calibration, and was −0.27°C for the verification coral. SST time series, derived by applying equation (3) to all Sr/Ca data for each coral, were also in good agreement with IGOSS SST (Figure 5b). A calibration constructed from BI, SC and BER yielded a similarly

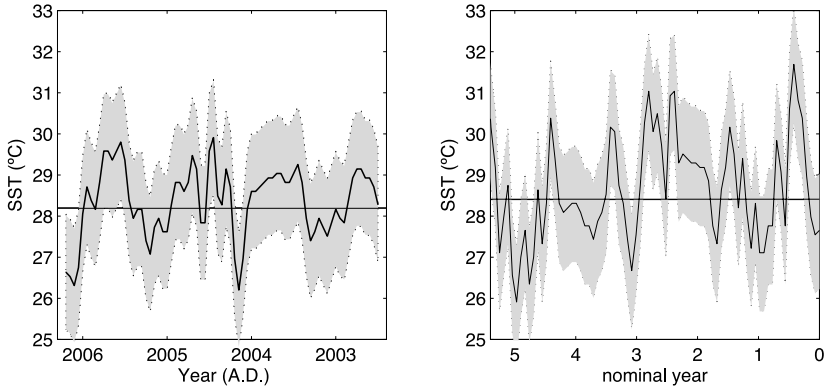

Figure 6. Coral-derived SST for BI (2003–2006 A.D.) and LIA (400 years B.P.) estimated from equation (3). BI is the modern site closest to the LIA drill core and is used to represent modern conditions. Shaded areas indicate the standard error of reconstructed SST at the 95% confidence interval.

good verification of GW. Including BI and BER in the calibration was required to accurately reconstruct SST in all four corals.

[22] We also derived SST from the Sr/Ca maxima and minima of each coral using a conventional nongrowth-dependent calibration based on the Sr/Ca–SST relationship derived from the BI coral. Excluding extension rate resulted in SST estimates as much as 9.0°C cooler than the observed IGOSS SST (Figure 5a). SC SST maxima derived from the nongrowth-dependent calibration were on average 4.0°C cooler than observed SST, while minima were on average 4.4°C cooler.

4.5. Little Ice Age

[23] The mean annual extension rate of the LIA *Montastrea* was 5.2 mm a^{-1}, based on x-radiograph gray scale analysis. The specimen exhibited no evidence of diagenetic alteration. Visual inspection of petrographic thin sections using transmitted light microscopy indicated that the LIA coral's centers of calcification were intact and that skeletal pore spaces were free of secondary aragonite.

[24] Mean SST derived from the LIA coral Sr/Ca ratios using our growth-dependent calibration was 28.4°C, with a seasonal amplitude of 3.5°C (Figure 6 and Table 1). In contrast, application of the conventional nongrowth-dependent Sr/Ca–SST calibration to LIA Sr/Ca yielded a mean SST of 22.6°C with a seasonal amplitude of 4.3°C. The modern coral BI was collected adjacent to the LIA drill site, and we used BI-derived SSTs to compare LIA reconstructions with the modern. Mean LIA SST derived from the growth-dependent calibration was within error of SST derived from the modern BI coral (28.0°C) using the same calibration. Conversely, mean LIA SST calculated using the nongrowth-dependent Sr/Ca–SST calibration was 5.3°C cooler than the modern BI coral.

5. Discussion

5.1. Sources of Sr/Ca Offsets

[25] The differences we observe between Sr/Ca–SST regressions derived for different *Montastrea* colonies indicate that *Montastrea* Sr/Ca ratios are not solely a function of SST. The observed offsets cannot be explained by local

Table 2. Proportion of Seasonal Coral Sr/Ca Variability Explained by Intersite SST and Seawater Sr/Ca Variations[a]

Sample	ΔCoral Sr/Ca$_{min}$ (mmol mol^{-1})	ΔSST (°C)	ΔSr/Ca$_{SST}$ (mmol mol^{-1})	ΔSr/Ca$_{sw}$ (mmol mol^{-1})	Total (mmol mol^{-1})	ΔCoral Sr/Ca$_{min}$ (%)
			Summer			
GW	0.14	0	0	0.02	0.02	14.3
SC	0.32	0.25	−0.02	0.07	0.05	14.7
			Winter			
GW	0.24	−0.25	0.02	0.02	0.04	17.9
SC	0.33	0	0	0.07	0.07	21.2

[a]Deltas (Δ) represent the difference in each parameter relative to that parameter at BI. Summer values compare mean minimum coral Sr/Ca with maximum SST measured by in situ SST loggers at each site. Winter values compare mean maximum coral Sr/Ca with minimum SST. Seawater Sr/Ca was not measured through a full annual cycle, and the same intersite differences (ΔSr/Ca$_{sw}$) are used in summer and winter. The difference in coral Sr/Ca expected from intersite SST differences (ΔSr/Ca$_{SST}$) assumes a sensitivity of −0.09 mmol mol^{-1} °C^{-1}. ΔSr/Ca$_{sw}$ and ΔSr/Ca$_{SST}$ were added to estimate the total coral Sr/Ca variability expected from intersite SST and seawater Sr/Ca variations. Total values were ~14–21% of the intersite Sr/Ca variations observed in corals (Δcoral Sr/Ca).

intersite variations in SST or seawater Sr/Ca. Assuming a Sr/Ca–SST sensitivity of −0.09 mmol mol^{-1} °C^{-1}, the differences in SST and seawater Sr/Ca ratios we measured between sites can account for no more than 22% of the observed variability in coral Sr/Ca among BI, GW and SC (Table 2).

[26] Two recent *Montastrea spp.* Sr/Ca–SST calibrations [*Swart et al.*, 2002; *Smith et al.*, 2006] have less negative slopes than those suggested by our data that may be caused by undersampling during part of an annual cycle (Figure 4). Separately applying *Swart et al.'s* [2002] summer and winter Sr/Ca values to our equation (3) calculates a summer SST that is within error of observed IGOSS summer SST (29.6°C), while the reconstructed winter value underestimates IGOSS winter SST (23.3°C) outside of error. This may indicate peak winter Sr/Ca was not captured in that calibration despite a high sampling rate. Furthermore, *Smith et al.* [2006] sampled considerably deeper (∼1 mm) into coral skeletons to produce up to 400 μg of carbonate powder. This approach may sample multiple skeletal elements, not just the thecal wall, a possibility that is consistent with their diminished $\delta^{18}O_c$-SST sensitivity (−0.08 to −0.12‰ °C^{-1}) compared to previous studies (−0.17 to −0.24‰ °C^{-1}).

[27] Instead, differences among Sr/Ca–SST calibrations derived from different *Montastrea* colonies may be caused by processes associated with biogenic mineralization referred to as "vital effects." Other studies have reported an inverse correlation between coral growth rate and Sr/Ca ratios [*deVilliers et al.*, 1995; *Cardinal et al.*, 2001; *Goodkin et al.*, 2005], but this relationship is not straightforward and is not apparent in all species. The Sr/Ca ratios of abiogenic aragonites precipitated experimentally from seawater show a positive correlation with crystal growth rate [*Gabitov et al.*, 2006], which is opposite from what we observe in *Montastrea*. This suggests crystal extension rate per se is not the mechanism linking coral Sr/Ca ratios with skeletal extension rate. Rather, we propose that the inverse relationship between Sr/Ca and growth rate in *Montastrea* is consistent with the Rayleigh fractionation model for coral biomineralization, in which compositional variability is driven in large part by variations in the mass fraction of aragonite precipitated by the coral from a batch of calcifying fluid [*Gaetani and Cohen*, 2006; *Cohen et al.*, 2006]. In the case of Sr/Ca, the more aragonite precipitated from a batch of fluid, the lower the Sr/Ca ratio of the coral aragonite will be because the partition coefficient for Sr^{2+} between fluid and aragonite is greater than that for Ca^{2+} [*Gaetani and Cohen*, 2006]. Interpreted within this framework, the correlation between Sr/Ca and growth rate in *Montastrea* suggests a correlation between the mass fraction aragonite precipitated ("precipitation efficiency") and average annual skeletal extension rate. Intra-annual variations in "precipitation efficiency" may cause higher-frequency Sr/Ca variations, but we cannot assess these impacts without improved knowledge of growth rate variability within a year. While there is clearly a link between skeletal composition and skeletal growth rate in the *Montastrea* analyzed in this study, such a link has not been observed in many *Porites spp.* corals where intercolony differences in Sr/Ca ratios have been observed [e.g., *Felis et al.*, 2004].

[28] Nevertheless, in the case of *Montastrea,* incorporating growth rate significantly improves the predictive capabilities of our calibration and allows us to apply a single equation to corals from several sites. SST estimates derived from application of the growth-dependent calibration to the modern corals are far more accurate than those derived from application of a nongrowth-dependent calibration (Figure 5). The implication of our results for interpreting Sr/Ca ratios of fossil corals in terms of SST is seen in our estimate of LIA SSTs derived using a nongrowth-dependent calibration. A cooling of 5.3°C relative to today exceeds most estimates of tropical SST cooling during the Last Glacial Maximum [*Pflaumann et al.*, 2003; *Schmidt et al.*, 2006] and would likely have caused significant changes in coral reef fauna that are not evident in the St. Croix drill cores [*Hubbard et al.*, 2005]. Further, a depression of mean annual SST below the 24°C isotherm would limit the growth of most *Montastrea* species [*Carricart-Ganivet*, 2004].

5.2. Comparison of LIA Paleoclimate Records

[29] While our short LIA record cannot be considered representative of the spatial and temporal variability of the entire 500-year long LIA period, our results are generally consistent with geochemical evidence from foraminifera that indicate slight (<1°C) SST cooling in the Florida Straits at ∼500 years B.P. [*Lund and Curry*, 2006]. Our results are inconsistent however, with LIA cooling estimates of >2–3°C from Caribbean corals, foraminiferal assemblages and sclerosponge geochemistry [*Winter et al.*, 2000; *Watanabe et al.*, 2001; *Nyberg et al.*, 2002, *Haase-Schramm et al.*, 2003, 2005]. *Winter et al.* [2000] interpreted coral $\delta^{18}O_c$ as a SST proxy although it is a function of both SST and $\delta^{18}O_{sw}$, and the 3°C LIA cooling estimate may reflect a small or negligible cooling accompanied by a large $\delta^{18}O_{sw}$ anomaly. If the $\delta^{18}O_c$ measured in our St. Croix corals is interpreted solely in terms of temperature (using equation (2) of *Watanabe et al.* [2001]), we calculate a similarly large LIA cooling of ∼5°C. Rather than measuring Sr/Ca, *Watanabe et al.* [2001] analyzed coral Mg/Ca ratios to estimate LIA SSTs. However, recent studies show that physiological processes, rather than temperature, exert the dominant influence on coral Mg/Ca ratios [*Meibom et al.*, 2006; *Gaetani and Cohen*, 2006; *Reynaud et al.*, 2007].

[30] In addition, a component of the apparent discrepancies between our LIA coral SST estimates and previous estimates based on coral and foraminifera may reflect natural variability. LIA Caribbean climate likely varied on multidecadal timescales [*Vellinga and Wu*, 2004; *Haase-Schramm et al.*, 2005], and foraminiferal Mg/Ca suggests relatively warm SSTs in the Caribbean from 400 to 500 years B.P. [*Black et al.*, 2007]. Though subject to large radiocarbon dating errors, even the 2σ age range for our LIA coral suggests it grew during a warmer LIA interval prior to the greatest cooling near 1700 A.D. [*Jones and Mann*, 2004; *Black et al.*, 2007], which may explain why we do not detect a large LIA SST change during this time.

[31] Assuming that LIA SSTs were not significantly cooler, the observed higher coral $\delta^{18}O_c$ is best explained

by higher $\delta^{18}O_{sw}$. This hint of a saltier Caribbean is consistent with evidence from a variety of other archives suggesting increased LIA aridity throughout the region because of a southerly migration of the ITCZ [*Haug et al.*, 2001; *Hodell et al.*, 2005; *Lund and Curry*, 2006]. The position of the ITCZ is sensitive to small (~0.5°C) perturbations of the Atlantic cross-equatorial SST gradient [*Chiang et al.*, 2002], suggesting that small variations in LIA SST do not preclude significant changes in the hydrologic cycle.

6. Conclusions

[32] 1. Sr/Ca ratios of *Montastrea* corals in this study are a function of both SST and mean annual colony extension rate.

[33] 2. The inverse relationship observed between growth rate and coral Sr/Ca is consistent with a biomineralization mechanism in which coral Sr/Ca is governed in large part by the mass fraction of aragonite precipitated and Rayleigh fractionation.

[34] 3. A Sr/Ca–SST calibration that incorporates coral growth rate significantly improves correlations between coral Sr/Ca ratios and instrumental SST.

[35] 4. Applying a conventional nongrowth-dependent Sr/Ca–SST calibration estimates modern SSTs that are up to 9.0°C cooler than observed, and calculates SSTs in a 5-year LIA (400 years B.P.) window that are more than 5.0°C cooler than today.

[36] 5. Application of the growth-dependent calibration yields SSTs during this 5-year LIA period that are within ±1.4°C of modern, i.e., our calibration error.

[37] 6. Higher Caribbean coral $\delta^{18}O_c$ during this 5-year LIA window suggests an increase in $\delta^{18}O_{sw}$ that is consistent with previous evidence of more arid conditions and may be explained by a southerly shift in mean ITCZ position.

[38] 7. Applying the approach presented here to existing and future *Montastrea spp.* across a wide range of annual linear extension rates may allow a single, robust calibration.

[39] **Acknowledgments.** The authors are grateful to Zandy Hillis-Starr, Liam Carr, Ian Lundgren, the University of the Virgin Islands, and the U.S. National Park Service for providing permits for coral collection and for assistance with sampling at Buck Island National Park, St. Croix. We are also grateful to the staff in the x-radiography unit at Falmouth Hospital, Massachusetts, for their time and assistance with x-raying the corals. We greatly appreciate the analytical assistance provided by Dorinda Ostermann, William Curry, Scot Birdwhistell, and Simon Thorrold. Andy Solow, Nathalie Goodkin, and Peter Huybers provided valuable insights into the statistical analysis. We thank Nancy Budd (University of Iowa) for identification of the *Montastrea* specimens to species level. The NOAA Coral Reef Early Warning System (CREWS) provided valuable SST data. This work was funded by National Science Foundation (NSF) grant OCE-0402728, the WHOI Ocean and Climate Change Institute, and an NSF Graduate Student Fellowship.

References

Bevington, P. R. (1969), Propagation of error, in *Data Reduction and Error Analysis for the Physical Sciences*, chap. 4, pp. 56–65, McGraw Hill, New York.

Black, D. E., R. C. Thunell, A. Kaplan, L. C. Peterson, and E. J. Tappa (2004), A 2000-year record of Caribbean and tropical North Atlantic hydrographic variability, *Paleoceanography*, *19*, PA2022, doi:10.1029/2003PA000982.

Black, D. E., R. C. Abahazi, R. C. Thunell, A. Kaplan, E. J. Tappa, and L. C. Peterson (2007), An 8-century tropical Atlantic SST record from the Cariaco Basin: Baseline variability, twentieth-century warming, and Atlantic hurricane frequency, *Paleoceanography*, *22*, PA4204, doi:10.1029/2007PA001427.

Cardinal, D., B. Hamelin, E. Bard, and J. Pätzold (2001), Sr/Ca, U/Ca and $\delta^{18}O$ records in recent massive corals from Bermuda: Relationships with sea surface temperature, *Chem. Geol.*, *176*, 213–233, doi:10.1016/S0009-2541(00)00396-X.

Carricart-Ganivet, J. P. (2004), Sea surface temperature and the growth of the west Atlantic reef-building coral Montastrea annularis, *J. Exp. Mar. Biol. Ecol.*, *302*, 249–260, doi:10.1016/j.jembe.2003.10.015.

Chiang, J. C. H., Y. Kushnir, and A. Giannini (2002), Deconstructing Atlantic Intertropical Convergence Zone variability: Influence of the local cross-equatorial sea surface temperature gradient and remote forcing from the eastern equatorial Pacific, *J. Geophys. Res.*, *107*(D1), 4004, doi:10.1029/2000JD000307.

Cobb, K. M., C. D. Charles, H. Cheng, M. Kastner, and R. L. Edwards (2003), U/Th-dating living and young fossil corals from the central tropical Pacific, *Earth Planet. Sci. Lett.*, *210*, 91–103, doi:10.1016/S0012-821X(03)00138-9.

Cohen, A. L., and R. A. Sohn (2004), Tidal modulation of Sr/Ca ratios in a Pacific reef coral, *Geophys. Res. Lett.*, *31*, L16310, doi:10.1029/2004GL020600.

Cohen, A. L., and S. R. Thorrold (2007), Recovery of temperature records from slow-growing corals by fine scale sampling of skeletons, *Geophys. Res. Lett.*, *34*, L17706, doi:10.1029/2007GL030967.

Cohen, A. L., S. R. Smith, M. S. McCartney, and J. van Etten (2004), How brain corals record climate: An integration of skeletal structure, growth and chemistry of *Diploria labyrinthiformis* from Bermuda, *Mar. Ecol. Prog. Ser.*, *271*, 147–158, doi:10.3354/meps271147.

Cohen, A. L., G. A. Gaetani, T. Lundalv, B. H. Corliss, and R. Y. George (2006), Compositional variability in a cold-water scleractinian Lophelia pertusa: New insights into "vital effects," *Geochem. Geophys. Geosyst.*, *7*, Q12004, doi:10.1029/2006GC001354.

Cronin, T. M., G. S. Dwyer, T. Kamiya, S. Schwede, and D. A. Willard (2003), Medieval Warm Period, Little Ice Age and 20th century temperature variability from Chesapeake Bay, *Global Planet. Change*, *36*, 17–29, doi:10.1016/S0921-8181(02)00161-3.

Department of Conservation and Cultural Affairs (1986), Marine water quality measurements in Chenay Bay, 1975–1986, report, Charlotte Amalie, St. Thomas, Virgin Islands.

deVilliers, S. B. (1999), Seawater strontium and Sr/Ca variability in the Atlantic and Pacific Oceans, *Earth Planet. Sci. Lett.*, *171*, 623–634, doi:10.1016/S0012-821X(99)00174-0.

deVilliers, S., B. K. Nelson, and A. R. Chivas (1995), Biological controls on coral Sr/Ca and $\delta^{18}O$ reconstructions of sea surface temperatures, *Science*, *269*, 1247–1249, doi:10.1126/science.269.5228.1247.

Felis, T., G. Lohmann, H. Kuhnert, S. J. Lorenz, D. S. Cholz, J. Patzold, S. A. Al-Rousan, and S. M. Al-Moghrabi (2004), Increased seasonality in Middle East temperatures during the last interglacial period, *Nature*, *429*, 164–168, doi:10.1038/nature02546.

Gabitov, R. I., A. L. Cohen, G. A. Gaetani, M. Holcomb, and E. B. Watson (2006), The impact of crystal growth rate on element ratios in aragonite: An experimental approach to understanding vital effects, *Geochim. Cosmochim. Acta*, *70*(18), A187–A220, doi:10.1016/j.gca.2006.06.377.

Gaetani, G. A., and A. L. Cohen (2006), Element partitioning during precipitation of aragonite from seawater: A framework for understanding paleoproxies, *Geochim. Cosmochim. Acta*, *70*, 4617–4634, doi:10.1016/j.gca.2006.07.008.

Goodkin, N. F., K. A. Hughen, A. L. Cohen, and S. R. Smith (2005), Record of Little Ice Age sea surface temperatures at Bermuda using a growth-dependent calibration of coral Sr/Ca, *Paleoceanography*, *20*, PA4016, doi:10.1029/2005PA001140.

Haase-Schramm, A., F. Böhm, A. Eisenhauer, W.-C. Dullo, M. M. Joachimski, B. Hansen, and J. Reitner (2003), Sr/Ca ratios and oxygen isotopes from sclerosponges: Temperature history of the Caribbean mixed layer and thermocline during the Little Ice Age, *Paleoceanography*, *18*(3), 1073, doi:10.1029/2002PA000830.

Haase-Schramm, A., F. Bohm, A. Eisenhauer, D. Garbe-Schonberg, W. C. Dullo, and J. Reitner (2005), Annual to interannual temperature variability in the Caribbean during the Maunder sunspot minimum, *Paleoceanography*, *20*, PA4015, doi:10.1029/2005PA001137.

Haug, G. H., K. A. Hughen, D. M. Sigman, L. C. Peterson, and U. Rohl (2001), Southward mi-

gration of the intertropical convergence zone through the Holocene, *Science*, *293*, 1304–1308, doi:10.1126/science.1059725.

Hendy, E. J., M. K. Gagan, C. A. Alibert, M. T. McCulloch, J. M. Lough, and P. J. Isdale (2002), Abrupt decrease in tropical Pacific Sea surface salinity at end of Little Ice Age, *Science*, *295*, 1511–1514, doi:10.1126/science.1067693.

Hernandez-Guerra, A., and T. M. Joyce (2000), Water masses and circulation in the surface layers of the Caribbean at 66°W, *Geophys. Res. Lett.*, *27*, 3497–3500, doi:10.1029/1999GL011230.

Hodell, D. A., M. Brenner, J. H. Curtis, R. Medina-Gonzalez, E. I. C. Can, A. Albornaz-Pat, and T. P. Guilderson (2005), Climate change on the Yucatan Peninsula during the Little Ice Age, *Quat. Res.*, *63*, 109–121, doi:10.1016/j.yqres.2004.11.004.

Hubbard, D. K., H. Zankl, I. Van Heerden, and I. P. Gill (2005), Holocene reef development along the northeastern St. Croix shelf, Buck Island, Virgin Islands, U.S., *J. Sediment. Res.*, *75*, 97–113, doi:10.2110/jsr.2005.009.

Hughen, K. A., et al. (2004), Marine radiocarbon age calibration, 26–0 ka BP, *Radiocarbon*, *46*, 1059–1086.

Jones, P. D., and M. E. Mann (2004), Climate over past millennia, *Rev. Geophys.*, *42*, RG2002, doi:10.1029/2003RG000143.

Leder, J. J., P. K. Swart, A. M. Szmant, and R. E. Dodge (1996), The origin of variations in the isotopic record of scleractinian corals. 1. Oxygen, *Geochim. Cosmochim. Acta*, *60*, 2857–2870, doi:10.1016/0016-7037(96)00118-4.

Lough, J. M. (2004), A strategy to improve the contribution of coral data to high-resolution paleoclimatology, *Palaeogeogr. Palaeoclimatol. Palaeoecol.*, *204*, 115–143.

Lund, D. C., and W. Curry (2006), Florida Current surface temperature and salinity variability during the last millennium, *Paleoceanography*, *21*, PA2009, doi:10.1029/2005PA001218.

Meibom, A., et al. (2006), Vital effects in coral skeletal composition display strict three-dimensional control, *Geophys. Res. Lett.*, *33*, L11608, doi:10.1029/2006GL025968.

Mohiuddin, M. M., A. Nishimura, Y. Tanaka, and A. Shimamoto (2004), Seasonality of biogenic particle and planktonic foraminifera fluxes: Response to hydrographic variability in the Kuroshio Extension, northwestern Pacific Ocean, *Deep Sea Res., Part I*, *51*, 1659–1683.

National Research Council (2006), *Surface Temperature Reconstructions for the Last 2,000 Years*, 196 pp., Natl. Acad. Press, Washington, D.C.

Nyberg, J., B. A. Malmgren, A. Kuijpers, and A. Winter (2002), A centennial-scale variability of tropical North Atlantic surface hydrography during the late Holocene, *Palaeogeogr. Palaeoclimatol. Palaeoecol.*, *183*, 25–41, doi:10.1016/S0031-0182(01)00446-1.

Ostermann, D. R., and W. B. Curry (2000), Calibration of stable isotopic data: An enriched $\delta^{18}O$ standard used for source gas mixing detection and correction, *Paleoceanography*, *15*, 353–360, doi:10.1029/1999PA000411.

Pflaumann, U., et al. (2003), Glacial North Atlantic: Sea-surface conditions reconstructed by GLAMAP 2000, *Paleoceanography*, *18*(3), 1065, doi:10.1029/2002PA000774.

Reynaud, S., C. Ferrier-Pages, A. Meibom, S. Mostefaoui, R. Mortlock, R. Fairbanks, and D. Allemand (2007), Light and temperature effects on Sr/Ca and Mg/Ca ratios in the scleractinian coral Acropora sp., *Geochim. Cosmochim. Acta*, *71*, 354–362, doi:10.1016/j.gca.2006.09.009.

Reynolds, R. W., and T. M. Smith (1994), Improved global sea surface temperature analyses using optimum interpolation, *J. Clim.*, *7*, 929–948, doi:10.1175/1520-0442(1994)007<0929:IGSSTA>2.0.CO;2.

Rosenthal, Y., M. P. Field, and R. M. Sherrell (1999), Precise determination of element/calcium ratios in calcareous samples using sector field inductively coupled plasma mass spectrometry, *Anal. Chem.*, *71*, 3248–3253, doi:10.1021/ac981410x.

Schmidt, M. W., M. J. Vautravers, and H. J. Spero (2006), Western Caribbean sea surface temperatures during the late Quaternary, *Geochem. Geophys. Geosyst.*, *7*, Q02P10, doi:10.1029/2005GC000957.

Smith, J. M., T. M. Quinn, K. P. Helmle, and R. B. Halley (2006), Reproducibility of geochemical and climatic signals in the Atlantic coral Montastraea faveolata, *Paleoceanography*, *21*, PA1010, doi:10.1029/2005PA001187.

Swart, P. K., H. Elderfield, and M. J. Greaves (2002), A high-resolution calibration of Sr/Ca thermometry using the Caribbean coral *Montastraea annularis*, *Geochem. Geophys. Geosyst.*, *3*(11), 8402, doi:10.1029/2002GC000306.

Thunell, R. C., and L. A. Reynolds (1984), Sedimentation of planktonic foraminifera: Seasonal changes in species flux in the Panama Basin, *Micropaleontology*, *30*, 243–262, doi:10.2307/1485688.

Vellinga, M., and P. L. Wu (2004), Low-latitude freshwater influence on centennial variability of the Atlantic thermohaline circulation, *J. Clim.*, *17*, 4498–4511, doi:10.1175/3219.1.

Watanabe, T., A. Winter, and T. Oba (2001), Seasonal changes in sea surface temperature and salinity during the Little Ice Age in the Caribbean Sea deduced from Mg/Ca and $^{18}O/^{16}O$ ratios in corals, *Mar. Geol.*, *173*, 21–35, doi:10.1016/S0025-3227(00)00166-3.

Weil, E., and N. Knowlton (1994), A multi-character analysis of the Caribbean coral *Montastraea annularis* (Ellis and Solander, 1786) and its two sibling species, *M. faveolata* (Ellis and Solander, 1786) and *M. franksi* (Gregory, 1895), *Bull. Mar. Sci.*, *55*, 151–175.

Winter, A., H. Ishioroshi, T. Watanabe, T. Oba, and J. Christy (2000), Caribbean sea surface temperatures: Two-to-three degrees cooler than present during the Little Ice Age, *Geophys. Res. Lett.*, *27*, 3365–3368, doi:10.1029/2000GL011426.

Yoo, J.-M., and J. A. Carton (1990), Annual and interannual variation of the freshwater budget in the tropical Atlantic Ocean and the Caribbean Sea, *J. Phys. Oceanogr.*, *20*, 831–845, doi:10.1175/1520-0485(1990)020<0831:AAIVOT>2.0.CO;2.

A. L. Cohen and D. W. Oppo, Department of Geology and Geophysics, Woods Hole Oceanographic Institution, Woods Hole, MA 02543, USA.

D. Hubbard, Department of Geology, Oberlin College, Oberlin, OH 44074, USA.

C. Saenger, MIT/WHOI Joint Program in Oceanography, Woods Hole Oceanographic Institution, Woods Hole, MA 02139, USA. (csaenger@mit.edu)

Chapter 3:

Surface-temperature trends and variability in the low-latitude North Atlantic since 1552

Saenger, C., A. L. Cohen, D. W. Oppo, R. B. Halley, and J. E. Carilli, 2009a: Surface temperature trends and variability in the low-latitude North Atlantic since 1552. *Nature Geoscience*, **2**, 492-495. doi: 10.1038/NGEO552

Abstract

Sea surface temperature variability in the North Atlantic Ocean recorded since about 1850 has been ascribed to a natural multidecadal oscillation superimposed on a background warming trend. It has been suggested that the multidecadal variability may be a persistent feature, raising the possibility that the associated climate impacts may be predictable. However, our understanding of the multidecadal ocean variability before the instrumental record is based on interpretations of high-latitude terrestrial proxy records. Here we present an absolutely dated and annually resolved record of sea surface temperature from the Bahamas, based on a 440-year time series of coral growth rates. The reconstruction indicates that temperatures were as warm as today from about 1552 to 1570, then cooled by about 1ºC from 1650 to 1730 before warming until the present. Our estimates of background variability suggest that much of the warming since 1900 was driven by anthropogenic forcing. Interdecadal variability with a period of 15–25 years is superimposed on most of the record, but multidecadal variability becomes significant only after 1730. We conclude that the multidecadal variability in sea surface temperatures in the low-latitude western Atlantic Ocean may not be persistent, potentially making accurate decadal climate forecasts more difficult to achieve.

nature geoscience

LETTERS

PUBLISHED ONLINE: 21 JUNE 2009 | DOI: 10.1038/NGEO552

Surface-temperature trends and variability in the low-latitude North Atlantic since 1552

Casey Saenger[1]*, Anne L. Cohen[2], Delia W. Oppo[2], Robert B. Halley[3] and Jessica E. Carilli[4]

Sea surface temperature variability in the North Atlantic Ocean recorded since about 1850 has been ascribed to a natural multidecadal oscillation superimposed on a background warming trend[1–6]. It has been suggested that the multidecadal variability may be a persistent feature[6–8], raising the possibility that the associated climate impacts may be predictable[9]. However, our understanding of the multidecadal ocean variability before the instrumental record is based on interpretations of high-latitude terrestrial proxy records[7,8]. Here we present an absolutely dated and annually resolved record of sea surface temperature from the Bahamas, based on a 440-year time series of coral growth rates. The reconstruction indicates that temperatures were as warm as today from about 1552 to 1570, then cooled by about 1 °C from 1650 to 1730 before warming until the present. Our estimates of background variability suggest that much of the warming since 1900 was driven by anthropogenic forcing. Interdecadal variability with a period of 15–25 years is superimposed on most of the record, but multidecadal variability becomes significant only after 1730. We conclude that the multidecadal variability in sea surface temperatures in the low-latitude western Atlantic Ocean may not be persistent, potentially making accurate decadal climate forecasts more difficult to achieve.

Fluctuations of North Atlantic sea surface temperature (SST) on decadal–multidecadal timescales can influence hemispheric temperature and precipitation patterns[3,5], tropical Atlantic hurricane behaviour[4,5] and may mask or augment warming due to anthropogenic causes[9]. The multidecadal portion of this SST variability, commonly referred to as the Atlantic Multidecadal Oscillation (AMO), is thought to reflect, at least partially, natural internal variations in the Atlantic Meridional Overturning Circulation[6,10,11] (MOC). In contrast, the lower-frequency background component of SST variability is considered to be externally forced by variations in solar activity, volcanism, greenhouse gases and tropospheric aerosols[2,12].

Model simulations[5,6,10,11] suggest that the AMO is a persistent mode of internal ocean variability, the climatic impacts of which may be predicted decades in advance once externally forced background SST variability is removed[9]. However, neither the AMO nor long-term changes in the background SST are well characterized in the brief (~150 year) observational record. Attempts to extend the instrumental record using proxy reconstructions have relied heavily on high-latitude tree-ring records[7,8], but these non-marine proxies do not respond directly to SST variability and may have significant biases at centennial timescales[13]. Reconstructions of Atlantic SST variability based strictly on oceanographic proxies lack either the age control[14–16] or the length[17–19] needed to separate the AMO from changes in externally forced background SST (see Supplementary Fig. S1).

Here we present continuous, absolutely dated and annually resolved proxy record of Atlantic SST spanning many centuries. Using computed axial tomography (CAT) imaging, we quantified temperature-dependent variations in the annual growth of a massive *Siderastrea siderea* coral collected from the Bahamas (25.84° N, 78.62° W) in 1991. We first established the growth–SST relationship for this coral over the full instrumental record (1857–1991), and then verified this calibration by applying it to an *S. siderea* colony from Belize (17.50° N, 87.76° W). Robust correlations between coral growth and SST in several other species[17,18,20–22] have yielded valuable palaeotemperature records[17,20], but these techniques have not been applied to *S. siderea*. In this and previous studies[20], CAT imaging was especially useful because unlike conventional two-dimensional X-ray techniques, three-dimensional CAT scans can be rotated electronically during data processing to ensure analyses are carried out along a coral's axis of maximum growth.

Greyscale analyses of CAT scan images revealed 440 (±1) annual high-density bands spanning 1552–1991 in the Bahamas coral and 66 bands spanning 1936–2001 in the Belize specimen (see Supplementary Fig. S2). We used the distance between successive high-density bands to calculate the annual upward growth of each coral. Annual growth rates, which ranged from 0.11–0.38 cm yr^{-1} in the Bahamas coral and 0.19–0.36 cm yr^{-1} in the Belize specimen, showed an inverse correlation with instrumental SST (Fig. 1a–c)[23]. Coral growth and observed annual average SST anomalies were significantly coherent (95%) at periods longer than ~6 years (see Supplementary Fig. S3). We calibrated coral growth rate anomalies against observed 1857–1991 Bahamas SST anomalies ($r = -0.67$, $p = 0.024$, $N_{effective} = 25$; Fig. 1a, see the Methods section). SST explains 45% of the variance in coral growth on 6-year timescales, and 78% of the variance on multidecadal (>30 year) timescales ($r = -0.88$, $p < 0.001$, $N_{effective} = 16$). Although it is well established that environmental parameters other than SST influence coral growth, we find SST to be the dominant forcing on the timescales of interest to this study, consistent with ref. 21. Furthermore, Belize SST anomalies reconstructed using our Bahamas coral calibration also correspond well with observations ($r = 0.70$, $p = 0.002$, $N_{effective} = 36$), capturing both the timing and amplitude of major SST excursions (Fig. 1c)[23].

Coral-based Bahamas SST anomalies show mild conditions from 1870–1900 and 1940–1960 separated by two decades of cooler SSTs from 1900–1920 (Fig. 1c). These multidecadal trends are significantly coherent (95%) with instrumental SST and the AMO index at periods longer than 6 years (Fig. 1d, see Supplementary Figs S3, S4). However, Bahamas SST anomalies did not cool markedly during the

[1]Massachusetts Institute of Technology and Woods Hole Oceanographic Institution Joint Program in Oceanography, Woods Hole, Massachusetts 02543, USA, [2]Department of Geology and Geophysics, Woods Hole Oceanographic Institution, Woods Hole, Massachusetts 02543, USA, [3]US Geological Survey (retired) 13765 2600 Rd. Cedaredge, Colorado 81413, USA, [4]University of California San Diego, Scripps Institution of Oceanography, La Jolla, California 92093, USA. *e-mail: csaenger@mit.edu.

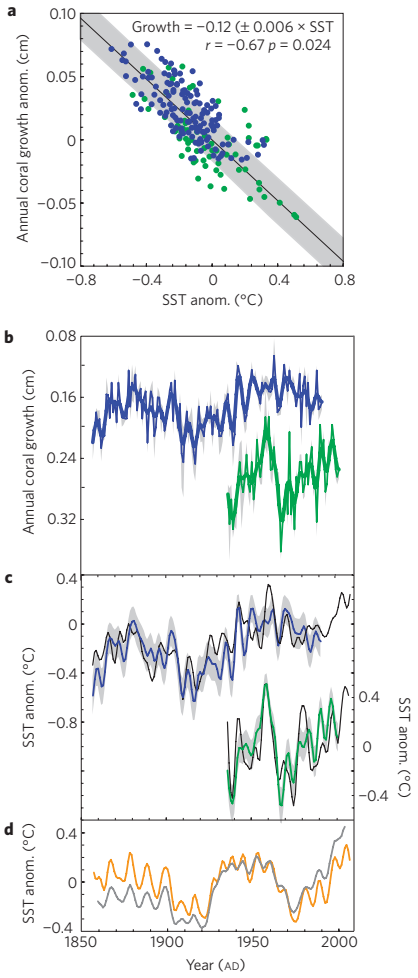

Figure 1 | Calibration and verification of the coral-based SST proxy. **a**, 1857–1991 Bahamas SST anomalies[23] regressed against Bahamas coral growth anomalies (blue). Belize coral growth anomalies and their equivalent SST anomalies (green) do not contribute to the calibration. **b**, Annual unfiltered (fine) and filtered (bold) coral growth measured from CAT scans of Bahamas (blue) and Belize (green) specimens. **c**, Coral-based SST anomalies reconstructed from Bahamas (blue) and Belize (green) corals compared with observed 1857–2008 filtered instrumental SST anomalies (black). The shading in **a**–**c** indicates 1σ standard error. **d**, The mean (grey) and linearly detrended mean (AMO; orange) SST anomalies from 0–75° N, 10–75° W.

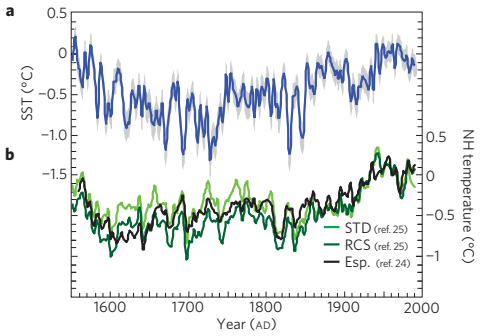

Figure 2 | Northern Hemisphere and Atlantic temperature variability since 1550. **a**, Bahamas coral-based SST anomaly and 1σ standard error (shading), estimated by applying the calibration in Fig. 1a to filtered annual coral growth rates (blue). **b**, Filtered hemispheric surface temperature anomalies from extratropical tree rings using standard curve fitting (STD; ref. 25), regional curve standardization (RCS; ref. 25) and Esper *et al.* (Esp.; ref. 24) methods.

recent negative AMO phase, indicating that regional-scale processes also influence low-latitude western Atlantic SST.

We applied our calibration to the entire record of Bahamas coral growth rate measurements to generate a continuous 440-year reconstruction of SST anomalies (Fig. 2a). Over this time period, which includes much of the Little Ice Age, Bahamas SST anomalies generally fluctuated within ~1 °C of the twentieth century mean. Our record suggests that SSTs were as warm as present from 1552 to 1570, but cooled steadily throughout the seventeenth century. Maximum cooling occurred from 1650 to 1730, and was punctuated by especially cool periods near 1672, 1694 and 1729. An ~70 year period of relatively stable warmth from ~1750 to 1830 ended with two abrupt cooling events between 1830 and 1850. A general warming trend after 1850 follows the instrumental record against which our SST reconstruction is calibrated.

Low-frequency variability in our Bahamas coral-based SST reconstruction is similar to that observed in annually resolved extratropical tree-ring-based estimates of Northern Hemisphere temperature variability (Fig. 2b)[24,25]. The major features of these hemispheric temperature reconstructions can be explained by variations in solar radiation, volcanic eruptions and the combined anthropogenic influence of greenhouse gases and tropospheric aerosols[12]. The similarities with our Bahamas record suggest the same forcings also influence low-latitude western Atlantic SST. Of note are two abrupt cold episodes in our record near 1830 and 1850 that occur ~15 years after similar volcanically driven hemispheric cool events. Although this relatively long delay suggests hemispheric and Bahamas cool episodes are unlikely to be responses to common volcanic forcings, similar abrupt events in a coral Sr/Ca record from Bermuda (see Supplementary Fig. S1c) are nearly synchronous with events in our reconstruction, suggesting that the cold excursions we observe are real features of low-latitude western Atlantic variability.

We estimate the externally forced background signal in our SST reconstruction using a multiple regression approach. To estimate the influence of individual radiative forcings, we simultaneously regressed an energy balance model's temperature response to solar, volcanic and anthropogenic variability[12] against Bahamas SST (Fig. 3a). Significant uncertainties are associated with radiative forcing estimates[26] and with applying the multiple regression approach to our single proxy record. However, because Bahamas SST is strongly correlated with low-latitude SST in other regions (see Supplementary Fig. S5), we consider this method to provide a useful approximation of externally forced SST variability across a broad region.

The results of our multiple regression approach suggest externally forced SST cooled by ~0.2 °C from ~1552 to 1600, remained cool from ~1600 to 1800 and warmed by ~0.8 °C after ~1800 (Fig. 3a). This trend, which accounts for 35% of the variance in our Bahamas SST reconstruction, is similar to lower-resolution SST reconstructions in the region that suggest a ~1 °C cooling from ~1600 to 1700 was the largest SST anomaly of the past few centuries[15,16]. Although it has been speculated that this cooling may reflect an oceanic response to reduced solar activity, a robust link has not been established owing to the relatively large chronological uncertainties inherent in lower-resolution sedimentary records[15].

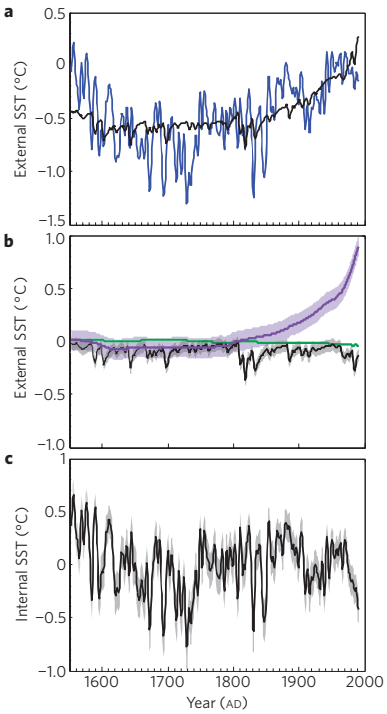

Figure 3 | Externally and internally forced SST variability a, Coral-based SST anomalies (blue) and estimated externally forced SST anomalies (black). **b**, SST variability and 1σ standard error attributed to volcanic (black), solar (green) and anthropogenic (purple) external forcings (see the Methods section). **c**, Internal SST variability (black) and standard error (1σ) calculated by subtracting the curves in **a**.

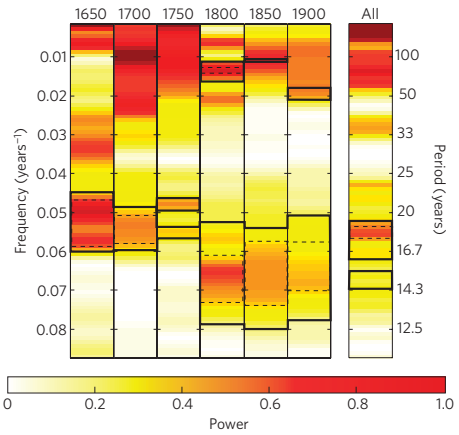

Figure 4 | Spectral analysis of internal SST variability. Spectral signature of internally driven SST variability from Fig. 3c. Spectra were calculated using the multitaper method[27] for the entire record (All) and in ~200-year bins spanning the periods 1552–1750, 1600–1800, 1650–1850, 1700-1900, 1750–1950 and 1800–1991. The centre year of each bin is shown (top). Gradients indicate the relative power at a given frequency (left *y* axis) and period (right *y* axis). Bounding boxes identify frequencies with significant power above red noise at 90% (bold) and 95% (dashed) confidence levels.

Using our absolutely dated record, we could not distinguish the effect of solar forcing from natural internal ocean variability, suggesting that it may not have been a dominant SST forcing on these timescales (Fig. 3b, c). In contrast, we did detect a significant SST response to volcanic and anthropogenic signals, the latter of which accounts for most of the warming in our coral-based SST record since ~1900.

Internal SST variations show clear multidecadal oscillations, but only back to ~1730 (Fig. 3c). In addition to the two AMO cycles inferred from the instrumental record, a third multidecadal cycle occurs from ~1740 to 1840 that is consistent with proxy evidence suggesting the AMO predates the instrumental record[7,8]. However, the longer period (100 years) and extended warm phase (70 years) of this extra cycle suggests that any multidecadal low-latitude western Atlantic SST variability is at best quasi-periodic. Before ~1730, there is little evidence for additional AMO-like oscillations, implying that multidecadal variability may not have been a persistent feature of low-latitude western Atlantic SST.

To characterize changes in the dominant periodicities of internal SST variability, we carried out multitaper method spectral analysis[27] in six overlapping ~200-year bins (Fig. 4). Bins centred on 1800, 1850 and 1900 show significant (90%) multidecadal power similar to the AMO, whereas no significant multidecadal power is evident in bins centred on 1650, 1700 and 1750. Although the absence of multidecadal variability before ~1730 may be caused by the same processes responsible for the recent divergence of observed Bahamas SST from the AMO (Fig. 1c, d), it may also reflect broad changes in multidecadal Atlantic SST variability. To the degree to which our record represents the larger North Atlantic, it suggests that if the AMO is a natural mode of internal ocean variability, it may be less persistent than previously suggested[6–8]. In contrast, interdecadal (15–25 year) internal variability is significant (>90%) throughout our record, hinting that variations on these timescales may be a more persistent feature of Atlantic SST.

Control runs of the HadCM3 coupled ocean–atmosphere global climate model show natural interdecadal to multidecadal MOC oscillations that may help explain the variability in our reconstructed SST. In the model, multidecadal oscillations are part of a coupled ocean–atmosphere process in which phase reversals rely on oceanic transport of density anomalies[10]. The model's interdecadal variability is not coupled however, but rather seems to arise from atmospherically driven oscillations of salt and heat advection into the subpolar Atlantic and Arctic oceans[11]. If the mechanisms of HadCM3 are accurate, the absence of multidecadal variability in the earliest centuries of our record may be related to a 15–25% reduction in northward Gulf Stream transport before ~1750 (ref. 28) and with a possible weakening of the MOC. We speculate that such a reduction may have diminished the effectiveness of the negative feedback responsible for multidecadal oscillations by increasing the time needed to transport low-latitude ocean density anomalies from the tropics to the subpolar Atlantic. The persistent interdecadal power in our record suggests that the atmospheric forcing potentially responsible for 15–25 year SST variability was not significantly changed by the weaker MOC. However, the mechanisms responsible for interdecadal–multidecadal SST oscillations remain poorly understood[29], and a link with multicentennial MOC vigour must be considered to be one of many possible explanations for the apparent lack of multidecadal variability before ~1730.

Methods

CAT scanning. A 9-cm-diameter coral core was split lengthwise, and one half was imaged using a Siemens Volume Zoom Spiral Computerized Tomography Scanner at the Woods Hole Oceanographic Institution. A 0.8-cm-thick by 5-cm-wide coral slab from Belize was scanned using the same method. Scans were conducted at 400 mA s and 120 kV using a 0.5 mm slice that was reconstructed at 0.2 mm. Siemens CT and eFilm software were used to identify the plane orthogonal to the coral's axis of maximum growth. We used ImageJ software to measure greyscale variations in

a 10-pixel-wide transect along parallel corallites in each image (see Supplementary Fig. S2). The lightest value of each sinusoidal annual cycle represented the location of each high-density band. The annual extension rate of each corallite was averaged for each year and is reported as a mean and standard error (1σ). Coral high-density band formation typically occurs during maximum SST and we assume annual extension represents growth between successive Augusts. Thus, data represents September (year -1) to August (year 0) of the date plotted.

Filtering. A second-order Butterworth low-pass filter with a cutoff frequency equivalent to 6 years was used to generate filtered data. This cutoff frequency was chosen on the basis of the coherence between coral extension and instrumental SST (see Supplementary Fig. S3).

Calibration and verification. Six-year filtered annual SST anomalies[23] in the $5° \times 5°$ gridbox centred on 22.5° N, 77.5° W were regressed against similarly filtered Bahamas coral growth rate anomalies for the period 1857–1991 and forced through the origin (Fig. 1a). Anomalies were calculated relative to the 1951–1980 mean, consistent with ref. 23. The effective number of samples in filtered data ($N_{\text{effective}}$) was estimated following the method of ref. 30 (pp. 261–263). Other reasonable choices for the filter cutoff frequency had a small influence on the calibration slope and do not affect our results with respect to frequency. A calibration based on SSTs in an adjacent $5° \times 5°$ gridbox centred on 27.5° N, 77.5° W yielded nearly identical results. Estimates of Belize SST anomalies were calculated by applying the calibration regression to 6-year filtered Belize coral growth anomalies. Statistical correlations of coral-based Belize SST anomalies are based on regression against 6-year filtered annual SST anomalies[23] in the $5° \times 5°$ gridbox centred on 17.5° N, 87.5° W.

Detection and attribution. Six-year filtered solar, volcanic and the sum of greenhouse gas and tropospheric aerosol radiative forcings (anthropogenic)[12] were simultaneously regressed against 6-year filtered coral-based Bahamas SST anomalies. Best-fit regression coefficients were multiplied by the original radiative forcings to estimate the SST contribution from solar, volcanic and anthropogenic influences (Fig. 3b).

The standard error (1σ) of each forcing's SST response was estimated using a Monte Carlo approach. Each year of our coral-based SST reconstruction was randomly sampled from its probability distribution. This was repeated 1,000 times to generate 1,000 SST estimates, each 440 years long. SST estimates were regressed against radiative forcings following the method above to estimate three series of SST responses to solar, volcanic and anthropogenic variability. Standard errors (1σ) were then calculated from these three series after accounting for reduced degrees of freedom[30].

The best estimate of externally forced SST was subtracted from the full Bahamas SST record (Fig. 3a) to estimate internal SST variability (Fig. 3c). We considered external signals (Fig. 3b) that were significantly different from internal variability at 95% based on a one-tailed t-test to be detectable.

Spectral analysis. The multitaper method ($p = 2$, $K = 2$; ref. 27) was applied to our estimate of internal SST variability (Fig. 3c) over the frequency range from 0 to 0.15 cycles yr^{-1}. Confidence levels were determined relative to a red noise AR(1) background.

Received 31 October 2008; accepted 21 May 2009; published online 21 June 2009

References

1. Schlesinger, M. E. & Ramankutty, N. An oscillation in the global climate system of period 65–70 years. *Nature* **367**, 723–726 (1994).
2. Andronova, N. G. & Schelsinger, M. E. Causes of global temperature changes during the 19th and 20th centuries. *Geophys. Res. Lett.* **27**, 2137–2140 (2000).
3. Enfield, D. B., Mestas-Nuñez, A. M. & Trimble, P. J. The Atlantic Multidecadal Oscillation and its relation to rainfall and river flows in the continental US. *Geophys. Res. Lett.* **28**, 2077–2080 (2001).
4. Goldenberg, S. B., Landsea, C. W., Mestas-Nuñez, A. M. & Gray, W. M. The recent increase in Atlantic hurricane activity: Causes and implications. *Science* **293**, 474–479 (2001).
5. Knight, J. R., Folland, C. K. & Scaife, A. A. Climate impacts of the Atlantic Multidecadal Oscillation. *Geophys. Res. Lett.* **33**, L17706 (2006).
6. Knight, J. R., Allan, R. J., Folland, C. K., Vellinga, M. & Mann, M. E. A signature of persistent natural thermohaline circulation cycles in observed climate. *Geophys. Res. Lett.* **32**, L20708 (2005).
7. Delworth, T. L. & Mann, M. E. Observed and simulated multidecadal variability in the Northern Hemisphere. *Clim. Dyn.* **16**, 661–676 (2000).
8. Gray, S. T., Graumlich, L. J., Betancourt, J. L. & Pederson, G. T. A tree-ring based reconstruction of the Atlantic Multidecadal Oscillation since 1567 A.D. *Geophys. Res. Lett.* **31**, L12205 (2004).
9. Latif, M., Collins, M., Pohlmann, H. & Keenlyside, N. A review of predictability studies of Atlantic sector climate on decadal timescales. *J. Clim.* **19**, 5971–5987 (2006).
10. Vellinga, M. & Wu, P. L. Low-latitude freshwater influence on centennial variability of the Atlantic thermohaline circulation. *J. Clim.* **17**, 4498–4511 (2004).
11. Dong, B. W. & Sutton, R. T. Mechanism of interdecadal thermohaline circulation variability in a coupled ocean-atmosphere GCM. *J. Clim.* **18**, 1117–1135 (2005).
12. Hegerl, G.C. *et al.* Detection of human influence on a new, validated 1500-year temperature reconstruction. *J. Clim.* **20**, 650–666 (2007).
13. D'Arrigo, R. D., Wilson, R., Liepert, B. & Cherubini, P. On the 'divergence problem' in northern forests: A review of the tree-ring evidence and possible causes. *Glob. Planet. Change* **60**, 289–205 (2008).
14. Haase-Schramm, A. *et al.* Sr/Ca ratios and oxygen isotopes from sclerosponges: Temperature history of the Caribbean mixed layer and thermocline during the Little Ice Age. *Paleoceanography* **18**, 1073 (2003).
15. Lund, D. C. & Curry, W. Florida Current surface temperature and salinity variability during the last millennium. *Paleoceanography* **21**, doi:10.1029/2005PA0011218 (2006).
16. Black, D. E. *et al.* An 8-century tropical Atlantic SST record from the Cariaco Basin. *Paleoceanography* **22**, PA4204 (2007).
17. Slowey, N. C. & Crowley, T. J. Interdecadal variability of northern hemisphere circulation recorded by Gulf of Mexico corals. *Geophys. Res. Lett.* **22**, 2345–2348 (1995).
18. Crueger, T., Kuhnert, H., Pätzold, J. & Zorita, E. Calibrations of Bermuda corals against large-scale sea surface temperature and sea level pressure pattern time series and implications for climate reconstructions. *J. Geophys. Res.* **111**, D23103 (2006).
19. Goodkin, N. F., Hughen, K. A., Curry, W. B., Doney, S. C. & Ostermann, D. R. Sea surface temperature and salinity variability at Bermuda during the end of the Little Ice Age. *Paleoceanography* **23**, PA3203 (2008).
20. Bessat, F. & Buigues, D. Two centuries of variation in coral growth in a massive *Porites* colony from Moorea (French Polynesia): A response of ocean-atmosphere variability from south central Pacific. *Palaeogeogr. Palaeoclimatol. Palaeoecol.* **175**, 381–392 (2001).
21. Lough, J. M. & Barnes, D. J. Environmental controls on growth of the massive coral *Porites*. *J. Exp. Mar. Biol. Ecol.* **245**, 225–243 (2000).
22. Carricart-Ganivet, J. P. Sea surface temperature and the growth of the West Atlantic reef-building coral *Montastrea annularis*. *J. Exp. Mar. Biol. Ecol.* **302**, 249–260 (2004).
23. Kaplan, A. *et al.* Analyses of global sea surface temperature 1856–1991. *Geophys. Res. Lett.* **103**, 18567–18589 (1998).
24. Esper, J., Cook, E. R. & Schweingruber, F. H. Low-frequency signals in long tree-ring chronologies for reconstructing past temperature variability. *Science* **295**, 2250–2253 (2002).
25. D'Arrigo, R., Wilson, R. & Jacoby, G. On the long-term context for late twentieth century warming. *J. Geophys. Res.* **111**, D03103 (2006).
26. Ammann, C. M., Joos, F., Schimel, D. S., Otto-Bliesner, B. L. & Tomas, R. A. Solar influence on climate during the past millennium: Results from transient simulations with NCAR Climate System Model. *Proc. Natl Acad. Sci. USA* **104**, 3713–3718 (2007).
27. Ghil, M. *et al.* Advanced spectral methods for climatic time series. *Rev. Geophys.* **40**, 3.1–3.41 (2002).
28. Lund, D. C., Lynch-Stieglitz, J. & Curry, W. B. Gulf Stream density structure and transport during the past millennium. *Nature* **444**, 601–604 (2006).
29. Delworth, T. L., Zhang, R. & Mann, M. E. in *Ocean Circulation: Mechanisms and Impacts* (eds Schmittner, A., Chiang, J. C. H. & Hemming, S. R.) 131–148 (American Geophysical Union, 2007).
30. Emery, W. J. & Thompson, R. E. *Data Analysis Methods in Physical Oceanography* (Elsevier, 1998).

Acknowledgements

We thank T. Crowley, P. Huybers, P. Chang, Y. Kwon, J. Woodruff, J. T. Farrar, N. Goodkin and G. Hegerl for discussion. We also thank D. Ketten and J. Arruda for CAT scan support and R. Petitt for initial growth measurements. This work was supported by the US National Science Foundation, WHOI's Ocean and Climate Change Institute, WHOI's Ocean Life Institute, award No. USA-0002, made by King Abdullah University of Science and Technology (KAUST), and the Inter-American Institute Global Change Research.

Author contributions

C.S., A.L.C. and D.W.O. designed the experiment. C.S. collected and analysed the data, and wrote the paper. C.S., A.L.C. and D.W.O. interpreted the data, discussed their implications and contributed to the manuscript. R.B.H. and J.E.C. provided sample material and manuscript comments.

Additional information

Supplementary information accompanies this paper on www.nature.com/naturegeoscience. Reprints and permissions information is available online at http://npg.nature.com/reprintsandpermissions. Correspondence and requests for materials should be addressed to C.S.

Chapter 4:

Internal variability and external forcing of Carolina Slope climate anomalies during the past 1800 years

Abstract

Western subtropical Atlantic oceanic and atmospheric circulations connect tropical and subpolar climates. Variations in these circulations can generate regional climate anomalies that are not reflected in Northern Hemisphere averages. Assessing the significance of anthropogenic climate change at regional scales requires proxy records that allow recent trends to be interpreted in the context of long-term regional variability. Here, I present a record of sea surface temperature (SST) and hydrographic variability in the western subtropical Atlantic over the past 1800 years. Magnesium/calcium (Mg/Ca) and oxygen isotopic ($\delta^{18}O$) records of planktonic foraminifera in two sediment cores suggest a steady increase in SSTs of <0.5ºC kyr^{-1} since 500 A.D. that may reflect either greater transport of warm Caribbean waters to the core site or a decrease in the frequency of seaward deflections in the Gulf Stream's path. Similar trends in other regional records support these possible mechanisms, and suggest that regional oceanic circulation near the Gulf Stream can give rise to SST variability that is distinctly different from the Northern Hemisphere mean. Multi-centennial SST variations superimposed upon millennial-scale trends may be caused by a natural, solar-forced oscillation of ocean circulation, but this cannot be verified without additional records. Comparing sedimentary SST reconstructions with a well-dated coral-based record suggests that internal variability has caused 20th century Carolina Slope SST to remain within the range of natural variability, while recent warming in regions further from the Gulf Stream may be anomalous. Carolina Slope hydrographic variability hints at an inverse correlation with tropical atmospheric circulation that may be related to enhanced moisture transport to the site during southerly migrations of the Intertropical Convergence Zone (ITCZ).

1. Introduction

Reconstructions of Northern Hemisphere surface temperature over the past two millennia provide a longer-term context in which to interpret recent climate changes. Natural low-frequency features in these records, such as the generally warm Medieval Climate Anomaly (MCA; ~700-1000 A.D.) and the generally cool Little Ice Age (LIA; ~1400-1850 A.D.), indicate that anthropogenic influences on climate are likely to be superimposed upon natural, low-frequency variations. Examining recent temperature changes on broad hemispheric scales within the context of multi-centennial variability suggests that the warming over the past few decades was likely anomalous [*Mann et al*., 2008] and anthropogenically forced [*Hegerl et al*., 2007]. However, on regional scales, sparse proxy reconstructions and a larger influence of internal climate dynamics make it difficult to assess the impacts of anthropogenic climate variability [*Goosse et al*., 2005].

Natural variations in the atmospheric and oceanic circulation of the western North Atlantic, including the Caribbean Sea and Gulf of Mexico, can strongly influence regional climate [*Enfield et al*., 2001; *Marshall et al*., 2001; *Hurrell et al*., 2003] and may alter the regional response to external radiative forcings such as anthropogenic greenhouse gases [*Lozier et al*., 2008; *Keenlyside et al*., 2008]. The Meridional Overturning Circulation (MOC) is a major component of regional ocean circulation. The shallow surface currents of this circulation carry large volumes of water [*DiNezio et al*., 2009] and heat [*Larsen,* 1992] to high latitudes, and subtle variations in its transport or path can cause significant climate anomalies [*Molinari,* 2004]. The North Atlantic Oscillation (NAO) is a leading mode of atmospheric variability in the Atlantic sector,

which influences regional climate by altering storm tracks, wind-driven circulation, surface buoyancy and deep convection [*Marshall et al., 2001*; *Visbeck et al.*, 2003]. Eddy-driven heat flux also likely influences regional climate, and may be of first-order importance in North Atlantic western boundary currents [*Wunsch*, 1999]. The brief (<150 year) instrumental record may not reflect the full range of these internal variations however, making it difficult to assess if recent anthropogenic forcing has lead to anomalous regional climate change. Determining the significance of recent climate variability in the western North Atlantic therefore requires proxy reconstructions that provide a longer record of the natural variations driven by the region's complex circulation regimes.

Here, we present an 1800-year, decadally-resolved proxy reconstruction of climate variability from the Carolina Slope region of the subtropical western Atlantic. Using variations in the magnesium/calcium (Mg/Ca) and oxygen isotopic ratios ($\delta^{18}O_c$) of the surface-dwelling foraminifera *Globigerinoides ruber* (white variety, *sensu stricto*) in two sediment cores, we explore the influence of external forcing and internal circulation on climate in the region. Our data indicate that sea surface temperature (SST) and hydrologic variations were subtle at our site in recent millennia and that these variations were strongly influenced by internal dynamics. The trends we observe suggest that complex regional processes can induce more diverse climatic responses than those suggested by Northern Hemisphere mean reconstructions.

2. Climatic setting

Data were generated from two Carolina Slope sediment cores: KNR140-2-59GGC (32.977ºN, 76.316ºW, 1205m) and CH07-98-MC22 (32.784ºN, 76.276ºW, 1895m), hereafter referred to as 59GGC and MC22 (Figure 1). Separated by ~22 km, the cores are located within a tongue of warm water on the southern flank of the Gulf Stream. The Gulf Stream is part of the larger MOC surface circulation in the region, the upstream components of which consist of transport through the Yucatan Straits to the Gulf of Mexico's Loop Current and subsequent Florida Current transport through the Florida Straits (Figure 1). Transport to our site consists of ~31 Sv (1 Sv = 1 x 10^6 m^3 s^{-1}) of Florida Current water (partitioned between surface MOC (~13 Sv) and a wind-driven (~17 Sv) components), and ~5-10 Sv from shallow southern Gulf Stream recirculation gyres [*Schmitz and Richardson*, 1991; *Schmitz and McCartney*, 1993; *Wang and Koblinsky*, 1996].

Mean annual SSTs at the 59GGC and MC22 core sites are 26.0 ± 0.3ºC (1σ) and 25.90 ± 0.3ºC (1σ), respectively, based on 0.044˚ x 0.044˚ NOAA Advanced Very-High-Resolution Radiometer (AVHRR) Pathfinder v5 data from 1982-2007 A.D. (http://www.nodc.noaa.gov/SatelliteData/pathfinder4km/). A lower mean of 24.7 ± 0.2ºC (1σ) over the same period in coarser 2º x 2º resolution NOAA Extended Reconstructed Sea Surface Temperature (ERSST) data [*Smith et al*., 2008] likely reflects the integration of cooler water masses flanking the narrow Gulf Stream. Complementary salinity timeseries are scarce, but reanalysis products and time-averaged data estimate a mean value near 36.3 psu [*Antonov et al*., 2006; *Carton and Giese*, 2008]. SST and salinity

from March-November, the months during which *G. ruber* (pink variety) may preferentially calcify [*Deuser and Ross*, 1989], show very similar trends to those of annual average data, but are systematically warmer by ~0.7ºC and fresher by ~0.04 psu.

3. Methods

3.1 Age model

The chronology for each core is based on several planktonic foraminiferal radiocarbon ages (Table 1). Assuming a standard reservoir correction of 400 years, three dates in MC22 support a constant sedimentation rate of 31 cm kyr^{-1}. However, a core-top fraction modern radiocarbon of only 97% suggests surface sediments in MC22 may not accurately capture modern conditions. Four radiocarbon ages in 59GGC suggest a constant sedimentation rate of 61 cm kyr^{-1}. A core-top age falls off this line, and has a fraction modern radiocarbon of only 95% that suggests the upper sediment layer may have been lost in the gravity coring process. A sedimentation rate of 61 cm kyr^{-1} is extrapolated through the upper 10 cm of the core to estimate a core-top age of ~1612 A.D. Based on these sedimentation rates, the average sampling interval for MC22 and 59GGC are 32 years and 16 years, respectively.

3.2 KNR140-2-59GGC

Approximately 100 *G. ruber* (white variety, *sensu stricto*) from the 212-300 μm size fraction were picked, weighed, gently crushed between glass slides and homogenized. The crushed sample was split into aliquots equivalent to ~80 and ~15

individuals for Mg/Ca and $\delta^{18}O_c$ analyses, respectively. This generally allowed two Mg/Ca and two $\delta^{18}O_c$ analyses at each depth interval. Mg/Ca samples were cleaned using the full trace metal method including clay removal, metal oxide reduction and organic matter oxidation [*Boyle and Keigwin*, 1985/6; *Rosenthal et al*., 1995].

Mg/Ca was measured at Rutgers University Inorganic Analytical Laboratory (RIAL) using a Thermo Element XR sector field inductively coupled plasma mass spectrometer (ICP-MS). The external precision of Mg/Ca analyses was ~1.1% (1σ RSD) based on repeated measurements of three consistency standards with Mg/Ca ratios between 1.2 and 7.5 mmol/mol. This is equivalent to ±0.12ºC at typical *G. ruber* ratios. Oxygen isotopes were measured at the Woods Hole Oceanographic Institution (WHOI) using a Finnigan-MAT 253 mass spectrometer with a Kiel III carbonate device. Calibration to the VPDB scale was made using the NBS-19 standard ($\delta^{18}O$ = -2.20‰), which has a reproducibility of ±0.08‰ (1σ, n=461).

3.3 CH07-98-MC22

Approximately 50 *G. ruber* (white variety, *sensu stricto*) were picked each centimeter from the 212-250 μm size fraction. Prior to crushing, samples were split into aliquots of 40 individuals for Mg/Ca and 10 individuals for $\delta^{18}O_c$ analyses. This generally allowed two $\delta^{18}O_c$ analyses at each depth interval, but only one Mg/Ca analysis. Mg/Ca samples were gently crushed and cleaned as above and were measured at WHOI using a Thermo-Finnigan Element2 sector field ICP-MS. Long-term external precision was ~1.2% (1σ RSD) based on repeated measurements of three consistency standards with

Mg/Ca ratios of 1.7, 3.3 and 5.0 mmol/mol. Stable isotope measurements were made at WHOI on uncrushed individuals following the method above.

3.4 SST and $\delta^{18}O_{sw}$ estimates

SST estimates were derived from Mg/Ca ratios using a general calibration based on a sediment trap study of ten Sargasso Sea planktonic foraminifera species: Mg/Ca (mmol/mol) = 0.38(±0.02) exp(0.09(±0.003*SST) [*Anand et al*., 2003]. SST estimates were combined with the δ^{18}O-SST relationship of *Bemis et al*. [1998] as presented by *Lynch-Stieglitz et al*., [1999] to calculate $\delta^{18}O_{sw}$. The δ^{18}O-SST equation of *Kim and O'Neil* [1997] yielded similar results.

To reduce uncertainties associated with age model errors and sedimentary smoothing when comparing records, we averaged 59GGC data in 100-year bins, which were shifted in 50-year increments such that only every other bin is independent. Because fewer replicate measurements were made at a coarser sampling resolution in MC22, its data were averaged in 200 year bins. Assuming similar analytical and calibration errors in all samples, SST and $\delta^{18}O_{sw}$ errors were estimated by calculating the standard error in each bin. This approach is reasonable for assessing relative changes, but does not consider calibration or analytical uncertainties. Assuming a Mg/Ca-SST calibration error of 0.5ºC [*Anand et al*., 2003], our measured analytical precisions and the method of *Rohling et al*. [2007] estimate absolute SST and $\delta^{18}O_{sw}$ uncertainties (1σ) of about ±0.67ºC and ±0.25‰, respectively.

4. Results

4.1 Core-top results

Applying the *Anand et al*. [2003] calibration to Mg/Ca data in the upper two centimeters of MC22, which likely represents early 20th century conditions, yields SSTs ranging from 27.3-27.7ºC, markedly warmer than the 1981-2007 A.D. climatological mean. Although a calibration specific to *G. ruber* (white variety) estimates MC22 core-top SSTs that are closer to the annual mean, the general equation we apply has significantly smaller errors on pre-exponential and exponential constants [*Anand et al*., 2003] that suggest it may be more appropriate for reconstructing relative SST changes. MC22 core-top $\delta^{18}O_{sw}$ values ranging from 0.92-1.01‰ are equivalent to salinities of 36.0-36.3 psu based on a subtropical Atlantic $\delta^{18}O_{sw}$–salinity relationship of $\delta^{18}O_{sw}$ (‰) = 0.26*salinity (psu) – 8.25 [*Schmidt et al*., 1999]. These values agree well with the 1981-2007 A.D. climatological mean.

4.2 Down core Mg/Ca and SST

Mg/Ca-based SSTs indicate subtle variability in the subtropical western Atlantic over the past two millennia (Figure 2a,b). Mean SSTs estimates of 27.26ºC and 27.31ºC in 59GGC and MC22, respectively, are similar to each other and to core-top values. Binned MC22 data show that SSTs cooled by almost 1ºC after ~200 A.D. to values ~0.5ºC colder than the long term mean around 500 A.D. This cooling, which is similar in magnitude to decadal SST variability observed in the modern, was followed by an increase of <0.5ºC kyr^{-1}in both records from 500-1600 A.D. Similar low-frequency

variability continues from 1600 A.D. to near the present in MC22. Both records also hint at synchronous multi-centennial variations with a period of ~250 years and an amplitude of ~0.5ºC. Cool intervals near 550, 900, 1200, and 1450 A.D. and warm periods near 750, 1000 and 1350 A.D. occur in both cores, while MC22 exhibits an additional warm and cool period near 1600 and 1750 A.D., respectively.

4.3 Down core $\delta^{18}O_c$

Mean values of -1.59±0.16‰ and -1.54±0.19‰ in MC22 and 59GCC, respectively indicate that $\delta^{18}O_c$ is reproduced relatively well in the two cores (Figure 2c,d). $\delta^{18}O_c$ in 59GGC decreases by ~0.5‰ from 500-800 A.D. to a relatively constant value near -1.6‰ from ~800-1400 A.D. before increasing again to -1.1‰ near the core-top. Depleted values near 800 and 1150 A.D., which are separated by relatively enriched periods around 950 and 1350 A.D., provide some evidence for multi-centennial variability. Similar multi-centennial variations during this interval are seen in MC22 $\delta^{18}O$, although the two cores show more divergent trends in the earliest and most recent intervals when age uncertainties are greater.

4.4 Down core $\delta^{18}O_{sw}$

The relatively small SST variations in both cores indicate that a significant portion of the observed $\delta^{18}O_c$ variability reflects changes in $\delta^{18}O_{sw}$. Mean $\delta^{18}O_{sw}$ of 0.86 ± 0.06‰ in MC22 is indistinguishable from a mean of 0.89 ± 0.10‰ in 59GGC (Figure 2e,f). Assuming the subtropical Atlantic $\delta^{18}O_{sw}$–salinity relationship used here is stable

through time, these mean $\delta^{18}O_{sw}$ values correspond to salinities near 35.8 psu that are fresher than modern values near 36.3 psu. During their period of overlap, both records show fresher conditions near 800 and 1150 A.D. that are separated by a more saline period centered on 950 A.D. MC22 hints at saline conditions around 1350 A.D. followed by a centennial-scale freshening in the 18th century. 59GGC suggests a more constant trend toward more saline conditions after 1150 A.D. that culminated in a sharp increase after 1500 A.D.

5. Discussion

5.1 Analytical inconsistencies and vital effects

Non-climatic factors associated with slightly different analytical protocols for MC22 and 59GGC samples may complicate the interpretation of our data. Changes in *G. ruber* Mg/Ca and $\delta^{18}O_c$ are assumed to reflect variations in SST, and SST plus $\delta^{18}O_{sw}$, respectively. However, biologically-mediated processes and/or different analytical methods may also contribute to the variability in our data. Decreasing calcification rates may lead to lower *G. ruber* $\delta^{18}O_c$ in coarser size fractions between 212-250 μm and >500 μm [*Ravelo and Fairbanks*, 1992; *Elderfield et al*. 2002]. Similar processes may explain a general increase in Mg/Ca over the same range of size fractions [*Elderfield et al*., 2002]. This suggests 59GGC specimens from the 212-300 μm size fraction may have preferentially lower $\delta^{18}O_c$ and higher Mg/Ca than those in the MC22 212-250 μm size fraction. To investigate this possibility we subtracted 59GGC $\delta^{18}O_c$ and Mg/Ca from the corresponding value in MC22 for each of their overlapping bins. No systematic offsets

were seen between the cores, and small mean differences of 3% and 0.1% for $\delta^{18}O$ and Mg/Ca, respectively, suggest differences between size fractions do not contribute significantly to our results.

Different analytical procedures between 59GGC and MC22 must also be considered. Poor reproducibility of foraminiferal Mg/Ca has been observed between laboratories, in part because of different cleaning methods [*Rosenthal et al*., 2004]. Oxygen isotopes in crushed samples may also be systematically depleted by ~0.2‰ relative to whole specimens due to isotopic exchanges associated with gas bubble formation [*Lund and Curry*, 2006]. These findings suggest that our analysis of Mg/Ca in different laboratories, and our measurement of stable isotopes on crushed samples for 59GGC, but whole samples for MC22, may bias our results. However, the exercise described above shows no large or systematic offsets between the two cores indicating these influence, if any, are minor.

5.2 SST variability

Independent *G. ruber* Mg/Ca-based SST reconstructions in the low-latitude western North Atlantic [*Lund and Curry,* 2006; *Richey et al*., 2007] provide a unique opportunity to compare our results with other regional SST estimates (Figure 3). This comparison suggests millennial-scale warming along the Carolina Slope may be a regional feature of Gulf Stream variability over the past two millennia (Figure 3). Two records from the Dry Tortugas, a region that is also sensitive to Gulf Stream variability, show a monotonic rise in SST from ~800-1800 A.D. [*Lund and Curry*, 2006] (Figure 3b).

Applying the paleotemperature calibration and averaging scheme used in our reconstruction to the Dry Tortugas record, we estimate a ~1.0ºC kyr^{-1} rise over this period that is similar to that reconstructed at the Carolina Slope.

The millennial-scale warming trend at the Dry Tortugas and Carolina Slope may reflect changes in ocean circulation that enhanced the transport of warm Caribbean water to both sites. This hypothesis is supported by recent work suggesting that wind-driven transport through the Florida Straits increased monotonically during the Holocene, including the last 2000 years [*Lynch-Stieglitz et al*., 2009]. The NAO provides one possible source for this apparent increase in transport. Observations suggest positive wind-stress curl anomalies during the positive phase of the NAO may lead to reduced Florida Current transport [*DiNezio et al*., 2009]. If a similar relationship occurs on longer timescales, more negative NAO conditions over the past millennium [*Trouet et al*., 2009] may have enhanced transport and warmed the Dry Tortugas and Carolina Slope.

Alternatively, *Lynch-Stieglitz et al*. [2009] argue their transport increase, and thus the Dry Tortugas and Carolina Slope warming, may have been caused by a southward shift of mean atmospheric circulation associated with changes in the seasonal distribution of solar radiation [*Braconnot et al*., 2007; *Haug et al*., 2001]. This possibility is consistent with evidence for monotonic cooling along the mid-Atlantic Bight [*Keigwin et al*., 2003; *Sachs*, 2007], which may reflect insolation-driven enhancement of Labrador Sea deep convection [*Renssen et al*., 2005].

A higher-resolution reconstruction of Florida Straits transport during the last millennium does not increase monotonically however, but rather suggests that transport

was reduced by about 15-25% from ~1200-1750 A.D. [*Lund et al.,* 2006]. If this reconstruction is correct, warming trends cannot simply reflect transport variations. SST variability in the region is also influenced by changes in the path of the Gulf Stream, which do not necessarily covary with transport. Seaward deflections in the path of the Gulf Stream near the Charleston Bump can influence Carolina Slope SST by altering the amount of cool South Atlantic Bight water in the region [*Bane and Dewar,* 1988; *Miller,* 1994]. Similarly, cool Tortugas eddies can persist near the Dry Tortugas for many months, leading to significant changes in SST [*Fratantoni et al.*, 1998; *Lund and Curry,* 2004, 2006]. Simulations suggest the amplitude of Florida Straits SST variability and the frequency of Gulf Stream deflection near the Carolina Slope are positively correlated and sensitive to small (~0.6ºC) anomalies [*Miller and Lee,* 1995]. If the millennial-scale warming trend near the Dry Tortugas was caused by a decrease in Tortugas eddy formation [*Lund and Curry,* 2006], this decrease may also have decreased the amplitude of Florida Straits SST variability. Subsequently, the frequency of Gulf Stream deflections near the Carolina Slope may have decreased leading to the warming we reconstruct.

Tortugas eddies form preferentially when a well-developed Loop Current penetrates deep into the Gulf of Mexico [*Fratantoni et al.*, 1998]. Although the Loop Current is influenced by vorticity input and transport in the Yucatan Straits [*Candela et al.,* 2002; *Oey et al.*, 2003], the mechanisms governing its variability remain poorly understood. We speculate that mesoscale variability in the Caribbean may have progressively inhibited the development of the Loop Current in recent millennia, leading

to an SST warming trend near the Dry Tortugas and Carolina Slope that differs from reconstructed Florida Straits transport.

Carolina Slope and Dry Tortugas SST variability differ from Northern Hemisphere trends and show no obvious MCA or LIA, consistent with the possibility that SSTs at these sites may be dominated by internal dynamics. In contrast, reconstructions from sites further away from the Gulf Stream show a distinctly different pattern of variability (Figure 3c,d). Records from the Gulf of Mexico and the Great Bahama Bank suggest that warm SSTs prior to ~1000 A.D. were followed by cooling until ~1600-1700 A.D. and warming during the past few centuries [*Lund and Curry*, 2006; *Richey et al*., 2007]. These trends are similar to the "classic" pattern of Northern Hemisphere surface temperature variability in which a warm MCA (~700-1000 A.D.) cools into the LIA (~1400-1850 A.D.) before warming throughout the 20th century [*Mann et al*., 2008] (Figure 4). *Hegerl et al*. [2007] concluded that external forcing, particularly volcanic and anthropogenic effects, could explain ~60% of this variability on the hemispheric scale. The similar trends in Northern Hemisphere, Gulf of Mexico and Great Bahama Bank temperatures suggest that these sites respond to external forcing in a similar way, with a smaller influence from internal ocean dynamics.

5.3 Comparison with a well-dated proxy record of regional SST

A 440-year coral-based SST reconstruction from the low-latitude western North Atlantic [*Saenger et al*., 2009a, Chapter 3] overlaps sedimentary Mg/Ca-based SST records in the region by many centuries and also extends into the late 20th century.

Comparing this coral-based record with Mg/Ca-based reconstructions may provide insight regarding the significance of 20th century SST trends. Although this comparison is complicated by the use of different SST proxies at different resolutions, we make the assumption that relative SST changes may be meaningful. This assumption is tenuous given that the errors of the two proxies are independent.

The coral-based SST reconstruction was averaged using the same 100-year binning scheme applied to 59GGC, and then was normalized to have the same 1600-1900 A.D. mean as MC22. We conducted the same exercise for the Great Bahama Bank records [*Lund and Curry,* 2006], which are the closest Mg/Ca-based records to the site of the coral-based reconstruction (Figure 1). Similar trends are evident between the coral-based and Mg/Ca-based SST estimates during their period of overlap at both sites (Figure 5) suggesting that our method may be reasonable.

Coral-based SST clearly warms during the 19th and 20th centuries in comparison to our Carolina Slope records, but earlier warm intervals in the region indicate that this warming may not be anomalous (Figure 5a). Although the mean coral-based SST during the 20th century is warmer than the mean of any other binned Carolina Slope interval, it is within the standard error (1σ) of the record's warm intervals. In contrast, when compared to Great Bahama Bank records, warm 20th century coral-based SSTs are outside the standard error (1σ) envelope of almost every other binned period (Figure 5b). However, these differences are unlikely to be significant when the absolute errors of SST estimates are considered. To the degree to which this coral-based record reflects variability in the larger North Atlantic, these results hint that recent warmth near the Great Bahama Bank

may be anomalous, while SSTs near the Carolina Slope may not be. This speculation is consistent with the possibility that the influence of internal variability on Carolina Slope SST may overprint or overwhelm the response to external forcing.

5.4 $\delta^{18}O_{sw}$ variability

Comparing our $\delta^{18}O_{sw}$ record with other *G. ruber*-based reconstructions in the region [*Lund and Curry,* 2006; *Richey et al*., 2007] suggests Carolina Slope hydrologic variability was also relatively small (Figure 6). Applying the subtropical $\delta^{18}O_{sw}$-salinity relationship $\delta^{18}O_{sw}$ (‰) = 0.26*salinity (psu) – 8.25 [*Schmidt et al*., 1999] to all records, we calculate a peak to peak range of 1.1-1.2 psu at the Carolina Slope that is close to the 1.2-1.5 psu estimated at the Great Bahama Bank. Salinity estimates from the Dry Tortugas and Pigmy Basin show larger ranges of 1.7-1.8 psu and 2.1 psu.

Dry Tortugas and Great Bahama Bank $\delta^{18}O_{sw}$ trends may reflect the northward advection of Tropical Atlantic salinity anomalies. *Lund and Curry* [2006] suggest southerly migrations of the Intertropical Convergence Zone (ITCZ), possibly due to reduced solar activity, might generate positive tropical Atlantic salinity anomalies that could be transported northward in surface circulations. Carolina Slope $\delta^{18}O_{sw}$ covaries with a proxy for ITCZ migrations [*Haug et al*., 2001], but in the opposite sense as the Florida Straits (Figure 7). This argues against a simple advective mechanism linking the sites. Climate model simulations show southerly ITCZ migrations forced by North Atlantic cooling are often accompanied by increased Carolina Slope precipitation [*Knight et al*., 2006; *Saenger et al*., 2009b, Chapter 5]. These simulations also show enhanced

southwesterly winds near the Carolina Slope, hinting that enhanced export of moisture from the Caribbean and Gulf of Mexico during southerly ITCZ displacements may explain the inverse relationship between $\delta^{18}O_{sw}$ and the ITCZ.

5.5 Pacific Interactions

Variations in tropical Pacific circulation related to the El Niño-Southern Oscillation (ENSO) can have global climatic impacts [*Cane*, 2005]. More evenly distributed heat in the eastern tropical Pacific during El Niño-like conditions may significantly impact the low-latitude Atlantic by shifting the ITCZ southward [*Newton et al*., 2006]. Conversely, La Niña-like conditions displace the SST maximum northward, leading to a more northerly ITCZ. If the inverse relationship between ITCZ displacements and Carolina Slope $\delta^{18}O_{sw}$ is correct, we would expect wetter conditions during more El Niño-like periods. Evidence for El Niño-like conditions from ~1000-1500 A.D., and less El Niño-like periods from ~500-1000 A.D. and ~1500-1900 A.D. [*Moy et al*., 2002; *Conroy et al*., 2009] coincide with a shift toward wetter conditions in 59GGC from 800-1500 A.D. supporting a possible ENSO influence (Figure 7b). Although this possibility may help explain some of the discrepancies between 59GGC and MC22, it seems unlikely for the two records to show such disparate responses to common forcings and their differences may simply reflect the errors of the method.

5.6 Centennial-scale variability

Multi-taper method spectral analysis (resolution = 2; tapers = 3) shows a significant (95%) spectral peak in 59GGC SST at ~225 years that is not an artifact of our binning scheme. Enhanced power at the same frequency occurs in MC22, but it is not significant, possibly because of the core's lower sampling resolution. Although higher frequency SST variability in our reconstructions must be interpreted cautiously, if centennial-scale oscillations are a real feature of Carolina Slope SST variability, they may be related to solar-induced MOC changes. Using an atmosphere-ocean model of intermediate complexity, *Weber et al*. [2004] found solar forcing could excite an internal mode of ocean circulation with a period of 200-250 years that was determined by the transit time of density anomalies within the MOC. Assuming SST anomalies advected from the Florida Straits are an important driver of Carolina Slope variability on multi-centennial timescales, similar centennial oscillations would be expected, but are not apparent, in the Dry Tortugas records. Although this may be a consequence of lower Dry Tortugas sedimentation rates (25-31 cm kyr^{-1}), another possibility is that mesoscale processes dominate multi-centennial SST variability near the Dry Tortugas, but are less influential along the Carolina Slope.

5.7 Salinity effects on Mg/Ca

Although Mg/Ca-based SSTs are reproduced well between 59GGC and MC22, their absolute value is too warm. Culturing experiments [*Kisakurek et al*., 2008] and core-top transects [*Ferguson et al*., 2008; *Arbuszewski et al*., 2009] indicate that elevated

salinities may increase Mg/Ca incorporation into *G. ruber* Mg/Ca at our subtropical site. Because the *Anand et al*. [2003] calibration does not account for salinity, we test this possibility by applying a calibration that describes *G. ruber* Mg/Ca as a function of SST and salinity [*Kisakurek et al*., 2008].

Combining the Mg/Ca-SST and Mg/Ca-salinity calibrations of *Kisakurek et al*. [2008] with the *Bemis et al*. [1998] and $\delta^{18}O_{sw}$-salinity relationships described above, we simultaneously solved for the SST and salinity values that minimize the residual between predicted and measured Mg/Ca and $\delta^{18}O_c$ (Figure 8a). The calculated MC22 core-top SSTs of 25.5-26.1ºC agree well with observations (Figure 8b). Salinity values of 34.7-34.9 psu are too fresh, but variability is smaller and possibly more realistic. If Carolina Slope salinity variability is more closely approximated by a thermocline relationship ($\delta^{18}O_{sw}$ = 0.50 * salinity - 17), as suggested by *Lund and Curry* [2006], we calculate slightly cooler and saltier MC22 core-top values of 25.3-25.7ºC and 35.2-35.1 psu, respectively. In either case, this exercise suggests that if salinity affects Mg/Ca, it does not significantly change the major trends we observe. We conclude that our interpretation of the data, particularly with respect to relative changes, remains valid.

6. Conclusions

Reconstructed Carolina Slope SST and $\delta^{18}O_{sw}$ over the past two millennia show small variations that do not follow larger Northern Hemisphere temperature trends. Similarities with equivalent proxy reconstructions from the Dry Tortugas suggests changes in Gulf Stream temperature, possibly associated with Tortugas Eddy formation,

may be an important control on Carolina Slope SST. We speculate that, due to the influence of internal dynamics, recent changes in Carolina Slope SST may not be anomalous within the context of natural variability. Unlike SST, hydrographic changes do not appear to be caused by the advection of Gulf Stream anomalies, but they may be impacted by atmospheric teleconnections with the tropical Atlantic and Pacific. Although some evidence for centennial-scale variability hints that internal oscillatory modes may be superimposed upon lower-frequency trends, their existence cannot be verified without further highly-resolved, well-dated SST reconstructions.

7. Acknowledgements

I would like to thank D. Oppo, R. Came, L. Keigwin and A. Cohen, who will be co-authors on the submitted version of this manuscript. I am also grateful for the sampling and analytical assistance of R. Came, Y. Rosenthal, P. Field, W. Curry, D. Ostermann, S. Praetorious, K. Rose and S. Birdwhistell. T. Joyce, M. McCartney, Y. Kwon, B. Peña-Molino, T. Cronin, F. Gibbons and C. Ponton provided thoughtful discussions and comments. This study was supported by the Ocean and Climate Change Institute (OCCI) at the Woods Hole Oceanographic Institution as well as by the National Science Foundation.

8. References

Anand, P., H. Elderfield, and M. H. Conte, 2003: Calibration of Mg/Ca thermometry in planktonic foraminifera from a sediment trap time series. *Paleoceanography*, **18**.

Antonov, J. I., R. A. Locarnini, T. P. Boyer, A. V. Mishonov, and H. E. Garcia, 2006. World Ocean Atlas 2005, Volume 2: Salinity. S. Levitus, Ed. NOAA Atlas NESDIS 62, U.S. Government Printing Office, Washington, D.C., 182 pp.

Arbuszewski, J., P. deMenocal, A. Kaplan, G. Klinkhammer, and A. Ungerer, 2009: Towards a Global Calibration of the *G. ruber* (White) Mg/Ca Paleothermometer. *Geochimica et Cosmochimica Acta*, A49.

Bane, J. M., and W. K. Dewar, 1988: Gulf-Stream bimodality and variability downstream of the Charleston Bump. *Journal of Geophysical Research-Oceans*, **93**, 6695-6710.

Bemis, B. E., H. J. Spero, J. Bijma, and D. W. Lea, 1998: Reevaluation of the oxygen isotopic composition of planktonic foraminifera: Experimental results and revised paleotemperature equations. *Paleoceanography*, **13,** 150-160.

Boyle, E. A. and L. D. Keigwin, 1985/6: Comparison of Atlantic and Pacific Paleochemical Records for the Last 215,000 Years - Changes in Deep Ocean Circulation and Chemical Inventories. *Earth and Planetary Science Letters*, **76,** 135-150.

Braconnot, P., B. Otto-Bliesner, S. Harrison, S. Joussaume, J.Y. Peterchmitt, A. Abe-Ouchi, M. Crucifix, E. Driesschaert, T. Fichefet, C. D. Hewitt, M. Kageyama,A. Kitoh, A. Laine, M. F. Loutre, O. Marti, U. Merkel, G. Ramstein, P. Valdes, S. L. Weber, Y. Yu and Y. Zhao, 2007: Results of PMIP2 coupled simulations of the Mid-Holocene and Last Glacial Maximum – Part 2: feedbacks with emphasis on the location of the ITCZ and mid- and high latitudes heat budget. *Climate of the Past*, **3**, 279-296.

Candela, J., J. Sheinbaum, J. Ochoa, A. Badan and R. Leben, 2002: The potential vorticity flux through the Yucatan Channel and the Loop Current in the Gulf of Mexico. *Geophysical Research Letters,* **29**.

Cane, M. A. Evolution of El Niño, past and future. Earth and Planetary Science Letters, **230**, 227-240.

Carton, J. A. and B. S. Giese, 2008: A reanalysis of ocean climate using Simple Ocean Data Assimilation (SODA). *Monthly Weather Review*, **136,** 2999-3017.

Conroy, J. L., A. Restrepo, J. T. Overpeck, M. Steinitz-Kannan, J. E. Cole, M. B. Bush, and P. A. Colinvaux, 2009: Unprecedented recent warming of surface temperatures in

the eastern tropical Pacific Ocean. *Nature Geoscience*, **2,** 46-50.

DiNezio, P. N., L. J. Gramer, W. E. Johns, C. S. Meinen and M. O. Baringer, 2009: Observed interannual variability of the Florida Current: wind forcing and the North Atlantic Oscillation. *Journal of Physical Oceanography*, **39**, p. 721-736.

Deuser, W. G. and E. H. Ross, 1989: Seasonally Abundant Planktonic-Foraminifera of the Sargasso Sea - Succession, Deep-Water Fluxes, Isotopic Compositions, and Paleoceanographic Implications. *Journal of Foraminiferal Research*, **19,** 268-293.

Elderfield, H., M. Vautravers, and M. Cooper, 2002: The relationship between shell size and Mg/Ca, Sr/Ca, delta O-18, and delta C-13 of species of planktonic foraminifera. *Geochemistry Geophysics Geosystems*, **3**.

Enfield, D. B., A. M. Mestas-Nunez, and P. J. Trimble, 2001: The Atlantic multidecadal oscillation and its relation to rainfall and river flows in the continental US. *Geophysical Research Letters*, **28,** 2077-2080.

Ferguson, J. E., G. M. Henderson, M. Kucera, and R. E. M. Rickaby, 2008: Systematic change of foraminiferal Mg/Ca ratios across a strong salinity gradient. *Earth and Planetary Science Letters*, **265,** 153-166.

Fratantoni, P. S., T. N. Lee, G. P. Podesta, and F. Muller-Karger, 1998: The influence of loop current perturbations on the formation and evolution of Tortugas eddies in the southern Straits of Florida. *Journal of Geophysical Research-Oceans*, **103,** 24759-24779.

Goosse, H., H. Renssen, A. Timmermann, and R. S. Bradley, 2005: Internal and forced climate variability during the last millennium: a model-data comparison using ensemble simulations. *Quaternary Science Reviews*, **24,** 1345-1360.

Haug, G. H., K. A. Hughen, D. M. Sigman, L. C. Peterson, and U. Rohl, 2001: Southward migration of the intertropical convergence zone through the Holocene. *Science*, **293,** 1304-1308.

Hegerl, G. C., T. J. Crowley, M. Allen, W. T. Hyde, H. N. Pollack, J. Smerdon, and E. Zorita, 2007: Detection of human influence on a new, validated 1500-year temperature reconstruction. *Journal of Climate*, **20,** 650-666.

Hurrell, J. W., Y. Kushnir, G. Ottersen and M. Visbeck, 2003: An Overview of the North Atlantic Oscillation, *in*, Hurrell, J. W., Y. Kushnir, G. Ottersen and M. Visbeck (eds.) The North Atlantic Oscillation: Climate Significance and Environmental Impact, American Geophysical Union, Washington D.C., p. 1-35.

Keenlyside, N. S., M. Latif, J. Jungclaus, L. Kornblueh, and E. Roeckner, 2008: Advancing decadal-scale climate prediction in the North Atlantic sector. *Nature*, **453,** 84-88.

Keigwin, L. D., J. P. Sachs, and Y. Rosenthal, 2003: A 1600-year history of the Labrador Current off Nova Scotia. *Climate Dynamics*, **21,** 53-62.

Kim, S. T. and J. R. O'Neil, 1997: Equilibrium and nonequilibrium oxygen isotope effects in synthetic carbonates. *Geochimica Et Cosmochimica Acta*, **61,** 3461-3475.

Kisakurek, B., A. Eisenhauer, F. Bohm, D. Garbe-Schonberg, and J. Erez, 2008: Controls on shell Mg/Ca and Sr/Ca in cultured planktonic foraminiferan, Globigerinoides ruber (white). *Earth and Planetary Science Letters*, **273,** 260-269.

Knight, J. R., C. K. Folland, and A. A. Scaife, 2006: Climate impacts of the Atlantic Multidecadal Oscillation. *Geophysical Research Letters*, **33**.

Larsen, J. C., 1992: Transport and heat-flux of the Florida Current at 27ºN derived from cross-stream voltages and profiling data – theory and observations. *Philosophical Transactions of the Royal Society of London Series A- Mathematical, Physical and Engineering Sciences,* **338**, 169-236.

Lozier, M. S., S. Leadbetter, R. G. Williams, V. Roussenov, M. S. C. Reed, and N. J. Moore, 2008: The spatial pattern and mechanisms of heat-content change in the North Atlantic. *Science*, **319,** 800-803.

Lund, D. C. and W. B. Curry, 2004: Late holocene variability in Florida current surface density: Patterns and possible causes. *Paleoceanography*, **19**.

Lund, D. C., J. Lynch-Stieglitz, and W. B. Curry, 2006: Gulf Stream density structure and transport during the past millennium. *Nature*, **444,** 601-604.

Lund, D. C. and W. Curry, 2006: Florida Current surface temperature and salinity variability during the last millennium. *Paleoceanography*, **21**.

Lynch-Stieglitz, J., W. B. Curry, and N. Slowey, 1999: A geostrophic transport estimate for the Florida Current from the oxygen isotope composition of benthic foraminifera. *Paleoceanography*, **14,** 360-373.

Lynch-Stieglitz, J., W. B. Curry, and D. C. Lund, 2009: Florida Straits density structure and transport over the last 8,000 years. *Paleoceanography,* in press.

Mann, M. E., Z. H. Zhang, M. K. Hughes, R. S. Bradley, S. K. Miller, S. Rutherford, and F. B. Ni, 2008: Proxy-based reconstructions of hemispheric and global surface

temperature variations over the past two millennia. *Proceedings of the National Academy of Sciences of the United States of America*, **105,** 13252-13257.

Marshall, J., Y. Kushner, D. Battisti, P. Chang, A. Czaja, R. Dickson, J. Hurrell, M. McCartney, R. Saravanan, and M. Visbeck, 2001: North Atlantic climate variability: Phenomena, impacts and mechanisms. *International Journal of Climatology*, **21,** 1863-1898.

Miller, J. L., 1994: Fluctuations of Gulf-Stream frontal position between Cape Hatteras and the Straits of Florida. *Journal of Geophysical Research – Oceans,* **99**, 5057-5064.

Miller, J. L. and T. N. Lee, 1995: Gulf-Stream meanders in the South-Atlantic Bight 1. Scaling and energetics. *Journal of Geophysical Research – Oceans,* **100**, 6687-6704.

Molinari, R. L., 2004: Annual and decadal variability in the western subtropical North Atlantic: signal characteristics and sampling methodologies. *Progress in Oceanography*, **62,** 33-66.

Moy, C. M., G. O. Seltzer, D. T. Rodbell, and D. M. Anderson, 2002: Variability of El Nino/Southern Oscillation activity at millennial timescales during the Holocene epoch. *Nature*, **420,** 162-165.

Newton, A., R. Thunell, and L. Stott, 2006: Climate and hydrographic variability in the Indo-Pacific Warm Pool during the last millennium. *Geophysical Research Letters*, **33**.

Oey, L. Y., H. C. Lee, W. J. Schmitz, 2003: Effects of winds and Caribbean eddies on the frequency of Loop Current eddy shedding: A numerical model study. *Journal of Geophysical Research – Oceans*, **108**.

Ravelo, A. C. and R. G. Fairbanks, 1992: Oxygen isotopic composition of multiple species of planktonic foraminifera: Recorders of the modern photic zone temperature gradient. *Paleoceanography*, **7**, 815-831.

Renssen, H., H. Goosse, T. Fichefet, V. Brovkin, E. Driesschaert and F. Wolk, 2005: Simulating the Holocene climate evolution at northern high latitudes using a coupled atmosphere-sea ice-ocean-vegetation model. *Climate Dynamics*, **24**, 23-43.

Richey, J. N., R. Z. Poore, B. P. Flower, and T. Quinn, 2007: 1400 yr multiproxy record of climate variability from the northern Gulf of Mexico. *Geology*, **35,** 423-426.

Rohling, E. J., 2007: Progress in paleosalinity: Overview and presentation of a new approach. *Paleoceanography*, **22**.

Rosenthal, Y., P. Lam, E. A. Boyle, and J. Thomson, 1995: Authigenic Cadmium

Enrichments in Suboxic Sediments - Precipitation and Postdepositional Mobility. *Earth and Planetary Science Letters*, **132,** 99-111.

Rosenthal, Y., S. Perron-Cashman, C. H. Lear, E. Bard, S. Barker, K. Billups, M. Bryan, M. L. Delaney, P. B. deMenocal, G. S. Dwyer, H. Elderfield, C. R. German, M. Greaves, D. W. Lea, T. M. Marchitto, D. K. Pak, G. L. Paradis, A. D. Russell, R. R. Schneider, K. Scheiderich, L. Stott, K. Tachikawa, E. Tappa, R. Thunell, M. Wara, S. Weldeab, and P. A. Wilson, 2004: Interlaboratory comparison study of Mg/Ca and Sr/Ca measurements in planktonic foraminifera for paleoceanographic research. *Geochemistry Geophysics Geosystems*, **5**.

Sachs, J. P., 2007: Cooling of Northwest Atlantic slope waters during the Holocene. *Geophysical Research Letters*, **34**.

Saenger, C., A. L. Cohen, D. W. Oppo, R. B. Halley, and J. E. Carilli, 2009a. Surface temperature trends and variability in the low-latitude North Atlantic since 1552. *Nature Geoscience*, **2**, 492-495.

Saenger, C., P. Chang, L. Ji, D. W. Oppo and A. L. Cohen, 2009b. Tropical Atlantic climate response to low-latitude and extratropical sea-surface temperature: A Little Ice Age perspective. *Geophysical Research Letters*, **36**.

Schmidt, G.A., G. R. Bigg and E. J. Rohling. 1999. "Global Seawater Oxygen-18 Database". http://data.giss.nasa.gov/o18data/

Schmitz, W. J. and P. L. Richardson, 1991: On the Sources of the Florida Current. *Deep-Sea Research Part a-Oceanographic Research Papers*, **38,** S379-S409.

Schmitz, W. J. and M. S. McCartney, 1993: On the North-Atlantic Circulation. *Reviews of Geophysics*, **31,** 29-49.

Smith, T.M., R.W. Reynolds, Thomas C. Peterson, and Jay Lawrimore, 2008: Improvements to NOAA's Historical Merged Land-Ocean Surface Temperature Analysis (1880-2006). *Journal of Climate*, **21**, 2283-2296.

Trouet, V., J. Esper, N. E. Graham, A. Baker, J. D. Scourse, and D. C. Frank, 2009: Persistent Positive North Atlantic Oscillation Mode Dominated the Medieval Climate Anomaly. *Science*, **324,** 78-80.

Visbeck, M., E. P. Chassignet, R. G. Curry, T. L. Delworth, R.R. Dickson, and G. Krahmann, 2003: The Ocean's Response to North Atlantic Oscillation Variability, *in*, Hurrell, J. W., Y. Kushnir, G. Ottersen and M. Visbeck (eds.) The North Atlantic Oscillation: Climate Significance and Environmental Impact, American Geophysical Union, Washington D.C., p. 113-145.

Wang, L. P. and C. J. Koblinsky, 1996: Annual variability of the subtropical recirculations in the North Atlantic and North Pacific: A Topex/Poseidon study. *Journal of Physical Oceanography*, **26,** 2462-2479.

Weber, S. L., T. J. Crowley, and G. van der Schrier, 2004: Solar irradiance forcing of centennial climate variability during the Holocene. *Climate Dynamics*, **22,** 539-553.

Wunsch, C., 1999: Where do ocean eddy heat fluxes matter? *Journal of Geophysical Research – Oceans*, **104**, 13235-13249.

Table 1. Radiocarbon ages for cores CH0798-MC22 and KNR140-2-59GGC

Core	depth (cm)	^{14}C age (years)	analytical error (years)	calendar age (years B.P.)	error (2 sigma)	species
CH0798-MC-22	0-1	260	35	modern*		*G. sacculifer*
CH0798-MC-22	30-31	1350	30	905	83	*G. sacculifer*
CH0798-MC-22	55-56	2160	40	1750	114	*G. sacculifer*
KNR140-2-59GGC	0-1	375	30	modern*		*G. sacculifer*
KNR140-2-59GGC	10-11	825	30	460	55	*G. sacculifer*
KNR140-2-59GGC	20-21	1100	30	666	60	*G. sacculifer*
KNR140-2-59GGC	35-36	1350	30	878	83	*G. sacculifer*
KNR140-2-59GGC	69-70	1910	30	1451	85	*G. sacculifer*

*fraction modern ^{14}C for CH0798-MC-22 and KNR140-2-59GGC core tops are 97% and 95%, respectively

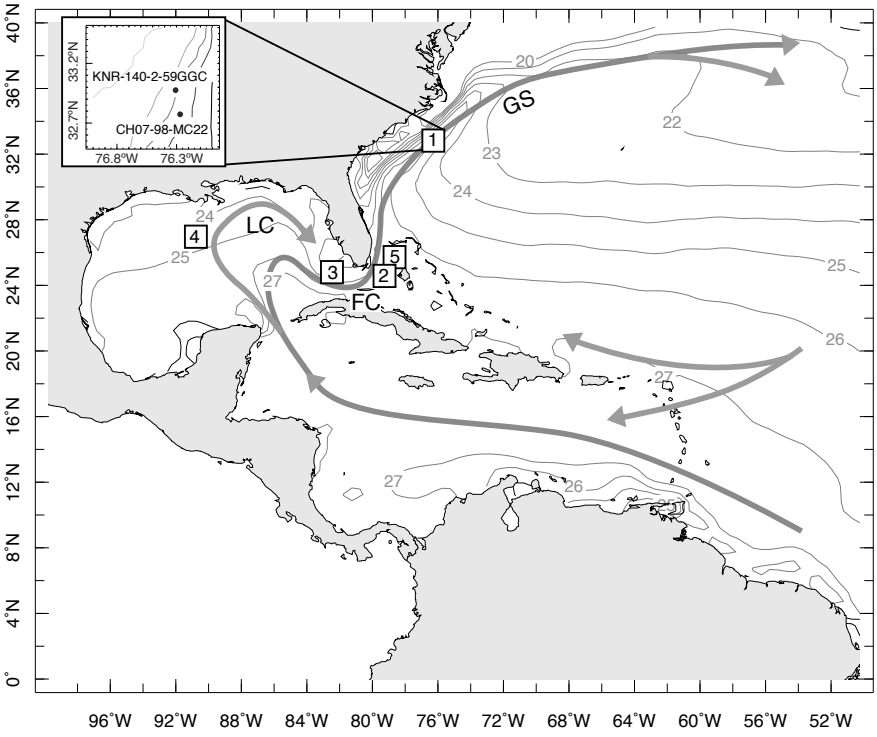

Figure 1. Map of low-latitude western North Atlantic mean annual SST 1958-2007 [*Carton and Giese,* 2008] and core sites discussed in the text, including 1. Carolina Slope (this study) 2. Great Bahama Bank [*Lund and Curry*, 2006] 3. Dry Tortugas [*Lund and Curry*, 2006], 4. Pigmy Basin [*Richey et al*., 2007] and 5. coral-based SST [*Saenger et al*., 2009a]. Arrows indicate the generalized regional ocean circulation including the Loop Current (LC), Florida Current (FC) and Gulf Stream (GS). The relative position of cores KNR-140-2-59GGC and CH07-98-MC22 is shown (inset) with 500 m bathymetric contours.

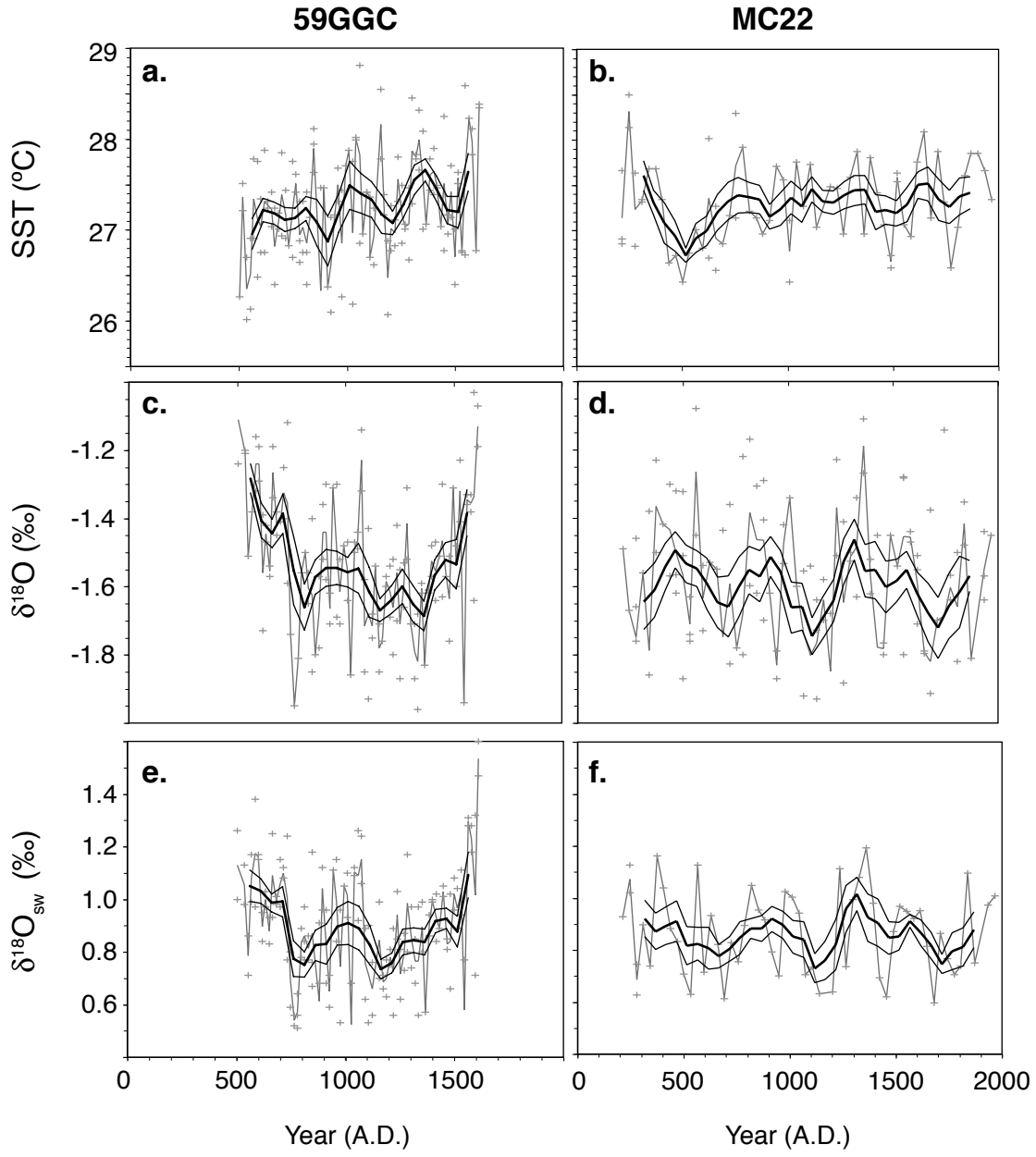

Figure 2. Mg/Ca-based SST in **a.** 59GGC and **b.** MC22. Individual analyses (crosses), and the mean value for each depth (thin black line) are shown. The mean value in each bin (100 years for 59GGC, 200 years for MC22) (bold line) shifted in 50 year increments is surrounded by its 1σ standard error bounds (thin lines). **c.-d.** As in **a.-b.** for oxygen isotopes. **e.-f.** As in **a.-b.** for the estimated oxygen isotopic composition of seawater.

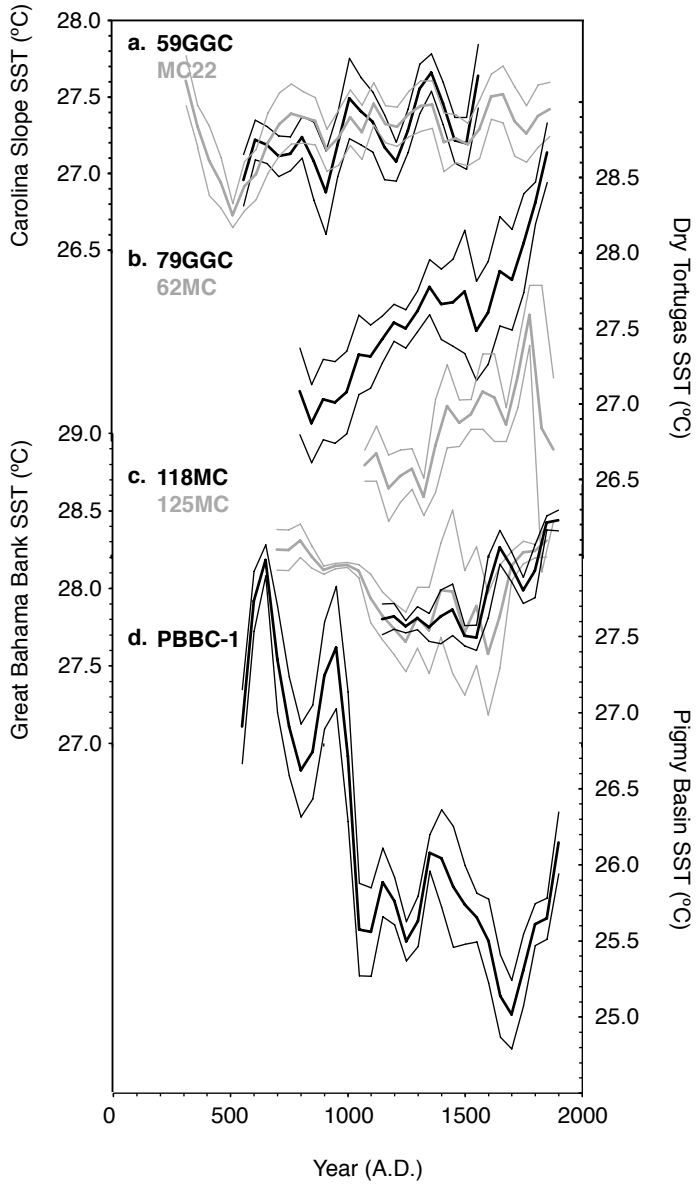

Figure 3. Mean and standard error of *G. ruber*-based SST estimates in successive bins from **a.** the Carolina Slope **b.** the Dry Tortugas **c.** the Great Bahama Bank **d.** the Pigmy Basin**.** All bins are 100 years except MC22 and 125MC, which are 200 years. All y-axes have the same scaling.

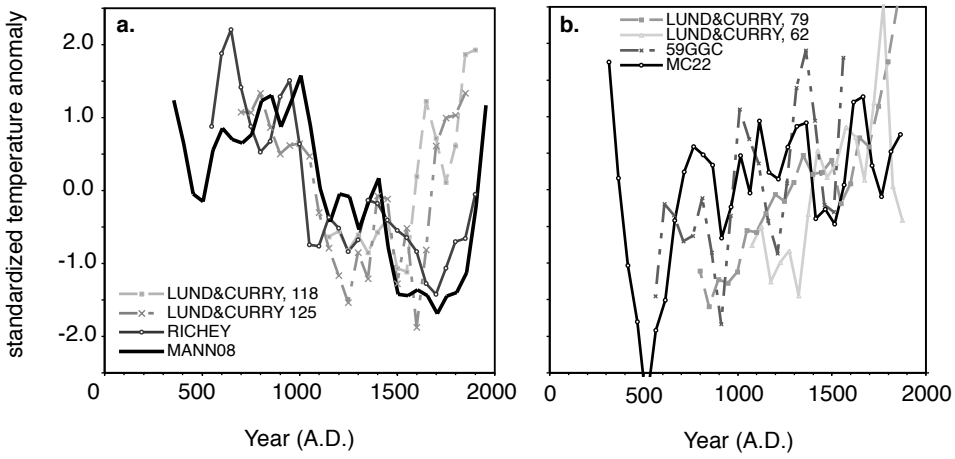

Figure 4. Standardized temperature anomalies for the binned SST estimates in Figure 3. **a**. Records that show a "classic" warm MCA, cool LIA, warm 20th century compared with a 100-year binned estimate of mean annual Northern Hemisphere surface temperature [*Mann et al*., 2008]. **b**. As in **a.** for records showing a steady increase since ~500 A.D. Standard error bounds have been omitted for clarity.

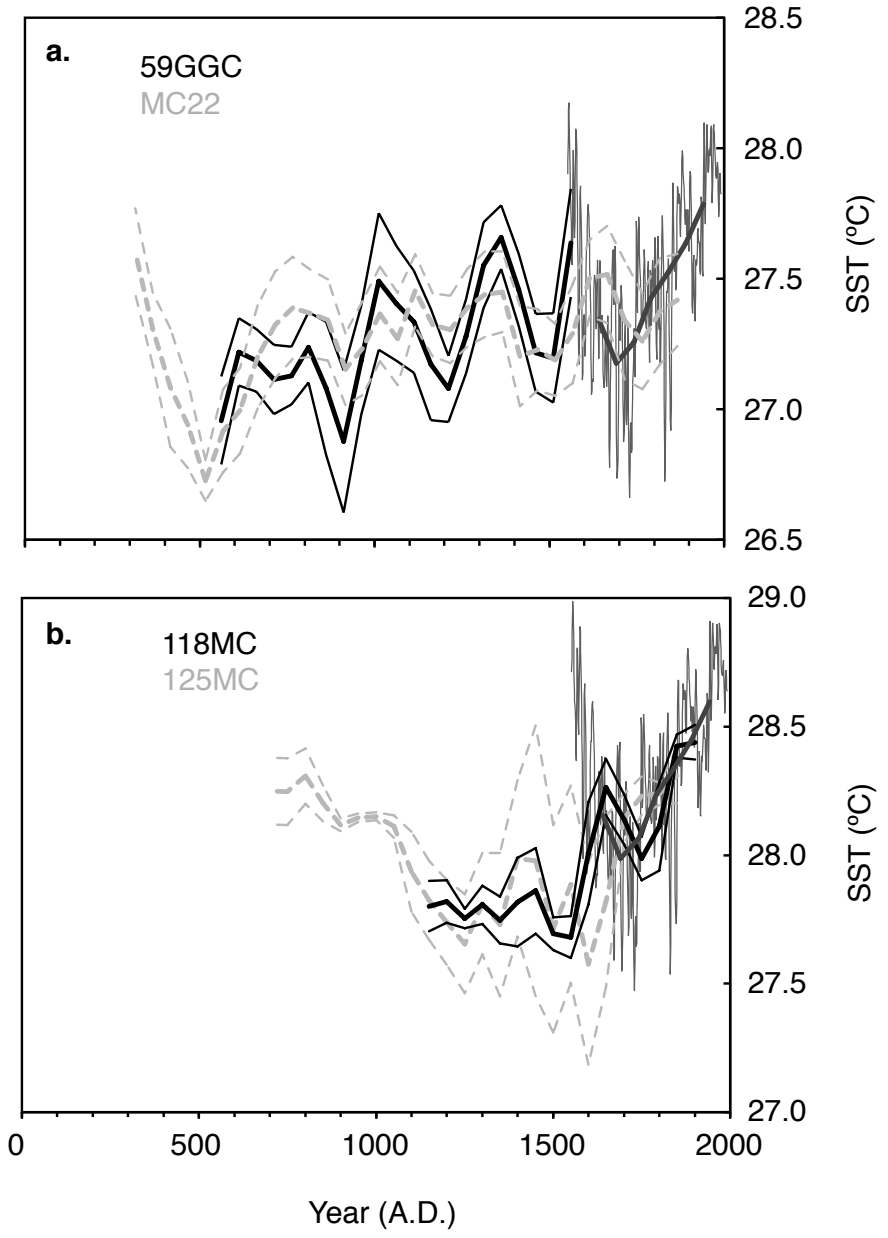

Figure 5. a. Binned 59GGC (black solid) and MC22 (grey dashed) mean SST compared with annually-resolved (fine dark grey) and 100-year binned (thick dark grey) coral-based SST [*Saenger et al*., 2009a]. Coral-based SST has been scaled to have the same 1600-1900 A.D. mean as MC22. **b.** As in **a.** for Great Bahama Bank records [*Lund and Curry*, 2006]. Coral-based SST has been scaled to have the same 1600-1900 A.D. mean as 118MC.

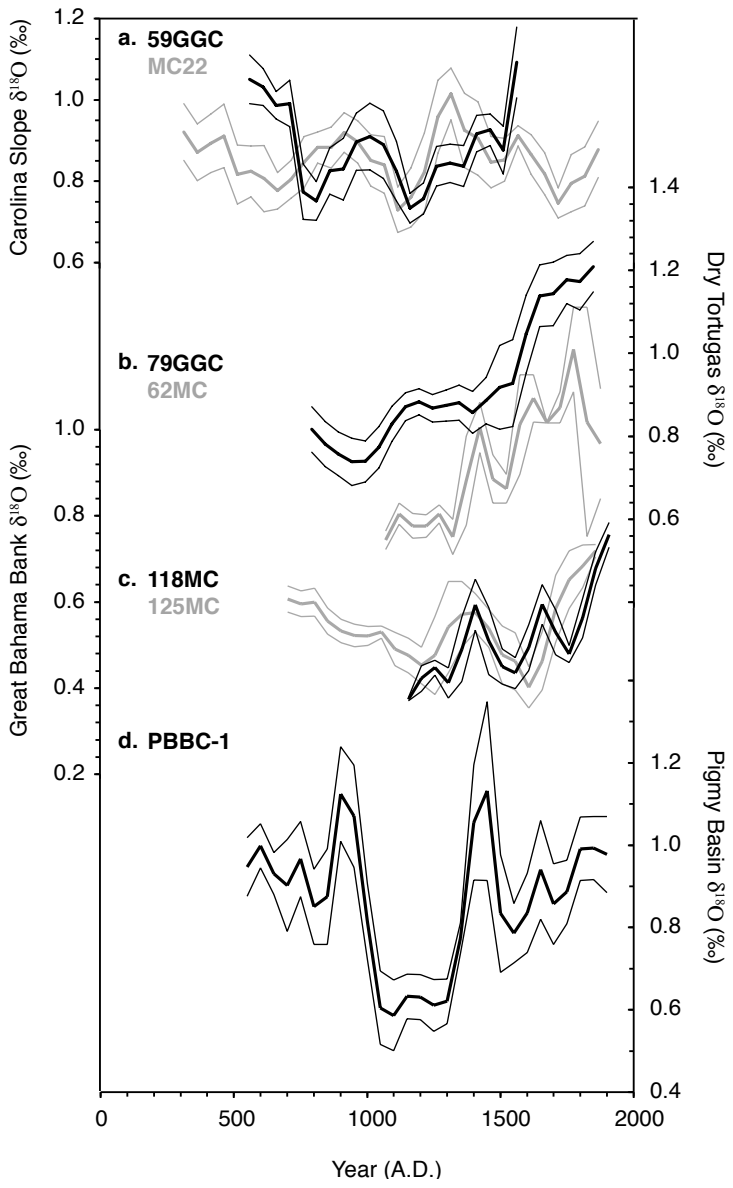

Figure 6. As in Figure 3 but for the oxygen isotopic composition of seawater.

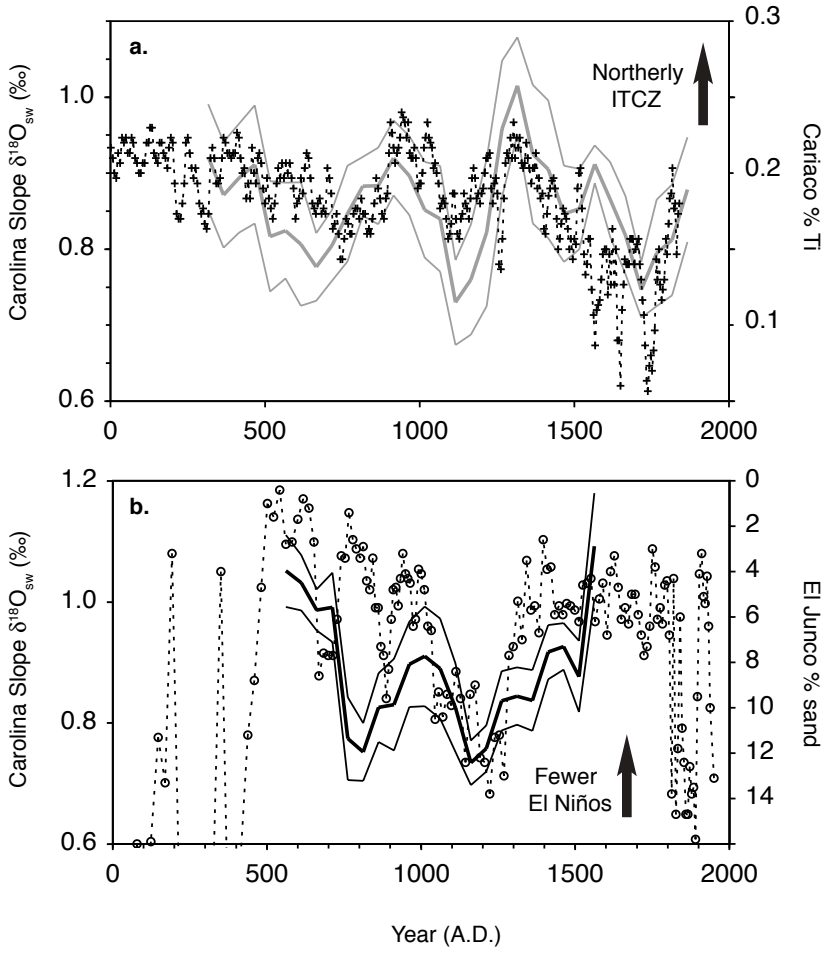

Figure 7. a. Binned MC22 $\delta^{18}O_{sw}$ and standard error bound (grey) plotted against the percent titanium in Cariaco Basin sediments, a proxy for ITCZ latitude (black dashed crosses) [*Haug et al*., 2001]. Southerly ITCZ migrations, such as those during the LIA as associated with *wetter* Carolina Slope conditions. **b.** Binned 59GGC $\delta^{18}O_{sw}$ (black) and standard error bounds plotted against El Junco Lake, Galapagos Islands, percent sand, an ENSO proxy (black dashed circles) [*Conroy et al*., 2009].

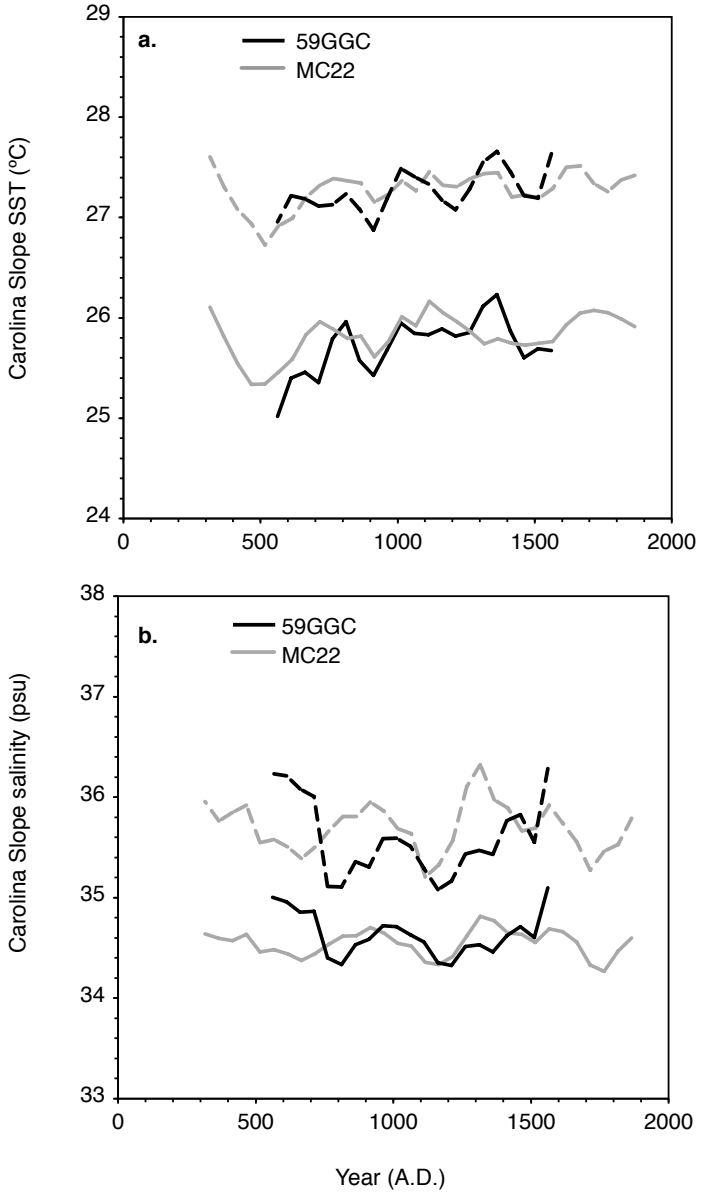

Figure 8. a. Binned 59GGC (black dashed) and MC22 (grey dashed) mean SST based on the general calibration of *Anand et al*. [2003]. Lower SSTs (solid lines) are estimated when the Mg/Ca-salinity and Mg/Ca-SST equations of *Kisakurek et al*., [2008] are solved simultaneously for SST and salinity using the $\delta^{18}O$ fractionation-SST relationship of *Bemis et al*. [1998] and our selected subtropical Atalntic $\delta^{18}O_{sw}$-salinity relationship [*Schmidt et al*., 1999] **b.** 59GGC (black dashed) and MC22 (grey dashed) salinity, estimated assuming Mg/Ca is only a function of SST. Lower, less variable salinities (solid lines) result from simultaneously solving for SST and salinity.

Chapter 5:

Tropical Atlantic climate response to low-latitude and extratropical sea-surface temperature: A Little Ice Age perspective

Saenger, C., P. Chang, L. Ji, D. W. Oppo, and A. L. Cohen, 2009: Tropical Atlantic climate response to low-latitude and extratropical sea-surface temperature: A Little Ice Age perspective. *Geophysical Research Letters*, **36**. L11703, doi:10.1029/2009GL038677

Abstract

Proxy reconstructions and model simulations suggest that steeper interhemispheric sea surface temperature (SST) gradients lead to southerly Intertropical Convergence Zone (ITCZ) migrations during periods of North Atlantic cooling, the most recent of which was the Little Ice Age (LIA; 100–450 yBP). Evidence suggesting low-latitude Atlantic cooling during the LIA was relatively small (<1ºC) raises the possibility that the ITCZ may have responded to a hemispheric SST gradient originating in the extratropics. We use an atmospheric general circulation model (AGCM) to investigate the relative influence of low-latitude and extratropical SSTs on the meridional position of the ITCZ. Our results suggest that the ITCZ responds primarily to local, low-latitude SST anomalies and that small cool anomalies (<0.5ºC) can reproduce the LIA precipitation pattern suggested by paleoclimate proxies. Conversely, even large extratropical cooling does not significantly impact low-latitude hydrology in the absence of ocean-atmosphere interaction.

GEOPHYSICAL RESEARCH LETTERS, VOL. 36, L11703, doi:10.1029/2009GL038677, 2009

Tropical Atlantic climate response to low-latitude and extratropical sea-surface temperature: A Little Ice Age perspective

Casey Saenger,[1] Ping Chang,[2] Link Ji,[2] Delia W. Oppo,[3] and Anne L. Cohen[3]

Received 13 April 2009; accepted 7 May 2009; published 5 June 2009.

[1] Proxy reconstructions and model simulations suggest that steeper interhemispheric sea surface temperature (SST) gradients lead to southerly Intertropical Convergence Zone (ITCZ) migrations during periods of North Atlantic cooling, the most recent of which was the Little Ice Age (LIA; ~100–450 yBP). Evidence suggesting low-latitude Atlantic cooling during the LIA was relatively small (<1°C) raises the possibility that the ITCZ may have responded to a hemispheric SST gradient originating in the extratropics. We use an atmospheric general circulation model (AGCM) to investigate the relative influence of low-latitude and extratropical SSTs on the meridional position of the ITCZ. Our results suggest that the ITCZ responds primarily to local, low-latitude SST anomalies and that small cool anomalies (<0.5°C) can reproduce the LIA precipitation pattern suggested by paleoclimate proxies. Conversely, even large extratropical cooling does not significantly impact low-latitude hydrology in the absence of ocean-atmosphere interaction. **Citation:** Saenger, C., P. Chang, L. Ji, D. W. Oppo, and A. L. Cohen (2009), Tropical Atlantic climate response to low-latitude and extratropical sea-surface temperature: A Little Ice Age perspective, *Geophys. Res. Lett.*, *36*, L11703, doi:10.1029/2009GL038677.

1. Introduction

[2] The Intertropical Convergence Zone (ITCZ) is a latitudinal band of intense precipitation with significant impacts on low-latitude Atlantic climate. Instrumental precipitation records suggest that the mean latitude of the ITCZ is strongly influenced by the sea surface temperature (SST) gradient between the relatively warm North Atlantic and the relatively cool South Atlantic [*Chiang et al.*, 2002]. Cool anomalies in the North tropical Atlantic reduce the interhemispheric SST gradient and drive enhanced cross-equatorial boundary layer flow into the Southern Hemisphere. Associated enhancement of northeasterly trade winds, and slackening of southeasterly trades, leads to a southerly displacement of the ITCZ.

[3] Proxy reconstructions of tropical Atlantic hydrology suggest that southerly ITCZ displacements coincide with high-latitude North Atlantic cooling on timescales ranging from hundreds to tens of thousands of years [*Peterson et al.*, 2000; *Haug et al.*, 2001]. One potential mechanism for these synchronous variations involves changes in the strength of the Atlantic Meridional Overturning Circulation (AMOC). General circulation model simulations of freshwater induced weakening of the AMOC commonly exhibit North Atlantic cooling, a steeper interhemispheric SST gradient and a southerly displacement of the ITCZ [*Zhang and Delworth*, 2005; *Stouffer et al.*, 2006].

[4] The Little Ice Age (LIA; ~100–450 yBP) was a recent interval of prominent extratropical North Atlantic cooling that may have been associated with a weaker AMOC [*Broecker*, 2000]. Proxy records suggest that a 1–2°C cooling of extratropical Atlantic SSTs during the LIA [e.g., *Keigwin et al.*, 2003; *Jiang et al.*, 2005] was accompanied by stronger northeasterly trade winds [*Black et al.*, 1999] higher salinities [*Linsley et al.*, 1994; *Watanabe et al.*, 2001; *Lund and Curry*, 2006] and more arid conditions [*Hodell et al.*, 2005] at low latitudes (Figure 1). Combined with evidence for increased precipitation in the Southern Hemisphere [*Baker et al.*, 2001; *Thompson et al.*, 2006], these proxy records suggest that a southerly migration of the ITCZ was a robust response to cooler North Atlantic SSTs during the LIA.

[5] Although some proxy records indicate that low latitude North Atlantic SSTs cooled by approximately 3°C during the LIA [*Winter et al.*, 2000], recent research suggests that LIA cooling was more subtle and was often within the range of modern instrumental values [*Lund and Curry*, 2006; *Black et al.*, 2007]. The possibility that low latitude Atlantic SSTs were not markedly cooler during the LIA suggests that the ITCZ may have responded to extratropical cooling. Idealized simulations [*Broccoli et al.*, 2006] and climate models of the last glacial maximum [*Chiang and Bitz*, 2005] indicate that high-latitude climate can influence the meridional position of the ITCZ, but these coupled simulations make it difficult to determine if the ITCZ's response necessarily requires changes to low-latitude Atlantic SST. Recent work suggesting southerly ITCZ migrations can be understood as the atmospheric adjustment to increased poleward energy fluxes [*Kang et al.*, 2008] allows for the possibility that the ITCZ could respond to extratropical cooling alone.

[6] In this paper, we explore the relative influence of low-latitude and extratropical North Atlantic SSTs on tropical precipitation within the context of the LIA. Using an atmospheric general circulation model (AGCM), we examine the potential for extratropical Atlantic cooling to alter tropical precipitation in the absence of low-latitude SST anomalies. In contrast to coupled model simulations, our approach isolates the specific influence of SST on Atlantic ITCZ variability. Our results indicate that without ocean-atmosphere coupling, cooler extratropical SSTs alone cannot force southerly Atlantic ITCZ migrations, suggesting

[1] MIT/WHOI Joint Program in Oceanography, Woods Hole, Massachusetts, USA.
[2] Department of Oceanography, Texas A&M University, College Station, Texas, USA.
[3] Department of Geology and Geophysics, Woods Hole Oceanographic Institution, Woods Hole, Massachusetts, USA.

0094-8276/09/2009GL038677$05.00

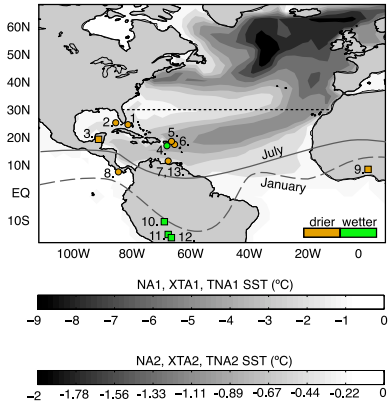

Figure 1. Imposed SST anomaly pattern (shading) for CAM3 simulations (note separate scales). XTA simulations applied SSTs only north of 30°N (dotted line). TNA simulations applied SSTs only south of 30°N. Marine (circles) and terrestrial (squares) proxy records indicating wetter (open/orange) and drier (filled/green) LIA conditions. Numbers correspond to Table 1. Modern seasonal ITCZ extremes are also shown.

that LIA ITCZ displacements were likely accompanied by some degree of low-latitude cooling.

2. Model Description and Methods

[7] We performed six simulations using the National Center for Atmospheric Research (NCAR) Community Atmosphere Model version 3 (CAM3) at T42 resolution (2.8° by 2.8° latitude-longitude, 26 vertical levels) [*Collins et al.*, 2006]. In general, CAM3 reproduces the pattern and amplitude of mean annual low-latitude Atlantic climate variability, as well as interannual migrations of tropical convergence zones [*Hack et al.*, 2006, *Hurrell et al.*, 2006] suggesting that it is appropriate for investigating the mean state of the ITCZ during the LIA. However, as in other AGCMs, CAM3 tends to overestimate Caribbean precipitation, particularly in boreal summer and autumn [*Hack et al.*, 2006; *Biasutti et al.*, 2006].

[8] Given the possibility that LIA SST and ITCZ variability was associated with a weaker AMOC, all simulations were forced using the North Atlantic SST pattern from the "hosing" experiment of *Zhang and Delworth* [2005] (hereinafter referred to as ZD05). Briefly, ZD05 applied a 0.6 Sv freshwater forcing to the high-latitude North Atlantic (55°–75°N, 63°W–4°E) for 60 years in an ocean-atmosphere global general circulation model. In response to this forcing, the entire North Atlantic cooled, with some SST anomalies reaching −9°C.

[9] Our first two simulations (NA1, NA2) prescribe the ZD05 SST pattern in the Atlantic north of the equator and use climatological SSTs elsewhere (Figure 1). NA1 uses the full magnitude of cooling, which reaches 9°C in the extratropical North Atlantic. NA2 is identical to NA1, but uniformly reduces SST anomalies by 78% such that extratropical Atlantic cooling does not exceed 2°C. NA1 is intended to be an idealized simulation that will yield a clear ITCZ response, while NA2 is designed to reflect the subtle cooling that may have characterized the LIA. Our second two simulations (XTA1, XTA2) are identical to NA1 and NA2, respectively, but apply ZD05 SSTs only north of 30°N. Our final two simulations (TNA1, TNA2) apply ZD05 SSTs only from the equator to 30°N. All simulations were run for 18 years, of which the final 14 years were analyzed. We assumed pre-industrial carbon dioxide concentrations, and assessed significant anomalies (95%) using a two-tailed t-test.

3. Modeled Precipitation and Wind Stress

[10] NA1 exhibits decreased annual average precipitation throughout the North Atlantic in response to cooler SSTs (Figure 2a). Negative precipitation anomalies extend in a zonal band from the eastern North Pacific to West Africa and can exceed −4 mm day^{-1}. Consistent with previous studies [*Zhang and Delworth*, 2005; Stouffer et al. 2006; *Sutton and Hodson*, 2007], increased precipitation immediately south of this zonal band can be interpreted as a southerly displacement of the Atlantic ITCZ. Cooler NA1 SSTs also lead to positive sea-level pressure (SLP) anomalies throughout the North Atlantic (not shown) that strengthen northeasterly wind stress at low-latitudes (Figure 2a). Enhanced northeasterly wind stress is most prominent along the northern coast of South America and in the southern Caribbean where anomalies extend across the Central American isthmus.

[11] Annual average results from NA2 are similar to those of NA1, suggesting an approximately linear response to the downscaled SST forcing (Figure 2b). A linear regression of NA1 and NA2 precipitation anomalies has a slope of 0.25 ± 0.1 that is close to the 0.22 expected for a perfectly linear response. As in NA1, NA2 precipitation anomalies exhibit a zonal band of increased aridity just north of the equator, although opposing positive precipitation anomalies to the south of this band are more subtle.

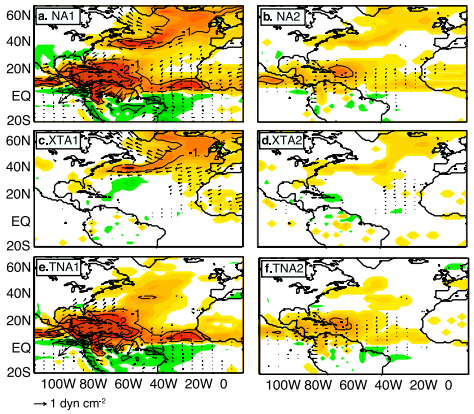

Figure 2. Significant mean annual precipitation (contours, mm day^{-1}) and wind stress (vectors, dyn cm^{-1}) anomalies for (a) NA1, (b) NA2, (c) XTA1, (d) XTA2, (e) TNA1, and (f) TNA2. Shading highlights positive (dark/green) and negative (light/orange) precipitation anomalies that are significant at 95%.

Table 1. Comparison of LIA Hydrologic and Trade Wind Proxies With Model Simulations[a]

Map	Location	LIA Conditions (Proxy)	Modelled Precip. Anomaly (mm day^{-1}) NA1/NA2	XTA1/XTA2	Reference
1	West Atlantic (Bahamas)	more saline (foram. δ^{18}O)	−1.78/−0.22	insig/+0.19	*Lund and Curry* [2006]
2	Florida, USA	more saline (foram. δ^{18}O)	−1.22/−0.22	insig/insig	*Lund and Curry* [2006]
3	Central America (Yucatan)	drier (ostracode δ^{18}O)	−1.41/insig	insig/insig	*Hodell et al.* [2005]
4	Caribbean (Puerto Rico)	less saline (foram. δ^{18}O)	−3.23/−0.79	+0.34/+0.32	*Nyberg et al.* [2002]
5	Caribbean (Puerto Rico)	more saline (coral δ^{18}O)	−3.23/−0.79	+0.34/+0.32	*Watanabe et al.* [2001]
6	Caribbean (St. Croix)	more saline (coral δ^{18}O)	−3.37/−1.41	+0.30/+0.23	*Saenger et al.* [2008]
7	Caribbean (Cariaco)	drier (%Ti)	−3.19/−0.65	insig/insig	*Haug et al.* [2001]
8	Tropical Pacific (Panama)	more saline (coral δ^{18}O)	−1.86/−0.47	insig/insig	*Linsley et al.* [1994]
9	West Africa	drier (lake level, model)	−0.97/−0.27	−0.25/insig	*Shanahan et al.* [2009]
10	South America (Andes)	wetter (mass accumulation)	insig/insig	insig/insig	*Thompson et al.* [2006]
11	South America (Andes)	wetter (multiproxy)	+0.40/insig	insig/insig	*Baker et al.* [2001]
12	South America (Andes)	wetter (mass accumulation)	+0.40/insig	insig/insig	*Liu et al.* [2005]
Map	Location	LIA Conditions (Proxy)	Modelled Wind Stress Anomaly (dyn cm^{-2}) NA1/NA2	XTA1/XTA2	Reference
13	Caribbean (Caricao)	strong NE trades (# *G. bulloides*)	0.14/0.41	insig/insig	*Black et al.* [1999]

[a]Results from TNA simulations were nearly identical to those of NA simulations. Map numbers 1–12 are for hydrologic proxies, and map number 13 is for a trade wind proxy.

Negative low-latitude precipitation anomalies are accompanied by enhanced northeasterly wind stress anomalies that are consistent with NA1.

[12] Neither XTA1 nor XTA2 exhibit significant low latitude precipitation or wind stress anomalies (Figures 2c and 2d). Even the idealized XTA1 exhibits precipitation anomalies that are generally heterogeneous with little evidence for robust patterns of change. Neither simulation exhibits significant northeasterly wind stress anomalies in the Caribbean or deep tropics. In contrast, low-latitude precipitation and wind stress anomalies in TNA1 and TNA2 (Figures 2e and 2f) are nearly indistinguishable from those in NA1 and NA2.

[13] Low-latitude precipitation and wind stress anomalies in NA and TNA simulations are clearly more similar to LIA proxy records than either XTA simulation (Figures 1 and 2 and Table 1). Considering that proxy records estimate the sign of hydrologic variability more accurately than its magnitude, we compare their spatial patterns with model results. Negative low-latitude North Atlantic annual average precipitation anomalies in NA and TNA simulations agree well with nearly unanimous proxy evidence for drier LIA conditions. In contrast, precipitation anomalies in XTA simulations are either insignificant or suggest increased precipitation that is at odds with proxy evidence. Furthermore, enhanced northeasterly wind stress in NA and TNA simulations agrees well with proxy evidence for greater wind-induced LIA upwelling [*Black et al.*, 1999], while insignificant wind stress anomalies in XTA simulations do not. In the Southern Hemisphere, only NA1 and TNA1 show significant precipitation increases as suggested by proxy records [*Baker et al.*, 2001; *Thompson et al.*, 2006], although similar precipitation anomaly patterns in NA2 and TNA2 agree qualitatively with proxy data.

4. Discussion

[14] Our results support suggestions that low latitude North Atlantic precipitation patterns during the LIA can be explained by a southerly displacement of the mean ITCZ. However, XTA simulations suggest this displacement was not forced by high-latitude SSTs alone, but must have been accompanied by some degree of low-latitude Atlantic cooling. Consistent with previous work illustrating the ITCZ's sensitivity to small SST gradients [*Chiang et al.*, 2002], NA2 and TNA2 simulations suggest that enhanced northeast trades and a southerly ITCZ displacement can occur in response to a mean low-latitude North Atlantic cooling anomaly of less than 0.5°C. The magnitude of this anomaly is at the upper detection limit of many commonly used paleotemperature proxies.

[15] The insensitivity of low-latitude precipitation to extratropical cooling is supported by an AGCM forced by 20th century multidecadal SST variability, which also shows that tropical precipitation is primarily driven by low-latitude SSTs [*Sutton and Hodson*, 2007]. Furthermore, the work of *Sutton and Hodson* [2007] suggests our results are insensitive to the exact pattern of SST forcing, and that they are likely to be relevant even if mechanisms other than a weakened AMOC caused LIA cooling.

[16] An idealized experiment that investigates the tropical response to extratropical heat anomalies describes the ITCZ in terms of a constraint imposed by atmospheric energy transport [*Kang et al.*, 2008]. Following a Northern Hemisphere cooling, *Kang et al.* [2008] suggest eddy energy transport can export heat from the northern tropics toward the northern pole, thus forcing the ITCZ toward the warmer Southern Hemisphere. Although the interhemispheric SST gradient steepens in these simulations, the mechanism for ITCZ variability does not explicitly require SST to change. In contrast, our results suggest cooler low-latitude North Atlantic SSTs were probably a necessary condition for southerly ITCZ migrations during the LIA.

[17] Coupled simulations often support the importance of tropical SST anomalies in determining the ITCZ's meridional position, but they suggest that these anomalies can propagate from high latitudes [*Chiang and Bitz*, 2005; *Broccoli et al.*, 2006]. A simulation in which the ITCZ was displaced southward by imposing high-latitude sea ice identified wind-evaporation-SST (WES) feedbacks as a

potential mechanism for communicating extratropical cooling to the tropics [*Chiang and Bitz*, 2005], although recent studies suggest that other atmospheric mechanisms are also important (S. Mahajan et al., The wind-evaporation-sea surface temperature (WES) feedback as a thermodynamic pathway for the equatorward propagation of high latitude sea-ice induced cold anomalies, submitted to *Journal of Climate,* 2009). Alternative mechanisms suggest high latitude signals may be transmitted to the tropics relatively rapidly via coastal Kelvin waves [*Yang*, 1999] and that interactions between a weakened AMOC and the wind-driven circulation may lead to changes in tropical Atlantic SST [*Chang et al.*, 2008].

[18] Ocean-atmosphere interactions, not captured by our uncoupled simulations, were likely important in shaping LIA climate. Such processes could enhance or dampen the precipitation and wind anomalies seen in our results. The stronger northeasterly trades in NA and TNA simulations would likely cause a positive WES feedback that could enhance or prolong cool SST anomalies. However, if cooler LIA SSTs were caused by a weaker AMOC, subsequent weakening of the low-latitude western boundary current would likely cause subsurface warming in the Caribbean and western tropical Atlantic leading to warmer SSTs in upwelling regions [*Wan et al.*, 2009]. The degree to which our simulations are realistic depends on the relative influences of these feedbacks. If the WES mechanism dominates, amplification of the small cooling imposed in NA2 and TNA2 may lead to a more pronounced tropical response. If the subsurface ocean warming has a larger influence, the imposed cooling would decay quickly, leading to a more subtle response [*Wan et al.*, 2009].

[19] Finally, some proxy evidence suggests that a southerly ITCZ migration during the LIA was a global phenomenon [*Newton et al.*, 2006] that may reflect remote climatic impacts of Atlantic SST anomalies. ZD05 suggest the cooler Atlantic SSTs and enhanced cross-isthmus winds seen in NA and TNA simulations could induce an El Niño-like tropical Pacific circulation capable of weakening the Indian and Asian monsoons. This mechanism is in agreement with evidence for weaker monsoons [e.g., *Gupta et al.*, 2003] and El Niño-like conditions [e.g., *Mann et al.*, 2005] during the LIA. However, without ocean feedbacks, our simulation exhibits an enhanced southwest Asian monsoon circulation (not shown) that further illustrates the important role of coupled atmosphere-ocean interactions in global climate teleconnections.

5. Summary and Conclusions

[20] We have identified a clear role for low-latitude Atlantic SST anomalies in forcing southerly ITCZ displacement. Low-latitude cooling within the range of recent LIA SST proxy estimates generates precipitation and wind stress anomalies that agree with available reconstructions. Conversely, without ocean-atmosphere interaction, even very large extratropical cooling cannot reproduce LIA precipitation and trade wind patterns. Additional highly-resolved and well-dated proxy reconstructions are clearly needed to better constrain the spatial and temporal evolution of Atlantic SST and hydrology during the LIA. Furthermore, additional simulations with both coupled and atmospheric GCMs that better resolve small-scale circulation features will help elucidate the important processes related to regional and remote influences of Atlantic SST on tropical hydrology.

[21] **Acknowledgments.** This work was supported by NSF grants OCE 0623364 and ATM 033746 as well as the student research fund of MIT's Department of Earth, Atmospheric and Planetary Science.

References

Baker, P. A., G. O. Seltzer, S. C. Fritz, R. B. Dunbar, M. J. Grove, P. M. Tapia, S. L. Cross, H. D. Rowe, and J. P. Broda (2001), The history of South American tropical precipitation for the past 25,000 years, *Science*, *291*, 640–643.

Biasutti, M., A. H. Sobel, and Y. Kushnir (2006), AGCM precipitation biases in the tropical Atlantic, *J. Clim.*, *19*, 935–958.

Black, D. E., L. C. Peterson, J. T. Overpeck, A. Kaplan, M. N. Evans, and M. Kashgarian (1999), Eight centuries of North Atlantic Ocean atmosphere variability, *Science*, *286*, 1709–1713.

Black, D. E., M. A. Abahazi, R. C. Thunell, A. Kaplan, E. J. Tappa, and L. C. Peterson (2007), An 8-century tropical Atlantic SST record from the Cariaco Basin: Baseline variability, twentieth-century warming, and Atlantic hurricane frequency, *Paleoceanography*, *22*, PA4204, doi:10.1029/2007PA001427.

Broccoli, A. J., K. A. Dahl, and R. J. Stouffer (2006), Response of the ITCZ to Northern Hemisphere cooling, *Geophys. Res. Lett.*, *33*, L01702, doi:10.1029/2005GL024546.

Broecker, W. S. (2000), Was a change in thermohaline circulation responsible for the Little Ice Age?, *Proc. Nat. Acad. Sci. U. S. A.*, *97*, 1339–1342.

Chang, P., R. Zhang, W. Hazeleger, C. Wen, X. Wan, L. Ji, R. J. Haarsma, W. P. Breugem, and H. Seidel (2008), Oceanic link between abrupt changes in the North Atlantic Ocean and the African monsoon, *Nat. Geosci.*, *1*, 444–448.

Chiang, J. C. H., and C. M. Bitz (2005), Influence of high latitude ice cover on the marine Intertropical Convergence Zone, *Clim. Dyn.*, *25*, 477–496.

Chiang, J. C. H., Y. Kushnir, and A. Giannini (2002), Deconstructing Atlantic Intertropical Convergence Zone variability: Influence of the local cross-equatorial sea surface temperature gradient and remote forcing from the eastern equatorial Pacific, *J. Geophys. Res.*, *107*(D1), 4004, doi:10.1029/2000JD000307.

Collins, W. D., P. J. Rasch, B. A. Boville, J. J. Hack, J. R. McCaa, D. L. Williamson, and B. P. Briegleb (2006), The formulation and atmospheric simulation of the Community Atmosphere Model version 3 (CAM3), *J. Clim.*, *19*, 2144–2161.

Gupta, A. K., D. M. Anderson, and J. T. Overpeck (2003), Abrupt changes in the Asian southwest monsoon during the Holocene and their links to the North Atlantic Ocean, *Nature*, *421*, 354–357.

Hack, J. J., J. M. Caron, S. G. Yeager, K. W. Oleson, M. M. Holland, J. E. Truesdale, and P. J. Rasch (2006), Simulation of the global hydrological cycle in the CCSM Community Atmosphere Model version 3 (CAM3) mean features, *J. Clim.*, *19*, 2199–2221.

Haug, G. H., K. A. Hughen, D. M. Sigman, L. C. Peterson, and U. Rohl (2001), Southward migration of the Intertropical Convergence Zone through the Holocene, *Science*, *293*, 1304–1308.

Hodell, D. A., M. Brenner, J. H. Curtis, R. Medina-Gonzalez, E. I. Can, A. Albornaz-Pat, and T. P. Guilderson (2005), Climate change on the Yucatan Peninsula during the Little Ice Age, *Quat. Res.*, *63*, 109–121.

Hurrell, J. W., J. J. Hack, A. S. Phillips, J. Caron, and J. Yin (2006), The dynamical simulation of the Community Atmosphere Model version 3 (CAM3), *J. Clim.*, *19*, 2162–2183.

Jiang, H., J. Eiriksson, M. Schulz, K. L. Knudsen, and M. S. Seidenkrantz (2005), Evidence for solar forcing of sea-surface temperature on the North Icelandic Shelf during the late Holocene, *Geology*, *33*, 73–76.

Kang, S. M., I. M. Held, D. M. W. Frierson, and M. Zhao (2008), The response of the ITCZ to extratropical thermal forcing: Idealized slab-ocean experiments with a GCM, *J. Clim.*, *21*, 3521–3532, doi:10.1175/2007JCLI2146.1.

Keigwin, L. D., J. P. Sachs, and Y. Rosenthal (2003), A 1600-year history of the Labrador Current off Nova Scotia, *Clim. Dyn.*, *21*, 53–62.

Linsley, B. K., R. B. Dunbar, G. M. Wellington, and D. A. Mucciarone (1994), A coral-based reconstruction of Intertropical Convergence Zone variability over Central-America since 1707, *J. Geophys. Res.*, *99*, 9977–9994.

Liu, K. B., C. A. Reese, and L. G. Thompson (2005), Ice-core pollen record of climatic changes in the central Andes during the last 400 yr, *Quat. Res.*, *64*, 272–278.

Lund, D. C., and W. Curry (2006), Florida Current surface temperature and salinity variability during the last millennium, *Paleoceanography*, *21*, PA2009, doi:10.1029/2005PA001218.

Mann, M. E., M. A. Cane, S. E. Zebiak, and A. Clement (2005), Volcanic and solar forcing of the tropical Pacific over the past 1000 years, *J. Clim.*, *18*, 447–456.

Newton, A., R. Thunell, and L. Stott (2006), Climate and hydrographic variability in the Indo-Pacific Warm Pool during the last millennium, *Geophys. Res. Lett.*, *33*, L19710, doi:10.1029/2006GL027234.

Nyberg, J., B. A. Malmgren, A. Kuijpers, and A. Winter (2002), A centennial-scale variability of tropical North Atlantic surface hydrography during the late Holocene, *Palaeogeogr. Palaeoclimatol. Palaeoecol.*, *183*, 25–41.

Peterson, L. C., G. H. Haug, K. A. Hughen, and U. Rohl (2000), Rapid changes in the hydrologic cycle of the tropical Atlantic during the last glacial, *Science*, *290*, 1947–1951.

Saenger, C., A. L. Cohen, D. W. Oppo, and D. Hubbard (2008), Interpreting sea surface temperature from strontium/calcium ratios in Montastrea corals: Link with growth rate and implications for proxy reconstructions, *Paleoceanography*, *23*, PA3102, doi:10.1029/2007PA001572.

Shanahan, T. M., J. T. Overpeck, K. J. Anchukaitis, J. W. Beck, J. E. Cole, D. L. Dettman, J. A. Peck, C. A. Scholz, and J. W. King (2009), Atlantic forcing of persistent drought in West Africa, *Science*, *324*, 377–380.

Stouffer, R. J., et al. (2006), Investigating the causes of the response of the thermohaline circulation to past and future climate changes, *J. Clim.*, *19*, 1365–1387.

Sutton, R. T., and D. L. R. Hodson (2007), Climate response to basin-scale warming and cooling of the North Atlantic Ocean, *J. Clim.*, *20*, 891–907.

Thompson, L. G., E. Mosley-Thompson, H. Brecher, M. Davis, B. León, D. Les, P. Lin, T. Mashiotta, and K. Mountain (2006), Abrupt tropical climate change: Past and present, *Proc. Nat. Acad. Sci. U. S. A.*, *103*, 10,536–10,543.

Wan, X. Q., P. Chang, R. Saravanan, R. Zhang, and M. W. Schmidt (2009), On the interpretation of Caribbean paleo-temperature reconstructions during the Younger Dryas, *Geophys. Res. Lett.*, *36*, L02701, doi:10.1029/2008GL035805.

Watanabe, T., A. Winter, and T. Oba (2001), Seasonal changes in sea surface temperature and salinity during the Little Ice Age in the Caribbean Sea deduced from Mg/Ca and $^{18}O/^{16}O$ ratios in corals, *Mar. Geol.*, *173*, 21–35.

Winter, A., H. Ishioroshi, T. Watanabe, T. Oba, and J. Christy (2000), Caribbean sea surface temperatures: Two-to-three degrees cooler than present during the Little Ice Age, *Geophys. Res. Lett.*, *27*, 3365–3368.

Yang, J. Y. (1999), A linkage between decadal climate variations in the Labrador Sea and the tropical Atlantic Ocean, *Geophys. Res. Lett.*, *26*, 1023–1026.

Zhang, R., and T. L. Delworth (2005), Simulated tropical response to a substantial weakening of the Atlantic thermohaline circulation, *J. Clim.*, *18*, 1853–1860.

P. Chang and L. Ji, Department of Oceanography, Texas A&M University, College Station, TX 77843, USA.

A. L. Cohen, D. W. Oppo, and C. Saenger, Department of Geology and Geophysics, Woods Hole Oceanographic Institution, MS 22, Woods Hole, MA 02543, USA. (csaenger@mit.edu)

Appendix A1:

Data for Chapter 2

BI: 12.6 mm yr^{-1}

depth (mm)	year (A.D.)	Sr/Ca (mmol/mol)	$\delta^{18}O$ (permil)
0.49	2006.20	8.64	-4.43
0.92	2006.14	8.67	-4.63
1.27	2006.08	8.52	-4.25
1.72	2006.02	8.42	-5.37
2.16	2005.96	8.61	-5.31
2.56	2005.89	8.39	-5.28
2.84	2005.83	8.38	-4.17
3.39	2005.76	8.37	-4.94
3.76	2005.69	8.36	-4.98
4.07	2005.57	8.50	-4.07
4.62	2005.45	8.50	-4.46
5.19	2005.39	8.51	-4.64
5.64	2005.32	8.50	-4.69
6.30	2005.23	8.54	-4.16
6.90	2005.13	8.63	-4.44
7.38	2005.10	8.57	-4.57
7.96	2005.08	8.50	-4.50
8.55	2005.05	8.52	-4.73
9.16	2005.03	8.58	-5.13
9.63	2005.00	8.55	-4.98
10.12	2004.98	8.49	-5.09
10.67	2004.95	8.45	-5.00
11.18	2004.93	8.45	-5.12
11.74	2004.90	8.44	-5.18
12.30	2004.88	8.46	-5.06
12.79	2004.85	8.42	-5.51
13.24	2004.83	8.41	-4.91
13.73	2004.80	8.38	-4.64
14.20	2004.78	8.36	-4.34
14.67	2004.75	8.45	-3.80
15.15	2004.61	8.48	-4.52
15.66	2004.48	8.47	-4.67
16.05	2004.34	8.37	-4.95
16.63	2004.20	8.64	-4.35
17.13	2004.10	8.64	-4.27
17.62	2004.08	8.49	-4.30
18.07	2004.06	8.49	-4.12
18.48	2004.03	8.44	-4.55
18.97	2004.01	8.47	-4.41
19.46	2003.99	8.48	-3.89
19.93	2003.97	8.40	-4.36
20.39	2003.94	8.45	-4.70
20.88	2003.92	8.43	-4.78
21.34	2003.90	8.41	-5.05
21.80	2003.88	8.46	-5.01

depth (mm)	year (A.D.)	Sr/Ca (mmol/mol)	$\delta^{18}O$ (permil)
22.28	2003.86	8.41	-5.04
23.76	2003.83	8.42	-4.96
24.25	2003.81	8.44	-4.87
24.74	2003.79	8.44	-4.70
25.18	2003.77	8.40	-4.60
25.65	2003.74	8.47	-4.34
26.14	2003.72	8.43	-4.31
26.58	2003.70	8.37	-4.54
27.07	2003.64	8.42	-4.47
27.59	2003.58	8.45	-4.41
28.09	2003.51	8.50	-4.19
28.55	2003.45	8.52	-4.38
29.00	2003.39	8.58	-4.19
29.47	2003.33	8.51	-4.34
29.91	2003.26	8.54	-4.46
30.34	2003.20	8.57	-4.76
30.79	2003.15	8.54	-4.74
31.27	2003.10	8.54	-4.72
31.73	2003.05	8.49	-4.59
32.18	2003.00	8.49	-4.85
32.58	2002.95	8.52	-4.99
33.11	2002.91	8.55	-4.94
33.52	2002.87	8.51	-4.76
33.86	2002.84	8.46	-4.98
34.34	2002.80	8.42	-5.15
34.83	2002.75	8.42	-4.89
35.31	2002.70	8.41	-4.94
35.78	2002.65	8.41	-4.64
36.30	2002.60	8.47	-4.93
36.75	2002.55	8.42	-4.66
37.17	2002.50	8.49	-4.70
37.63	2002.45	8.45	-4.59
38.11	2002.40	8.48	-4.08
38.58	2002.35	8.59	-4.29
39.10	2002.30	8.53	-4.26

GW:10.1 mm yr^{-1}

depth (mm)	year (A.D.)	Sr/Ca (mmol/mol)	$\delta^{18}O$ (permil)
0.15	2000.27	8.77	-4.09
0.47	2000.22	8.87	-4.63
0.86	2000.17	8.82	-4.16
1.36	2000.12	8.78	-4.27
1.72	2000.07	8.74	-4.56
2.01	2000.02	8.87	-4.79
2.44	2000.02	8.81	-4.30
2.83	2000.01	8.80	-4.62

depth (mm)	year (A.D.)	Sr/Ca (mmol/mol)	$\delta^{18}O$ (permil)
3.29	2000.01	8.70	-4.60
3.75	2000.00	8.82	-4.51
4.27	1999.94	8.83	-4.74
4.73	1999.89	8.61	-5.22
5.35	1999.80	8.63	-5.28
5.77	1999.71	8.61	-5.35
6.26	1999.62	8.53	-4.88
6.69	1999.58	8.78	-4.59
6.97	1999.55	8.76	-4.78
7.19	1999.51	8.64	-4.59
7.53	1999.47	8.72	-4.58
7.94	1999.43	8.72	-4.52
8.31	1999.39	8.73	-4.65
8.76	1999.36	8.79	-4.55
9.26	1999.32	8.82	-4.33
9.67	1999.28	8.87	-4.51
10.05	1999.24	8.88	-4.42
10.50	1999.20	8.92	-4.34
10.91	1999.19	8.73	-4.17
11.26	1999.17	8.83	-4.12
11.73	1999.16	8.79	-4.40
12.25	1999.14	8.88	-4.40
12.74	1999.12	8.88	-4.28
13.21	1999.10	8.85	-4.32
13.69	1999.08	8.85	-4.12
14.14	1999.06	8.83	-4.21
14.66	1999.04	8.91	-4.45
15.02	1999.02	8.88	-4.47
15.68	1999.00	8.90	-4.43
16.16	1998.94	8.86	-4.51
16.51	1998.87	8.86	-4.40
16.80	1998.81	8.67	-5.00
16.96	1998.74	8.52	-5.09
17.27	1998.68	8.46	-5.19
17.57	1998.62	8.57	-5.16
17.80	1998.55	8.74	-5.20
18.02	1998.49	8.59	-5.43
18.16	1998.43	8.80	-4.90
18.68	1998.36	8.69	-5.17
19.05	1998.34	8.73	-5.28
19.74	1998.32	8.78	-4.61
20.33	1998.29	8.78	-4.58
20.99	1998.27	8.79	-4.54
21.62	1998.25	8.88	-4.34
22.01	1998.23	8.84	-4.59
22.22	1998.22	8.76	-4.33

depth (mm)	year (A.D.)	Sr/Ca (mmol/mol)	$\delta^{18}O$ (permil)
22.59	1998.20	8.79	-4.14
22.84	1998.18	8.80	-4.24
23.07	1998.17	8.80	-4.15
23.22	1998.15	8.88	-4.34
23.40	1998.12	8.78	-4.58
23.53	1998.08	8.74	-4.28
24.07	1998.05	8.89	-4.80
24.51	1997.96	8.90	-4.81
24.86	1997.88	8.91	-4.60
25.18	1997.79	8.77	-5.18
25.60	1997.70	8.55	-5.06
25.99	1997.64	8.80	-5.11
26.39	1997.57	8.76	-4.92
26.86	1997.51	8.79	-5.03
27.34	1997.44	8.78	-4.89
27.75	1997.41	8.88	-4.94
28.16	1997.37	8.78	-4.85
28.59	1997.34	8.88	-4.75
29.07	1997.30	8.84	-4.58
29.52	1997.28	8.89	-4.56
29.84	1997.26	8.86	-4.22
30.39	1997.24	8.94	-4.36
30.87	1997.22	8.93	-4.41
31.31	1997.21	8.89	-4.41
31.73	1997.19	8.90	-4.08
31.73	1997.17	8.98	-4.02
32.25	1997.12	8.94	-3.91
32.83	1997.10	8.90	-4.01
33.09	1997.08	8.91	-3.91
33.45	1997.06	8.91	-4.05
33.82	1997.04	8.96	-4.13
34.20	1997.01	8.92	-4.21
34.15	1996.99	8.87	-4.52
34.62	1996.90	8.67	-4.69
35.03	1996.87	8.65	-4.88
35.42	1996.87	8.67	-4.37
35.82	1996.86	8.65	-4.77
36.28	1996.86	8.68	-4.72
36.73	1996.86	8.81	-4.87
37.18	1996.85	8.81	-4.53
37.64	1996.85	8.80	-4.62
38.08	1996.82	8.83	-4.73
38.45	1996.78	8.62	-4.97
38.84	1996.75	8.49	-4.88
39.30	1996.72	8.52	-4.74
39.77	1996.68	8.53	-4.62

depth (mm)	year (A.D.)	Sr/Ca (mmol/mol)	$\delta^{18}O$ (permil)
40.23	1996.65	8.62	-4.47
40.84	1996.62	8.77	-4.45
41.49	1996.62	8.81	-4.35
42.13	1996.61	8.87	-4.09
42.77	1996.61	8.90	-4.16
43.26	1996.61	8.92	-4.11
43.73	1996.61	8.89	-4.14
44.22	1996.60	8.75	-4.15
44.71	1996.60	8.74	-4.41
45.20	1996.58	8.80	-4.45
45.68	1996.55	8.77	-4.86
46.18	1996.53	8.74	-4.78
46.71	1996.50	8.75	-4.57
47.28	1996.37	8.82	-4.86
47.77	1996.34	8.83	-4.69
48.23	1996.31	8.83	-4.36
48.72	1996.28	8.99	-4.44
49.14	1996.25	8.99	-4.59
49.47	1996.24	8.81	-4.22
49.85	1996.23	8.80	-4.40
50.27	1996.23	8.88	-4.44
51.19	1996.22	8.83	-4.40
51.42	1996.21	8.81	-4.45
51.65	1996.20	8.98	-4.37
52.12	1996.15	8.94	-4.29
52.58	1996.12	8.90	-4.35
52.98	1996.08	8.81	-4.50
52.99	1995.96	8.72	-4.48
53.44	1995.95	8.81	-4.71
53.96	1995.94	8.75	-4.58
54.44	1995.92	8.85	-4.67
54.93	1995.91	8.78	-4.85
55.41	1995.90	8.78	-4.79
55.84	1995.89	8.75	-4.99
56.29	1995.88	8.66	-5.04
56.73	1995.87	8.67	-5.05
57.20	1995.86	8.64	-5.03

SC1: 8.0 mm yr^{-1}

depth (mm)	year (A.D.)	Sr/Ca (mmol/mol)	$\delta^{18}O$ (permil)
0.25	2000.5	8.72	-4.42
0.74	2000.42	8.83	-4.45
1.26	2000.35	8.95	-4.46
1.83	2000.27	9.05	-4.57
2.42	2000.08	9.01	-4.89
3.01	1999.89	8.96	-5.12

depth (mm)	year (A.D.)	Sr/Ca (mmol/mol)	$\delta^{18}O$ (permil)
3.56	1999.7	8.73	-5.12
4.13	1999.63	8.78	-5.11
4.73	1999.56	8.92	-5.12
5.40	1999.49	8.83	-5.03
6.06	1999.41	8.86	-4.80
6.65	1999.34	8.85	-4.89
7.27	1999.27	8.96	-4.97
7.99	1999.2	9.03	-4.43
8.56	1999.15	9.03	-4.31
9.05	1999.09	8.94	-4.28
9.70	1999.04	8.85	-4.23
10.26	1998.98	8.83	-4.43
10.80	1998.93	8.84	-4.78
11.15	1998.88	8.86	-4.33
11.53	1998.82	8.94	-4.70
12.17	1998.77	8.96	-4.43
12.86	1998.71	8.98	-4.75
13.76	1998.66	8.70	-4.60
14.34	1998.61	8.73	-4.85
14.67	1998.55	8.82	-4.92
15.21	1998.5	8.82	-4.99
15.80	1998.44	8.83	-5.04
16.39	1998.39	8.83	-4.75
16.90	1998.33	8.85	-4.41
17.39	1998.28	8.90	-4.77
17.87	1998.27	8.80	-4.43
18.38	1998.25	8.85	-4.56
18.90	1998.24	8.86	-4.46
19.42	1998.22	8.85	-4.47
19.92	1998.21	8.86	-4.48
20.45	1998.19	8.84	-4.43
20.98	1998.18	8.85	-4.42
21.47	1998.11	8.78	-4.69
21.94	1998.03	8.79	-4.78
22.39	1997.96	8.76	-4.93
22.88	1997.89	8.74	-4.93
23.41	1997.81	8.78	-5.01
23.89	1997.74	8.66	-5.08
24.33	1997.68	8.76	-4.85

BER: 2.3 mm yr^{-1}

depth (mm)	year (A.D.)	Sr/Ca (mmol/mol)
0.13	2001.50	9.54
0.19	2001.46	9.73
0.24	2001.41	9.83
0.30	2001.37	9.44

depth (mm)	year (A.D.)	Sr/Ca (mmol/mol)
0.36	2001.33	9.75
0.41	2001.29	10.02
0.47	2001.14	9.52
0.53	2001.09	9.23
0.58	2001.05	9.52
0.64	2001.01	9.21
0.69	2001.00	9.75
0.74	2000.97	9.34
0.80	2000.96	9.07
0.80	2000.96	9.43
0.85	2000.95	9.21
0.95	2000.95	9.59
1.03	2000.92	9.25
1.10	2000.92	9.44
1.17	2000.91	9.03
1.25	2000.91	9.49
1.32	2000.91	9.45
1.39	2000.91	9.42
1.47	2000.87	9.05
1.54	2000.83	8.97
1.60	2000.79	9.13
1.67	2000.75	8.93
1.73	2000.71	8.99
1.80	2000.66	9.03
1.86	2000.63	9.36
1.93	2000.62	9.00
1.99	2000.60	9.21
2.06	2000.58	9.12
2.12	2000.54	9.29
2.18	2000.51	9.30
2.25	2000.48	9.69
2.31	2000.44	9.75
2.38	2000.41	9.47
2.44	2000.38	9.67
2.51	2000.34	9.85
2.57	2000.31	10.01
2.64	2000.29	9.57
2.70	2000.27	9.34
2.76	2000.25	9.86
2.83	2000.23	9.86
2.89	2000.21	10.05
2.96	2000.19	9.95
3.02	2000.17	9.44
3.07	2000.15	9.95
3.12	2000.14	9.82
3.17	2000.12	9.48

depth (mm)	year (A.D.)	Sr/Ca (mmol/mol)	$\delta^{18}O$ (permil)
3.21	2000.10	9.69	
3.26	2000.08	9.49	
3.31	2000.06	9.45	
3.36	2000.04	9.70	
3.40	2000.02	9.48	
3.45	2000.00	9.33	
3.50	1999.98	9.66	
3.55	1999.96	9.64	
3.59	1999.94	9.46	
3.64	1999.92	9.37	
3.69	1999.91	9.62	
3.74	1999.89	9.27	
3.78	1999.87	9.53	
3.83	1999.85	9.45	
3.88	1999.83	9.21	
3.93	1999.81	9.24	
3.98	1999.79	9.26	
4.02	1999.77	9.29	
4.12	1999.75	9.03	
4.21	1999.73	9.05	
4.31	1999.71	9.13	
4.41	1999.68	9.05	
4.48	1999.66	9.08	
4.55	1999.64	9.07	
4.62	1999.60	9.15	
4.69	1999.57	9.22	
4.76	1999.55	9.19	
4.83	1999.55	9.23	
4.90	1999.53	9.20	
4.97	1999.51	9.28	
5.04	1999.49	9.55	
5.11	1999.46	9.63	
5.18	1999.43	9.71	
5.25	1999.36	9.85	
5.32	1999.25	9.70	
5.39	1999.17	9.29	
5.46	1999.17	9.29	
5.54	1999.17	9.34	
5.61	1999.16	9.50	
5.67	1999.05	9.54	
5.74	1998.98	9.36	
5.80	1998.95	9.24	
5.87	1998.90	9.15	
5.94	1998.89	9.52	
6.00	1998.89	9.64	
6.07	1998.89	9.24	

depth (mm)	year (A.D.)	Sr/Ca (mmol/mol)	$\delta^{18}O$ (permil)
6.14	1998.87	9.04	
6.20	1998.84	9.26	
6.27	1998.82	9.13	
6.33	1998.78	9.18	
6.40	1998.77	9.29	
6.47	1998.77	9.15	
6.53	1998.76	9.28	
6.60	1998.74	9.05	
6.66	1998.70	9.09	
6.73	1998.70	9.27	
6.80	1998.69	9.45	
6.86	1998.68	9.26	
6.93	1998.68	9.13	
7.00	1998.67	9.11	
7.06	1998.67	9.11	
7.12	1998.66	9.11	
7.18	1998.63	9.26	
7.24	1998.60	9.41	
7.30	1998.57	9.56	
7.36	1998.54	9.77	
7.42	1998.52	9.43	
7.48	1998.49	9.45	
7.54	1998.46	9.37	
7.60	1998.43	9.83	
7.66	1998.40	9.42	
7.72	1998.37	9.36	
7.77	1998.34	9.40	
7.83	1998.31	10.06	

LIA: 5.2 mm yr^{-1}

depth (mm)	year (A.D.)	Sr/Ca (mmol/mol)	$\delta^{18}O$ (permil)
0	5.50	8.62	-3.51
0.46	5.42	8.77	-3.65
0.88	5.35	8.85	-3.86
1.3	5.27	9.12	-3.08
1.71	5.19	8.82	-2.82
2.61	5.11	8.95	-3.45
2.9	5.04	9.21	-3.81
3	4.96	9.05	-3.63
3.32	4.88	8.98	-3.23
3.76	4.80	9.09	-3.93
4.15	4.73	9.05	-3.58
4.58	4.65	8.85	-3.61
5.03	4.63	8.98	-3.82
5.46	4.60	9.01	-4.24
5.88	4.58	9.04	-3.96

depth (mm)	year (A.D.)	Sr/Ca (mmol/mol)	$\delta^{18}O$ (permil)
6.31	4.55	8.91	-3.80
6.74	4.52	8.98	-3.67
7.17	4.50	8.66	-3.53
7.6	4.29	8.95	-3.83
8.01	4.08	8.91	-3.90
8.43	3.86	8.97	-3.72
8.87	3.65	8.99	-3.67
9.31	3.63	8.93	-3.44
9.75	3.60	8.89	-3.52
10.2	3.58	9.04	-3.13
10.63	3.55	8.84	-3.33
11.04	3.52	9.06	-3.24
11.85	3.50	8.69	-2.70
12.24	3.10	9.09	-3.43
12.64	2.99	8.89	-3.41
13.03	2.88	8.67	-3.27
13.03	2.76	8.73	-3.60
13.41	2.65	8.79	-3.93
13.81	2.63	8.73	-3.90
14.22	2.61	8.95	-3.72
14.62	2.59	8.93	-4.40
15.01	2.56	8.92	-3.87
15.39	2.54	9.13	-3.34
15.78	2.52	9.05	-3.41
16.19	2.50	8.61	-3.29
16.57	2.41	8.73	-3.44
16.94	2.31	8.84	-3.55
17.33	2.22	8.81	-2.95
17.69	2.12	8.83	-3.90
18.08	2.03	8.83	-3.89
18.49	1.93	8.84	-4.16
18.89	1.84	8.88	-4.49
19.29	1.74	9.05	-3.67
19.69	1.65	8.89	-3.42
20.11	1.50	8.76	-3.17
20.56	1.43	8.79	-2.93
21.01	1.37	8.96	-4.72
21.42	1.30	8.78	-3.36
21.82	1.24	8.96	-4.19
22.25	1.17	9.03	-3.69
22.65	1.11	8.89	-3.74
23.07	1.04	9.03	-2.89
23.52	0.98	9.05	-3.51
23.95	0.91	8.96	-3.60
24.35	0.85	9.03	-2.63
24.76	0.78	8.86	-3.42

depth (mm)	year (A.D.)	Sr/Ca (mmol/mol)	$\delta^{18}O$ (permil)
25.17	0.72	8.79	-3.01
25.58	0.65	8.82	-3.79
26.02	0.63	8.85	-3.65
26.45	0.60	9.00	-3.00
26.89	0.58	8.70	-3.56
27.32	0.55	8.71	-3.06
27.74	0.52	8.68	-3.55
28.14	0.50	8.60	-3.57
28.53	0.33	8.72	-3.92
28.95	0.17	8.98	-3.33
29.35	0.00	8.99	-3.58

Appendix A2:

Supplemental information for Chapter 3

Surface temperature trends and variability in the low-latitude North Atlantic since 1552. Saenger et al., NGS-2008-10-01089A, Supplementary Information

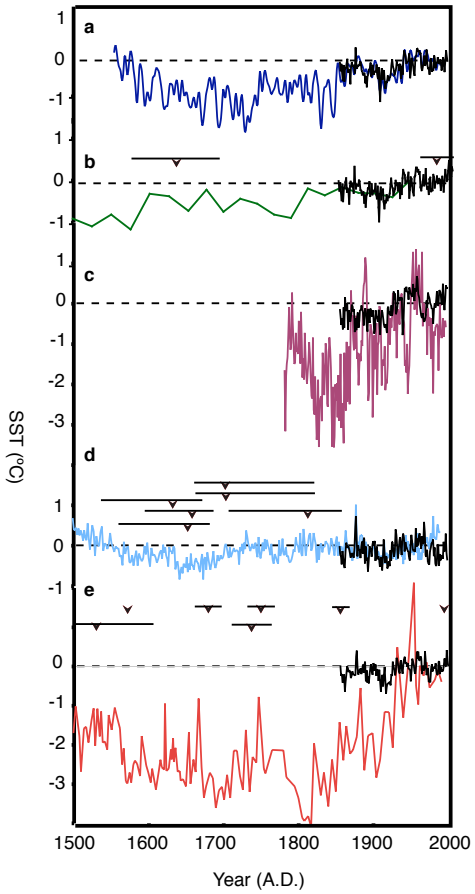

Figure S1: Previous low-latitude Atlantic SST reconstructions. Proxy-based SST (colour) and Kaplan instrumental SST[23] in the 5º x 5º grid box closest to the proxy site (black) from **a.** this study **b.** Great Bahama Bank foraminifera Mg/Ca[15] **c.** Bermuda coral Sr/Ca and growth rate[19] **d.** Cariaco Basin foraminifera Mg/Ca[16] and **e.** Jamaican sclerosponge Sr/Ca[14]. SST estimates in **e**. applied the calibration of Rosenheim et al. (2004). Black triangles represent ^{14}C dates in **b.** and **d.,** and U/Th dates in **e.** Black bars indicate 2σ age uncertainty. This plot is not comprehensive, but it is representative of the best available coral, sedimentary and sclerosponge SST reconstructions based on length, age-control and sampling resolution.

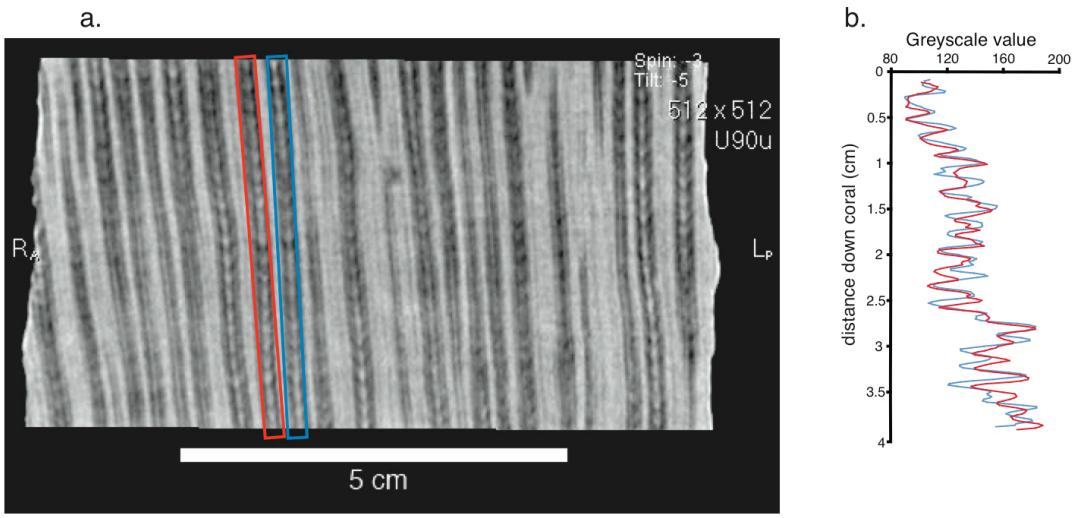

Figure S2: Greyscale variations in Bahamas *Siderastrea siderea.* a. A representative 2-D slice from a CAT scan of our Bahamas coral. Higher density regions along parallel vertical corallites (red and blue boxes) are lighter, while lower density regions are darker. **b.** Greyscale analysis of parallel corallites illustrating reproducible annual density variations upon which annual growth rates are based.

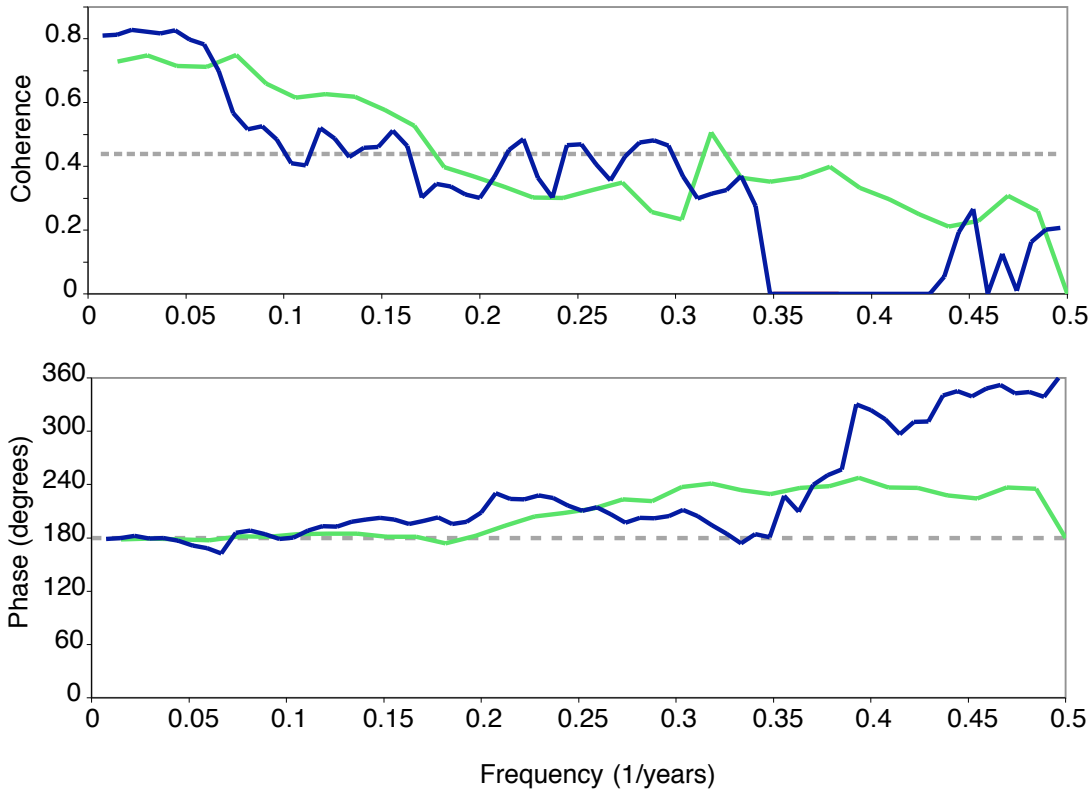

Figure S3: Coherence and phase between SST and coral growth. A multitaper method with 8 windows was used to calculate coherence (top) and phase (bottom) between annual mean Kaplan SST[23] and annual extension rates for corals from the Bahamas (dark) and Belize (light). Dashed line (top) indicates 95% coherence confidence level. See http://www.people.fas.harvard. edu/ ~phuybers/Mfiles/index.html

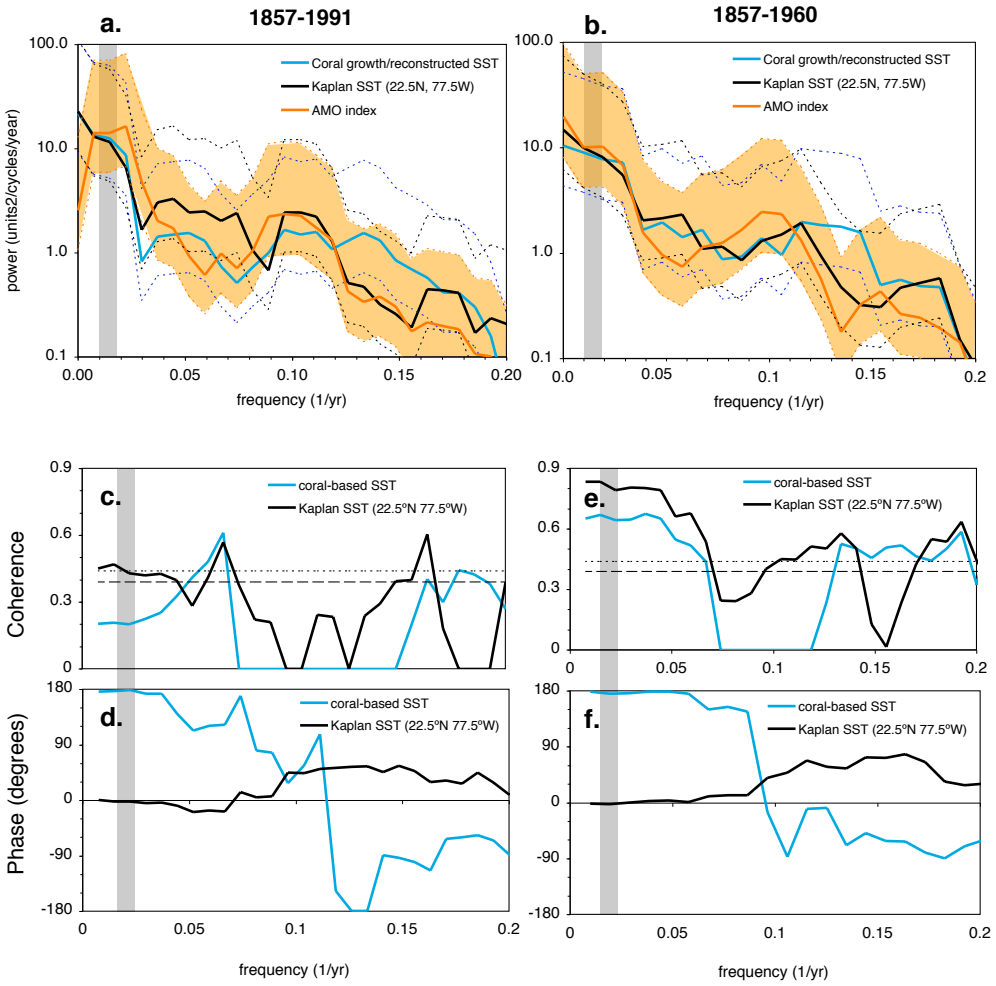

Figure S4: Coherence and phase of SST, AMO and coral growth. Power spectrum of the AMO index (light, shaded), instrumental Bahamas SST[23] (black) and coral extension (light) from **a.** 1857-1991 and **b.** 1857-1960. Shaded region and dashed lines indicate 95% confidence interval. Vertical grey bar is the AMO band. The power spectra of SST and coral extension are statistically indistinguishable from the AMO. Power spectra are calculated using the multi-taper method (nw =3, nfft = 134) see http://www.people.fas.harvard.edu/ ~phuybers/Mfiles/index.html. **c.** Coherence of SST23 (black) and coral extension (blue) with the AMO. Horizontal lines are the 90% (long dash) and 95% (short dash) confidence intervals. **d.** Phase of SST[23] (black) and coral extension (blue). **e., f.** As in **c.** and **d.**, respectively, for the period 1857-1960. Coherence is calculated as in Figure S3.

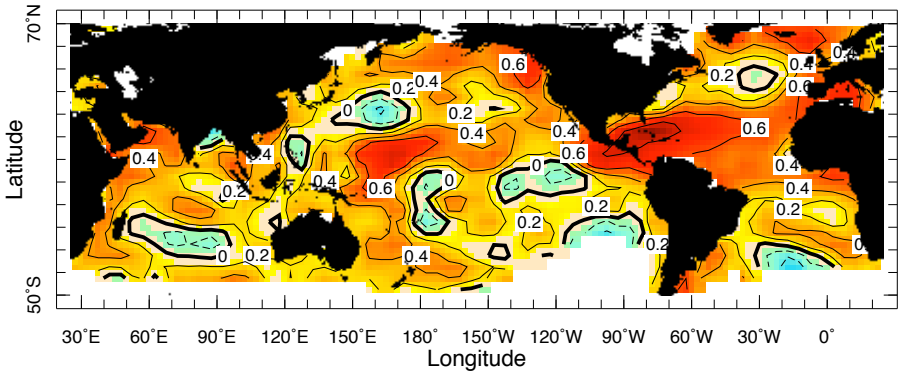

Figure S5: Comparison of Bahamas SST with global SST. Correlations of 6-year running mean linearly-detrended Kaplan SST in the 5º x 5º gridbox centred on 22.5ºN, 77.5ºW, and all global gridboxes for the period 1856-2008[23].

References

Rosenheim, B. E. et al. High-resolution Sr/Ca records in sclerosponges calibrated to temperature in situ *Geology* **32**, doi: 10.1130/G20117.1 (2004).

Appendix A3:

Enlarged figures for Chapter 3

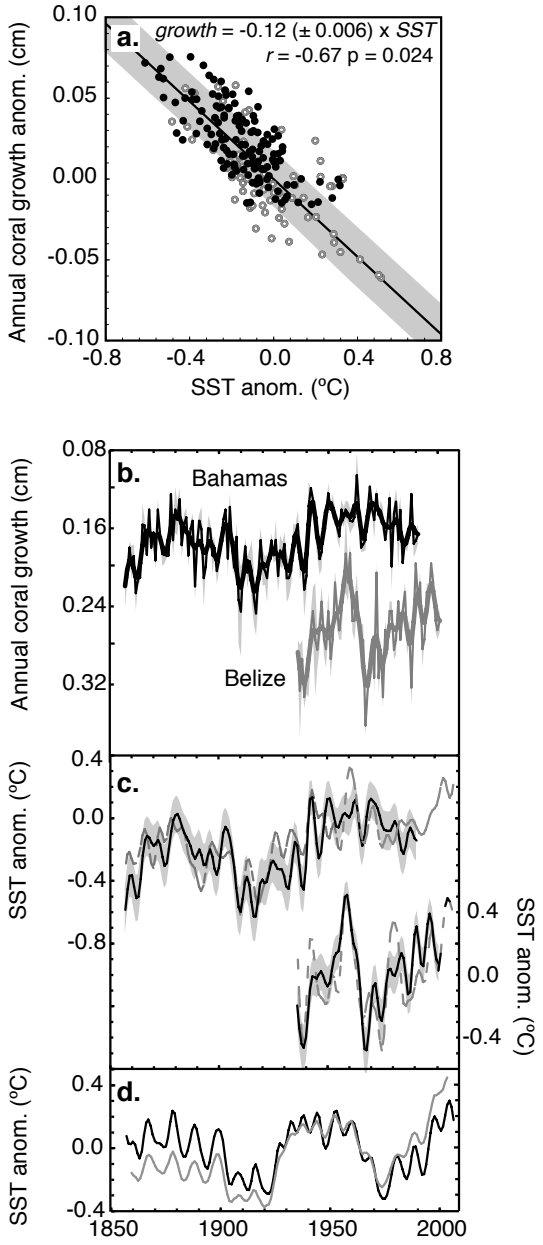

Figure 1. Calibration and verification of the coral-based SST proxy. a, 1857–1991 Bahamas SST anomalies regressed against Bahamas coral growth anomalies (filled). Belize coral growth anomalies and their equivalent SST anomalies (open) do not contribute to the calibration. b, Annual unfiltered (fine) and filtered (bold) coral growth measured from CAT scans of Bahamas (black) and Belize (grey) specimens. c, Coral-based SST anomalies reconstructed from Bahamas (black, top) and Belize (black, below) corals compared with observed 1857–2008 filtered instrumental SST anomalies (grey, dashed). The shading in a–c indicates 1 σstandard error. d, The mean (grey) and linearly detrended mean (AMO; black) SST anomalies from 0–75 N, 10–75 W.

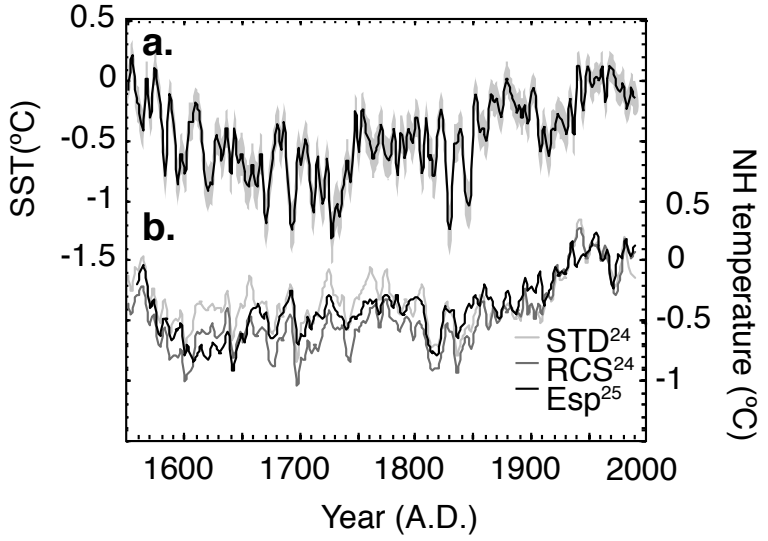

Figure 2: Northern Hemisphere and Atlantic temperature variability since 1550. a, Bahamas coral-based SST anomaly and 1 standard error (shading), estimated by applying the calibration in Fig. 1a to filtered annual coral growth rates (black). b, Filtered hemispheric surface temperature anomalies from extratropical tree rings using standard curve fitting (STD; ref. 25), regional curve standardization (RCS; ref. 25) and Esper et al. (Esp.; ref. 24) methods.

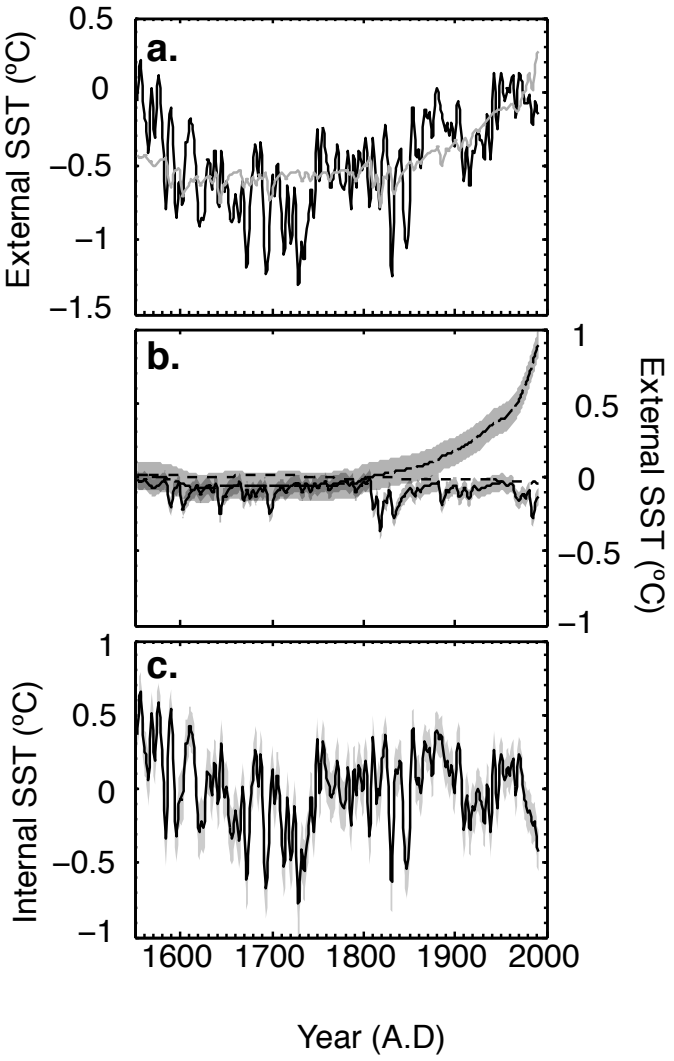

Figure 3 Externally and internally forced SST variability a, Coral-based SST anomalies (black) and estimated externally forced SST anomalies (grey). b, SST variability and 1 standard error attributed to volcanic (black), solar (short dash) and anthropogenic (long dash) external forcings (see the Methods section). c, Internal SST variability (black) and standard error (1σ) calculated by subtracting the curves in a.

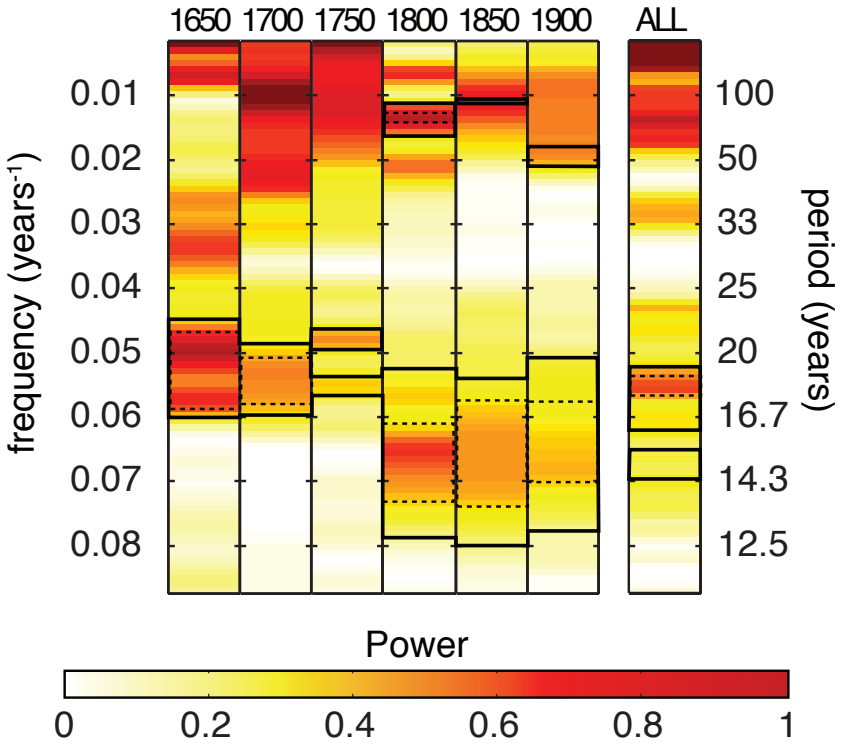

Figure 4 Spectral analysis of internal SST variability. Spectral signature of internally driven SST variability from Fig. 3c. Spectra were calculated using the multitaper method for the entire record (All) and in 200-year bins spanning the periods 1552–1750, 1600–1800, 1650–1850, 1700-1900, 1750–1950 and 1800–1991. The centre year of each bin is shown (top). Gradients indicate the relative power at a given frequency (left y axis) and period (right y axis). Bounding boxes identify frequencies with significant power above red noise at 90% (bold) and 95% (dashed) confidence levels.

Appendix A4:

Data for Chapter 3

Chapter 3 data. Year (column 1), mean annual linear coral extension (column 2), the standard error (1σ) on the linear extension estimate (column 3), the number of corallites analyzed in each year (column 4), 6-year filtered sea surface temperature (SST) anomaly (column 5) and the standard error (1σ) on the SST estimate (column 6)

Year A.D.	extension cm yr^{-1}	std. error cm yr^{-1}	# corallites	SSTa (ºC)	std. error (ºC)
1991	0.166	0.010	3	-0.09	0.21
1990	0.173	0.011	3	-0.07	0.21
1989	0.176	0.014	3	-0.02	0.21
1988	0.125	0.007	3	0.02	0.21
1987	0.167	0.004	3	-0.03	0.21
1986	0.176	0.008	3	-0.14	0.21
1985	0.172	0.008	3	-0.21	0.21
1984	0.196	0.004	3	-0.18	0.21
1983	0.141	0.014	3	-0.07	0.22
1982	0.172	0.029	3	0.04	0.22
1981	0.133	0.013	3	0.07	0.22
1980	0.145	0.010	3	0.04	0.22
1979	0.199	0.024	3	-0.01	0.22
1978	0.129	0.010	3	-0.01	0.21
1977	0.157	0.000	3	-0.01	0.21
1976	0.172	0.000	3	0.00	0.21
1975	0.153	0.014	3	0.05	0.21
1974	0.142	0.010	3	0.12	0.21
1973	0.146	0.004	3	0.19	0.21
1972	0.125	0.007	3	0.22	0.21
1971	0.152	0.020	3	0.25	0.21
1970	0.141	0.008	3	0.27	0.21
1969	0.118	0.004	3	0.24	0.21
1968	0.141	0.008	3	0.12	0.21
1967	0.172	0.011	4	-0.06	0.21
1966	0.177	0.007	3	-0.14	0.21
1965	0.180	0.005	3	-0.05	0.21
1964	0.137	0.023	3	0.14	0.22
1963	0.106	0.022	4	0.26	0.22
1962	0.149	0.008	4	0.24	0.22
1961	0.153	0.007	4	0.15	0.21
1960	0.153	0.013	4	0.11	0.21
1959	0.145	0.012	4	0.12	0.21
1958	0.141	0.009	4	0.14	0.21
1957	0.149	0.010	4	0.13	0.21

1956	0.141	0.011	4	0.07	0.21
1955	0.168	0.012	4	0.02	0.21
1954	0.159	0.011	4	0.03	0.21
1953	0.146	0.006	4	0.10	0.21
1952	0.138	0.013	4	0.20	0.21
1951	0.141	0.000	4	0.27	0.21
1950	0.124	0.011	4	0.27	0.21
1949	0.144	0.006	4	0.16	0.21
1948	0.151	0.004	4	-0.03	0.21
1947	0.184	0.017	4	-0.20	0.21
1946	0.192	0.016	4	-0.25	0.22
1945	0.169	0.021	4	-0.12	0.22
1944	0.151	0.018	4	0.10	0.22
1943	0.131	0.008	4	0.28	0.21
1942	0.119	0.000	4	0.27	0.21
1941	0.137	0.025	4	0.02	0.22
1940	0.209	0.016	4	-0.32	0.22
1939	0.223	0.028	4	-0.52	0.22
1938	0.192	0.010	4	-0.49	0.22
1937	0.192	0.021	4	-0.31	0.22
1936	0.156	0.014	4	-0.14	0.21
1935	0.165	0.008	4	-0.11	0.21
1934	0.168	0.013	4	-0.22	0.21
1933	0.204	0.014	4	-0.41	0.22
1932	0.211	0.020	3	-0.51	0.22
1931	0.211	0.024	3	-0.49	0.22
1930	0.176	0.012	3	-0.40	0.22
1929	0.187	0.014	3	-0.35	0.22
1928	0.183	0.016	3	-0.34	0.22
1927	0.209	0.016	3	-0.34	0.22
1926	0.172	0.021	3	-0.30	0.21
1925	0.188	0.008	3	-0.27	0.21
1924	0.173	0.008	3	-0.29	0.21
1923	0.188	0.000	3	-0.38	0.21
1922	0.211	0.024	5	-0.46	0.21
1921	0.204	0.014	5	-0.47	0.22
1920	0.200	0.019	5	-0.43	0.22
1919	0.172	0.012	5	-0.47	0.22
1918	0.209	0.026	5	-0.61	0.22
1917	0.247	0.022	5	-0.76	0.22
1916	0.232	0.027	5	-0.76	0.22
1915	0.204	0.031	5	-0.63	0.22
1914	0.194	0.012	5	-0.48	0.22
1913	0.205	0.016	5	-0.41	0.21

1912	0.179	0.009	5	-0.46	0.21
1911	0.203	0.010	5	-0.60	0.22
1910	0.245	0.046	5	-0.72	0.23
1909	0.234	0.045	5	-0.67	0.23
1908	0.169	0.014	5	-0.51	0.22
1907	0.200	0.006	5	-0.33	0.22
1906	0.181	0.020	5	-0.18	0.22
1905	0.138	0.014	5	-0.07	0.21
1904	0.191	0.018	4	0.00	0.21
1903	0.141	0.000	4	0.03	0.21
1902	0.151	0.002	4	-0.03	0.21
1901	0.172	0.006	4	-0.17	0.21
1900	0.194	0.011	4	-0.33	0.21
1899	0.204	0.013	4	-0.39	0.21
1898	0.180	0.008	4	-0.34	0.21
1897	0.188	0.019	4	-0.23	0.21
1896	0.161	0.007	4	-0.17	0.21
1895	0.160	0.013	4	-0.22	0.21
1894	0.200	0.004	4	-0.30	0.21
1893	0.211	0.029	4	-0.31	0.22
1892	0.161	0.023	4	-0.22	0.22
1891	0.153	0.008	4	-0.17	0.22
1890	0.176	0.020	4	-0.22	0.22
1889	0.220	0.013	4	-0.25	0.21
1888	0.153	0.007	4	-0.21	0.21
1887	0.160	0.007	4	-0.14	0.21
1886	0.188	0.011	4	-0.10	0.21
1885	0.149	0.010	4	-0.06	0.21
1884	0.157	0.011	4	-0.02	0.21
1883	0.177	0.012	4	0.03	0.21
1882	0.130	0.012	4	0.10	0.22
1881	0.151	0.016	4	0.14	0.22
1880	0.141	0.024	4	0.13	0.22
1879	0.172	0.017	4	0.08	0.22
1878	0.125	0.007	4	-0.02	0.21
1877	0.188	0.000	4	-0.17	0.21
1876	0.188	0.003	3	-0.29	0.20
1875	0.187	0.009	3	-0.32	0.21
1874	0.186	0.012	3	-0.24	0.21
1873	0.165	0.005	3	-0.13	0.21
1872	0.141	0.011	3	-0.09	0.21
1871	0.193	0.009	3	-0.12	0.21
1870	0.165	0.005	3	-0.14	0.21
1869	0.180	0.006	3	-0.11	0.20

1868	0.141	0.000	3	-0.07	0.20
1867	0.187	0.000	3	-0.05	0.21
1866	0.157	0.008	3	-0.09	0.21
1865	0.157	0.022	3	-0.23	0.21
1864	0.211	0.005	3	-0.43	0.21
1863	0.212	0.005	3	-0.58	0.21
1862	0.227	0.017	3	-0.59	0.21
1861	0.189	0.012	3	-0.50	0.21
1860	0.195	0.017	3	-0.43	0.21
1859	0.180	0.006	3	-0.44	0.21
1858	0.211	0.006	3	-0.50	0.21
1857	0.220	0.022	3	-0.48	0.21
1856	0.181	0.006	3	-0.33	0.21
1855	0.163	0.006	3	-0.15	0.21
1854	0.164	0.005	3	-0.04	0.21
1853	0.166	0.003	6	-0.03	0.20
1852	0.170	0.001	6	-0.18	0.20
1851	0.176	0.000	6	-0.50	0.21
1850	0.254	0.028	6	-0.91	0.21
1849	0.294	0.021	6	-1.21	0.21
1848	0.249	0.003	7	-1.33	0.21
1847	0.287	0.019	7	-1.33	0.21
1846	0.253	0.018	7	-1.27	0.21
1845	0.274	0.012	7	-1.16	0.21
1844	0.246	0.023	7	-0.98	0.22
1843	0.227	0.030	7	-0.74	0.22
1842	0.196	0.007	7	-0.54	0.21
1841	0.194	0.009	7	-0.43	0.21
1840	0.194	0.005	7	-0.44	0.21
1839	0.214	0.015	6	-0.51	0.21
1838	0.199	0.025	6	-0.57	0.21
1837	0.219	0.007	6	-0.61	0.21
1836	0.225	0.007	4	-0.60	0.21
1835	0.207	0.013	4	-0.62	0.21
1834	0.189	0.018	4	-0.79	0.21
1833	0.288	0.013	3	-1.11	0.21
1832	0.264	0.006	3	-1.44	0.21
1831	0.319	0.020	3	-1.60	0.21
1830	0.306	0.006	3	-1.49	0.21
1829	0.244	0.023	3	-1.17	0.21
1828	0.240	0.005	3	-0.82	0.21
1827	0.156	0.010	3	-0.59	0.21
1826	0.254	0.010	3	-0.47	0.21
1825	0.196	0.017	3	-0.33	0.21

1824	0.150	0.015	3	-0.21	0.21
1823	0.150	0.005	3	-0.22	0.21
1822	0.234	0.010	3	-0.34	0.21
1821	0.196	0.000	3	-0.43	0.21
1820	0.195	0.028	3	-0.55	0.21
1819	0.169	0.015	3	-0.77	0.21
1818	0.313	0.010	3	-0.99	0.22
1817	0.267	0.030	3	-0.98	0.22
1816	0.202	0.015	3	-0.80	0.22
1815	0.157	0.026	3	-0.74	0.22
1814	0.286	0.011	3	-0.80	0.21
1813	0.252	0.005	4	-0.75	0.20
1812	0.190	0.001	4	-0.50	0.20
1811	0.156	0.000	4	-0.31	0.21
1810	0.177	0.033	4	-0.39	0.22
1809	0.244	0.013	4	-0.64	0.22
1808	0.230	0.020	4	-0.87	0.21
1807	0.244	0.013	4	-0.96	0.21
1806	0.246	0.007	4	-0.88	0.21
1805	0.210	0.009	4	-0.68	0.21
1804	0.197	0.020	4	-0.46	0.22
1803	0.186	0.029	4	-0.32	0.22
1802	0.181	0.020	4	-0.32	0.22
1801	0.182	0.005	4	-0.43	0.22
1800	0.228	0.028	4	-0.57	0.22
1799	0.228	0.023	4	-0.61	0.22
1798	0.179	0.011	4	-0.57	0.22
1797	0.215	0.021	4	-0.50	0.21
1796	0.203	0.009	4	-0.45	0.21
1795	0.191	0.022	4	-0.44	0.22
1794	0.195	0.014	4	-0.52	0.22
1793	0.200	0.018	4	-0.68	0.22
1792	0.264	0.029	4	-0.78	0.22
1791	0.239	0.033	4	-0.69	0.22
1790	0.166	0.007	4	-0.52	0.21
1789	0.192	0.006	5	-0.49	0.21
1788	0.222	0.006	5	-0.66	0.20
1787	0.227	0.005	5	-0.89	0.21
1786	0.277	0.016	5	-0.97	0.21
1785	0.238	0.037	5	-0.83	0.22
1784	0.191	0.020	5	-0.58	0.23
1783	0.172	0.027	5	-0.44	0.23
1782	0.219	0.022	5	-0.49	0.22
1781	0.215	0.025	5	-0.61	0.22

1780	0.219	0.016	5	-0.72	0.21
1779	0.227	0.011	5	-0.78	0.21
1778	0.234	0.007	5	-0.80	0.21
1777	0.227	0.018	5	-0.79	0.21
1776	0.203	0.015	5	-0.78	0.21
1775	0.246	0.005	5	-0.74	0.21
1774	0.231	0.025	5	-0.62	0.22
1773	0.176	0.025	5	-0.45	0.22
1772	0.172	0.013	5	-0.38	0.22
1771	0.219	0.018	5	-0.43	0.22
1770	0.207	0.020	5	-0.52	0.22
1769	0.191	0.017	5	-0.60	0.21
1768	0.239	0.015	5	-0.66	0.21
1767	0.218	0.007	5	-0.69	0.21
1766	0.196	0.000	5	-0.73	0.21
1765	0.244	0.021	5	-0.78	0.21
1764	0.238	0.013	5	-0.78	0.21
1763	0.211	0.011	5	-0.70	0.21
1762	0.203	0.009	5	-0.62	0.21
1761	0.215	0.016	5	-0.57	0.21
1760	0.203	0.020	5	-0.54	0.22
1759	0.207	0.020	5	-0.48	0.22
1758	0.190	0.019	5	-0.39	0.22
1757	0.183	0.015	5	-0.29	0.22
1756	0.190	0.017	5	-0.21	0.22
1755	0.160	0.013	5	-0.24	0.22
1754	0.172	0.030	5	-0.42	0.22
1753	0.242	0.018	5	-0.65	0.22
1752	0.230	0.008	5	-0.71	0.21
1751	0.227	0.015	5	-0.54	0.21
1750	0.160	0.021	5	-0.29	0.22
1749	0.156	0.020	3	-0.23	0.21
1748	0.194	0.000	3	-0.46	0.21
1747	0.244	0.007	3	-0.81	0.21
1746	0.264	0.021	3	-1.04	0.21
1745	0.254	0.028	3	-1.05	0.21
1744	0.234	0.000	3	-0.92	0.21
1743	0.221	0.006	4	-0.79	0.21
1742	0.215	0.013	4	-0.80	0.21
1741	0.239	0.017	4	-0.92	0.21
1740	0.278	0.009	4	-1.03	0.21
1739	0.244	0.006	4	-1.08	0.21
1738	0.234	0.014	4	-1.15	0.21
1737	0.288	0.015	4	-1.30	0.21

1736	0.274	0.011	4	-1.43	0.21
1735	0.317	0.022	4	-1.45	0.21
1734	0.264	0.017	4	-1.36	0.21
1733	0.259	0.009	4	-1.29	0.21
1732	0.273	0.026	4	-1.35	0.21
1731	0.289	0.009	4	-1.51	0.21
1730	0.317	0.027	4	-1.66	0.21
1729	0.303	0.026	4	-1.68	0.21
1728	0.303	0.010	4	-1.53	0.21
1727	0.264	0.012	4	-1.25	0.21
1726	0.254	0.014	4	-0.95	0.21
1725	0.195	0.014	4	-0.79	0.21
1724	0.231	0.010	3	-0.84	0.21
1723	0.267	0.005	3	-1.04	0.21
1722	0.261	0.015	3	-1.21	0.21
1721	0.273	0.017	3	-1.30	0.21
1720	0.267	0.006	3	-1.27	0.21
1719	0.273	0.034	3	-1.11	0.21
1718	0.241	0.015	3	-0.89	0.22
1717	0.189	0.011	3	-0.76	0.21
1716	0.247	0.015	3	-0.85	0.21
1715	0.228	0.030	3	-1.11	0.21
1714	0.326	0.005	3	-1.34	0.21
1713	0.267	0.011	3	-1.39	0.21
1712	0.267	0.015	3	-1.30	0.21
1711	0.247	0.011	3	-1.17	0.21
1710	0.274	0.017	3	-1.02	0.21
1709	0.221	0.020	3	-0.86	0.22
1708	0.209	0.022	3	-0.72	0.22
1707	0.228	0.015	3	-0.63	0.22
1706	0.215	0.017	3	-0.57	0.21
1705	0.199	0.011	3	-0.58	0.21
1704	0.189	0.005	3	-0.70	0.21
1703	0.254	0.010	3	-0.86	0.21
1702	0.287	0.015	3	-0.86	0.21
1701	0.182	0.023	3	-0.71	0.22
1700	0.189	0.023	3	-0.66	0.22
1699	0.242	0.005	3	-0.84	0.21
1698	0.266	0.009	5	-1.14	0.21
1697	0.288	0.012	5	-1.37	0.20
1696	0.294	0.015	5	-1.48	0.20
1695	0.262	0.009	5	-1.55	0.20
1694	0.312	0.007	5	-1.58	0.20
1693	0.316	0.016	5	-1.52	0.21

1692	0.242	0.011	5	-1.33	0.21
1691	0.270	0.022	5	-1.06	0.21
1690	0.230	0.015	5	-0.76	0.22
1689	0.195	0.020	3	-0.48	0.22
1688	0.176	0.026	3	-0.36	0.22
1687	0.189	0.005	3	-0.44	0.22
1686	0.215	0.039	3	-0.60	0.22
1685	0.247	0.006	3	-0.67	0.21
1684	0.202	0.015	3	-0.59	0.21
1683	0.182	0.005	3	-0.45	0.21
1682	0.196	0.017	3	-0.38	0.21
1681	0.195	0.017	3	-0.41	0.22
1680	0.195	0.017	3	-0.50	0.22
1679	0.215	0.017	3	-0.62	0.22
1678	0.249	0.009	3	-0.70	0.21
1677	0.186	0.031	3	-0.79	0.21
1676	0.249	0.005	4	-0.95	0.21
1675	0.279	0.009	4	-1.15	0.21
1674	0.268	0.012	4	-1.33	0.21
1673	0.244	0.019	4	-1.48	0.21
1672	0.378	0.020	4	-1.52	0.21
1671	0.215	0.010	3	-1.40	0.21
1670	0.293	0.010	3	-1.17	0.21
1669	0.241	0.006	3	-0.92	0.21
1668	0.201	0.015	3	-0.74	0.21
1667	0.222	0.020	3	-0.73	0.21
1666	0.235	0.017	3	-0.85	0.21
1665	0.260	0.005	3	-1.01	0.21
1664	0.228	0.020	3	-1.10	0.22
1663	0.299	0.031	3	-1.08	0.22
1662	0.222	0.034	3	-0.95	0.22
1661	0.215	0.020	3	-0.85	0.22
1660	0.241	0.011	3	-0.86	0.21
1659	0.247	0.011	3	-0.95	0.21
1658	0.241	0.025	3	-1.05	0.21
1657	0.273	0.017	3	-1.11	0.21
1656	0.248	0.015	3	-1.10	0.21
1655	0.241	0.015	3	-1.07	0.21
1654	0.254	0.026	3	-1.02	0.22
1653	0.260	0.024	4	-0.92	0.22
1652	0.200	0.028	4	-0.80	0.22
1651	0.233	0.016	4	-0.73	0.23
1650	0.221	0.041	4	-0.73	0.23
1649	0.210	0.022	4	-0.79	0.22

1648	0.250	0.015	4	-0.82	0.22
1647	0.237	0.025	4	-0.73	0.22
1646	0.198	0.012	4	-0.55	0.22
1645	0.195	0.020	4	-0.44	0.21
1644	0.166	0.007	4	-0.53	0.21
1643	0.254	0.010	4	-0.78	0.21
1642	0.249	0.005	4	-0.95	0.21
1641	0.254	0.021	4	-0.92	0.21
1640	0.215	0.014	4	-0.73	0.22
1639	0.176	0.026	4	-0.53	0.22
1638	0.230	0.015	4	-0.44	0.22
1637	0.176	0.014	4	-0.45	0.22
1636	0.209	0.015	4	-0.57	0.21
1635	0.195	0.020	4	-0.74	0.21
1634	0.303	0.007	4	-0.80	0.21
1633	0.186	0.007	4	-0.69	0.21
1632	0.177	0.006	4	-0.57	0.21
1631	0.223	0.010	4	-0.53	0.21
1630	0.223	0.008	4	-0.53	0.21
1629	0.203	0.014	4	-0.52	0.21
1628	0.173	0.003	4	-0.59	0.21
1627	0.238	0.010	4	-0.80	0.20
1626	0.268	0.003	4	-1.00	0.20
1625	0.258	0.005	4	-1.07	0.20
1624	0.238	0.013	4	-1.06	0.20
1623	0.235	0.005	4	-1.07	0.20
1622	0.278	0.008	4	-1.12	0.21
1621	0.244	0.012	4	-1.14	0.21
1620	0.272	0.027	4	-1.07	0.21
1619	0.230	0.019	4	-0.92	0.22
1618	0.220	0.020	4	-0.74	0.22
1617	0.204	0.014	4	-0.58	0.22
1616	0.202	0.016	4	-0.46	0.22
1615	0.208	0.029	4	-0.34	0.22
1614	0.143	0.005	4	-0.25	0.22
1613	0.198	0.019	4	-0.21	0.21
1612	0.175	0.003	4	-0.18	0.21
1611	0.178	0.012	4	-0.15	0.21
1610	0.150	0.000	4	-0.16	0.21
1609	0.177	0.011	4	-0.26	0.21
1608	0.214	0.009	4	-0.36	0.21
1607	0.205	0.023	4	-0.36	0.22
1606	0.156	0.026	4	-0.36	0.22
1605	0.189	0.006	4	-0.49	0.22

1604	0.244	0.032	4	-0.72	0.22
1603	0.235	0.018	4	-0.89	0.21
1602	0.249	0.009	4	-0.94	0.21
1601	0.225	0.010	4	-0.89	0.21
1600	0.235	0.011	4	-0.79	0.21
1599	0.225	0.017	4	-0.72	0.22
1598	0.210	0.022	4	-0.74	0.22
1597	0.215	0.029	4	-0.87	0.22
1596	0.287	0.015	4	-1.03	0.21
1595	0.225	0.007	4	-1.06	0.21
1594	0.274	0.014	4	-0.91	0.21
1593	0.201	0.004	4	-0.64	0.21
1592	0.166	0.007	4	-0.38	0.21
1591	0.195	0.014	4	-0.21	0.21
1590	0.166	0.007	4	-0.11	0.21
1589	0.186	0.007	4	-0.05	0.21
1588	0.127	0.014	4	-0.11	0.22
1587	0.196	0.021	3	-0.37	0.22
1586	0.215	0.020	3	-0.74	0.22
1585	0.273	0.024	3	-0.98	0.22
1584	0.254	0.023	3	-0.95	0.22
1583	0.215	0.024	3	-0.71	0.22
1582	0.156	0.020	3	-0.47	0.22
1581	0.215	0.020	3	-0.32	0.22
1580	0.195	0.023	3	-0.18	0.22
1579	0.117	0.020	3	-0.01	0.22
1578	0.176	0.020	3	0.13	0.22
1577	0.137	0.022	3	0.23	0.23
1576	0.117	0.025	3	0.25	0.23
1575	0.156	0.025	3	0.15	0.23
1574	0.150	0.020	3	-0.04	0.22
1573	0.176	0.022	3	-0.23	0.22
1572	0.215	0.024	3	-0.32	0.22
1571	0.156	0.023	3	-0.24	0.22
1570	0.196	0.022	3	-0.04	0.22
1569	0.117	0.023	3	0.14	0.23
1568	0.132	0.023	3	0.13	0.23
1567	0.166	0.024	3	-0.09	0.23
1566	0.200	0.024	3	-0.35	0.22
1565	0.215	0.024	3	-0.46	0.22
1564	0.196	0.021	3	-0.39	0.22
1563	0.156	0.023	3	-0.26	0.22
1562	0.176	0.024	3	-0.17	0.22
1561	0.175	0.024	3	-0.15	0.22

1560	0.170	0.024	3	-0.10	0.23
1559	0.159	0.024	3	0.01	0.23
1558	0.145	0.024	3	0.16	0.23
1557	0.131	0.024	3	0.31	0.23
1556	0.121	0.024	3	0.39	0.23
1555	0.117	0.024	3	0.35	0.23
1554	0.136	0.023	3	0.21	0.23
1553	0.176	0.021	3	0.08	0.22
1552	0.157	0.020	3	0.01	0.22

Appendix A5:

Data for Chapter 4

Chapter 4 59GGC Mg/Ca and stable isotope data

depth (cm)	Year (A.D.)	Year (B.P.)	Mg/Ca (mmol/mol)	SST (ºC)	$\delta^{13}C$ (per mil)	$\delta^{18}O$ (per mil)
1.5	1618	332	4.87	28.34	1.02	-1.19
1.5	1618	332	4.89	28.39	0.92	-1.07
2.5	1601	349	4.23	26.78	1.10	-1.64
3.5	1585	365	4.77	28.11	1.01	-1.03
3.5	1585	365	4.65	27.83	0.50	-1.33
3.5	1585	365			0.56	-1.38
4.5	1569	381	4.82	28.23	0.66	-1.36
4.5	1569	381			0.59	-1.33
5.5	1552	398	4.21	26.72	0.13	-1.94
5.5	1552	398	4.98	28.59		
6.5	1536	414	4.23	26.78	0.48	-1.41
6.5	1536	414	4.22	26.75	0.45	-1.23
7.5	1519	431	4.52	27.51	0.30	-1.60
7.5	1519	431	4.57	27.63	0.61	-1.48
8.5	1503	447	4.32	27.01	0.45	-1.31
8.5	1503	447	4.09	26.40		
9.5	1487	463	4.60	27.71	0.61	-1.51
9.5	1487	463	4.37	27.14	0.11	-1.76
10.5	1470	480	4.38	27.16	0.50	-1.57
10.5	1470	480	4.30	26.96		
11.5	1454	496	4.23	26.78	0.42	-1.30
11.5	1454	496	4.83	28.25	0.76	-1.63
12.5	1437	513	4.33	27.04	0.62	-1.51
13.5	1421	529	4.50	27.46	0.61	-1.64
13.5	1421	529	4.51	27.49	0.45	-1.47
14.5	1405	545	4.47	27.39	0.38	-1.48
14.5	1405	545	4.68	27.90	0.67	-1.57
15.5	1388	562	4.49	27.44	0.45	-1.62
15.5	1388	562	4.63	27.78	0.49	-1.61
16.5	1372	578	4.34	27.06	0.56	-1.83
17.5	1355	595	4.32	27.01	0.46	-1.59
17.5	1355	595	4.76	28.09	0.39	-1.62
18.5	1339	611	4.86	28.32	0.52	-1.68
18.5	1339	611	4.58	27.66	0.21	-1.96
19.5	1323	627	4.65	27.83	0.09	-1.71
19.5	1323	627	4.63	27.78	0.41	-1.87
20.5	1306	644	4.43	27.29	0.63	-1.71
20.5	1306	644	4.92	28.45		
21.5	1290	660	4.50	27.46	0.33	-1.31
21.5	1290	660	4.19	26.67	1.01	-1.52
22.5	1274	676	4.34	27.06	0.76	-1.53
22.5	1274	676	4.32	27.01	0.41	-1.66
23.5	1257	693	4.51	27.49	0.48	-1.87
23.5	1257	693	4.26	26.85	0.47	-1.55

24.5	1241	709	4.64	27.80	0.40	-1.70
24.5	1241	709	4.44	27.31	0.84	-1.42
25.5	1224	726	4.25	26.83	0.39	-1.80
25.5	1224	726	4.36	27.11	0.58	-1.52
26.5	1208	742	4.42	27.26	0.37	-1.69
26.5	1208	742	4.23	26.78	0.75	-1.54
27.5	1192	758	4.27	26.88	0.13	-1.60
27.5	1192	758	3.97	26.07	0.55	-1.57
28.5	1175	775	4.38	27.16	0.45	-1.76
28.5	1175	775	4.47	27.39		
29.5	1159	791	4.96	28.54	0.34	-1.71
29.5	1159	791	4.63	27.78	0.22	-1.85
30.5	1142	808			0.17	-1.54
31.5	1126	824	4.41	27.24	0.44	-1.68
31.5	1126	824	4.17	26.62	0.64	-1.75
32.5	1110	840	4.20	26.70	0.43	-1.43
32.5	1110	840	4.46	27.36	0.05	-1.93
33.5	1093	857	4.48	27.41	0.24	-1.85
33.5	1093	857	4.48	27.41	0.31	-1.58
34.5	1077	873	4.30	26.96	0.51	-1.32
34.5	1077	873			0.82	-1.14
35.5	1060	890	5.08	28.81	0.41	-1.49
35.5	1060	890	4.26	26.85	0.40	-1.44
36.5	1044	906	4.72	27.99	0.63	-1.50
36.5	1044	906	4.73	28.02	0.62	-1.47
37.5	1028	922	4.01	26.18	0.05	-1.86
37.5	1028	922	4.62	27.76		
38.5	1011	939	4.67	27.87	0.32	-1.47
38.5	1011	939			0.37	-1.64
39.5	995	955	4.60	27.71	0.49	-1.48
40.5	978	972	4.04	26.26	0.36	-1.71
40.5	978	972	4.49	27.44	0.15	-1.52
41.5	962	988	4.44	27.31	0.39	-1.30
41.5	962	988	4.59	27.68	0.46	-1.69
42.5	946	1004	4.38	27.16	0.33	-1.31
43.5	929	1021	4.37	27.14	0.53	-1.71
43.5	929	1021	3.98	26.10	0.09	-1.62
44.5	913	1037	4.08	26.37	0.61	-1.30
44.5	913	1037			1.03	-1.58
45.5	896	1054	4.50	27.46	0.58	-1.52
45.5	896	1054			0.41	-1.36
46.5	880	1070	3.67	25.20	0.80	-1.78
46.5	880	1070	4.50	27.46	0.51	-1.57
47.5	864	1086				-1.80
48.5	847	1103	4.70	27.95	0.43	-1.40
48.5	847	1103	4.57	27.63	0.93	-1.85
48.5	847	1103	4.77	28.11		

49.5	831	1119	4.37	27.14	0.37	-1.56
49.5	831	1119			0.17	-1.65
50.5	814	1136	4.09	26.40	0.42	-1.50
50.5	814	1136	4.22	26.75		
50.5	814	1136	4.48	27.41		
51.5	798	1152	4.44	27.31	0.56	-1.56
51.5	798	1152	4.22	26.75		
52.5	782	1168	4.18	26.64	0.55	-1.81
52.5	782	1168	4.44	27.31		
52.5	782	1168	4.27	26.88		
53.5	765	1185	4.56	27.61	0.01	-1.95
53.5	765	1185	4.48	27.41		
54.5	749	1201	4.20	26.70	0.12	-1.74
54.5	749	1201	4.62	27.76		
55.5	733	1217	4.25	26.83	0.88	-1.59
55.5	733	1217			0.86	-1.12
56.5	716	1234	4.49	27.44	1.19	-1.40
56.5	716	1234	4.28	26.91	0.83	-1.25
57.5	700	1250	4.66	27.85	1.05	-1.41
57.5	700	1250	4.29	26.93	0.42	
58.5	683	1267	4.39	27.19	0.42	-1.45
58.5	683	1267	4.32	27.01	0.65	-1.38
59.5	667	1283	4.41	27.24	0.63	-1.19
59.5	667	1283	4.09	26.40	0.58	-1.34
60.5	651	1299	4.48	27.41	-0.30	-1.54
60.5	651	1299	4.33	27.04	0.39	-1.57
61.5	634	1316	4.44	27.31	0.21	-1.42
61.5	634	1316	4.41	27.24	0.74	-1.47
62.5	618	1332	4.22	26.75	0.86	-1.39
62.5	618	1332	4.67	27.87	0.48	-1.73
63.5	601	1349	4.45	27.34	0.68	-1.29
63.5	601	1349	4.22	26.75	0.67	-1.19
64.5	585	1365	4.12	26.48	0.10	-1.32
64.5	585	1365	4.62	27.76	0.64	-1.16
65.5	569	1381	4.63	27.78	0.58	-1.38
65.5	569	1381	4.28	26.91		
66.5	552	1398	4.28	26.91	0.13	-1.51
66.5	552	1398	3.99	26.13		
67.5	536	1414	3.95	26.01	0.65	-1.21
67.5	536	1414	4.20	26.70	0.89	-1.20
68.5	519	1431	4.52	27.51		
68.5	519	1431	4.40	27.21		
69.5	503	1447	4.04	26.26	0.78	-1.24
69.5	503	1447			0.40	-0.98

Chapter 4 MC22 Mg/Ca and stable isotope data

depth (cm)	Year (A.D.)	Year (B.P.)	Mg/Ca (mmol/mol)	SST (ºC)	$\delta^{13}C$ (per mil)	$\delta^{18}O$ (per mil)
0.5	1966	-16	4.45	27.34	0.65	-1.45
1.5	1934	16	4.58	27.66	0.58	-1.57
1.5	1934	16			0.63	-1.64
1.5	1934	16			0.84	-1.44
2.5	1902	48	4.66	27.85		
3.5	1870	80	4.66	27.85	0.48	-1.81
4.5	1839	111	4.56	27.61	0.58	-1.48
4.5	1839	111			0.92	-1.35
5.5	1807	143	4.33	27.04	0.48	-1.50
5.5	1807	143			0.56	-1.82
6.5	1775	175	4.16	26.59	0.61	-1.64
6.5	1775	175			0.45	-1.57
7.5	1743	207	4.44	27.31	0.64	-2.23
7.5	1743	207			0.96	-1.14
8.5	1711	239	4.67	27.87	0.25	-1.70
9.5	1679	271	4.37	27.14	0.02	-2.17
9.5	1679	271			0.46	-1.91
9.5	1679	271			-0.07	-1.38
10.5	1647	303	4.76	28.09	0.16	-1.79
10.5	1647	303			-0.08	-1.80
11.5	1616	334	4.62	27.76	0.80	-1.51
11.5	1616	334			0.32	-1.71
11.5	1616	334			0.52	-1.55
12.5	1584	366	4.29	26.93	0.60	-1.47
12.5	1584	366			-0.32	-1.44
13.5	1552	398	4.34	27.06	0.29	-1.28
13.5	1552	398			-0.01	-1.80
13.5	1552	398			0.62	-1.28
14.5	1520	430	4.57	27.63	0.79	-1.54
14.5	1520	430	4.53	27.54		
15.5	1488	462	4.16	26.59	0.16	-1.45
15.5	1488	462	4.21	26.72		
16.5	1456	494	4.34	27.06	0.94	-1.80
16.5	1456	494			0.30	-1.77
17.5	1425	525	4.48	27.41	0.76	-1.45
17.5	1425	525			0.33	-2.11
18.5	1393	557	4.64	27.80	0.46	-1.52
18.5	1393	557			0.64	-1.62
19.5	1361	589	4.30	26.96	0.68	-1.11
19.5	1361	589			0.62	-1.27
20.5	1329	621	4.67	27.87	0.91	-1.63
20.5	1329	621			0.31	-1.34
21.5	1297	653	4.55	27.59	0.30	-1.50
21.5	1297	653			0.61	-1.53

22.5	1265	685	4.30	26.96	0.70	-1.41
22.5	1265	685			0.56	-1.88
23.5	1233	717	4.50	27.46	0.73	-1.51
23.5	1233	717			0.48	-1.23
24.5	1202	748	4.51	27.49	-0.21	-1.68
24.5	1202	748			0.48	-2.02
25.5	1170	780			-0.18	-1.58
25.5	1170	780			0.43	-1.70
26.5	1138	812	4.33	27.04	0.32	-1.93
26.5	1138	812			-0.26	-1.64
26.5	1138	812			-0.25	-1.73
27.5	1106	844	4.61	27.73	0.44	-1.54
27.5	1106	844			-0.64	-2.06
28.5	1074	876	4.42	27.26	0.16	-1.92
28.5	1074	876			0.45	-1.55
29.5	1042	908	4.62	27.76	1.08	-1.60
30.5	1011	939	4.10	26.43	0.55	-1.34
30.5	1011	939	4.36	27.11		
31.5	979	971	4.54	27.56	0.68	-1.42
31.5	979	971			0.70	-1.53
32.5	947	1003	4.60	27.71	-0.08	-1.79
32.5	947	1003			0.47	-1.87
33.5	915	1035	4.36	27.11	0.44	-1.62
34.5	883	1067	4.30	26.96	0.58	-1.70
34.5	883	1067			0.94	-1.29
34.5	883	1067			0.76	-1.41
35.5	851	1099	4.37	27.14	0.48	-1.62
35.5	851	1099			0.75	-1.31
36.5	820	1131	4.40	27.21	0.45	-1.17
36.5	820	1131			0.66	-1.60
37.5	788	1162	4.69	27.92	0.70	-1.80
37.5	788	1162			0.29	-1.22
37.5	788	1162			0.05	-2.02
38.5	756	1194	4.37	27.14	0.42	-1.78
38.5	756	1194	4.85	28.30		
39.5	724	1226	4.38	27.16	0.51	-1.36
39.5	724	1226			0.43	-1.83
40.5	692	1258	4.26	26.85	0.77	-2.06
40.5	692	1258			0.46	-1.44
41.5	660	1290	4.42	27.26	-0.04	-1.55
41.5	660	1290	4.15	26.56		
42.5	628	1322	4.20	26.70	0.45	-1.53
42.5	628	1322	4.73	28.02		
43.5	597	1354	4.24	26.80	0.52	-1.73
43.5	597	1354			0.11	-1.54
44.5	565	1385	4.32	27.01	0.78	-1.08
44.5	565	1385			0.58	-1.45

45.5	533	1417	4.22	26.75	1.11	-1.74
45.5	533	1417			0.88	-1.63
45.5	533	1417			0.86	-1.76
46.5	501	1449	4.10	26.43	0.29	-1.87
46.5	501	1449			0.81	-1.51
46.5	501	1449			0.63	-1.32
47.5	469	1481	4.21	26.72	0.18	-1.62
47.5	469	1481			0.51	-1.32
47.5	469	1481			0.32	-1.57
48.5	437	1513	4.18	26.64	0.92	-1.30
48.5	437	1513			0.75	-1.57
49.5	406	1545	4.45	27.34	0.37	-1.42
50.5	374	1576	4.59	27.68	0.75	-1.50
50.5	374	1576			0.45	-1.23
51.5	342	1608	4.59	27.68	0.41	-1.86
51.5	342	1608			0.64	-1.38
51.5	342	1608			0.68	-2.12
52.5	310	1640	4.44	27.31	0.69	-1.56
52.5	310	1640	4.45	27.34		
53.5	278	1672	4.57	27.63	0.47	-1.46
53.5	278	1672	4.25	26.83	0.80	-1.76
53.5	278	1672			0.28	-1.66
53.5	278	1672			0.62	-2.12
54.5	246	1704	4.78	28.13	0.08	-1.67
54.5	246	1704	4.94	28.50		
55.5	214	1736	4.28	26.91	0.52	-1.49
55.5	214	1736	4.58	27.66		
55.5	214	1736	4.26	26.85		

Appendix A6:

Enlarged figures for Chapter 5

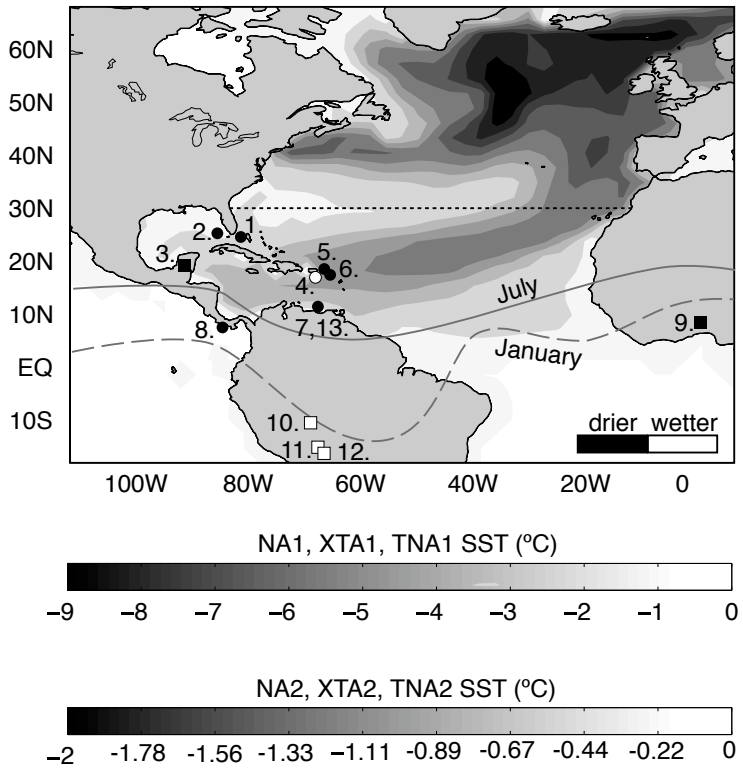

Figure 1. Imposed SST anomaly pattern (shading) for CAM3 simulations (note separate scales). XTA simulations applied SSTs only north of 30 N (dotted line). TNA simulations applied SSTs only south of 30 N. Marine (circles) and terrestrial (squares) proxy records indicating wetter (open) and drier (filled/green) LIA conditions. Numbers correspond to Table 1. Modern seasonal ITCZ extremes are also shown.

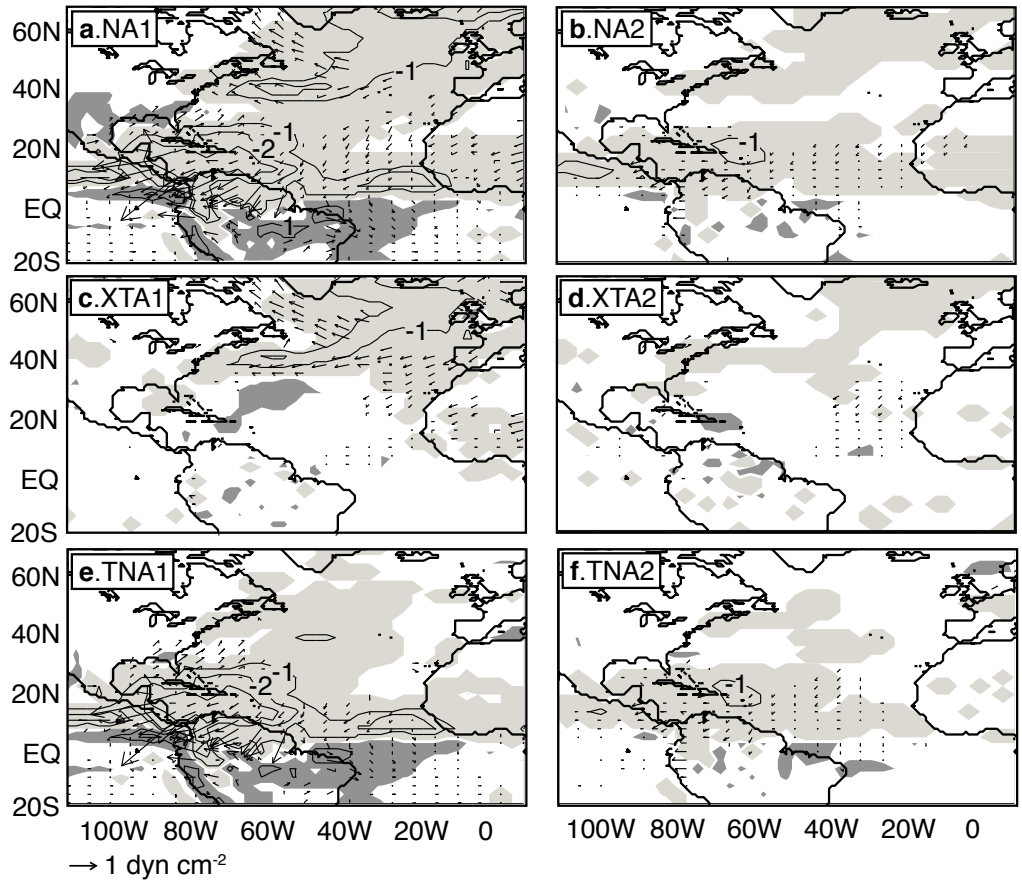

Figure 2. Significant mean annual precipitation (contours,mm day^{-1}) and wind stress (vectors, dyn cm^{-1}) anomalies for (a) NA1, (b) NA2, (c) XTA1, (d) XTA2, (e) TNA1, and (f) TNA2. Shading highlights positive (dark) and negative (light) precipitation anomalies that are significant at 95%.